DEPARTAMENTO DE CIÊNCIAS DA VIDA

FACULDADE DE CIÊNCIAS E TECNOLOGIA
UNIVERSIDADE DE COIMBRA

Role of p66shc Signaling on Doxorubicin-Induced Cardiac Mitochondrial Dysfunction

Susana Filipa Pereira Sampaio

2012

DEPARTAMENTO DE CIÊNCIAS DA VIDA

FACULDADE DE CIÊNCIAS E TECNOLOGIA
UNIVERSIDADE DE COIMBRA

Role of p66shc Signaling on Doxorubicin-Induced Cardiac Mitochondrial Dysfunction

Dissertação apresentada à Universidade de Coimbra para cumprimento dos requisitos necessários à obtenção do grau de Mestre em Biologia Celular e Molecular, realizada sob a orientação cientifica do Doutor Paulo Jorge Oliveira (Centro de Neurociências e Biologia Celular, Universidade de Coimbra) e da Doutora Maria Sancha Santos (Departamento de Ciências da Vida, Universidade de Coimbra)

Susana Filipa Pereira Sampaio

2012

AGRADECIMENTOS

No final de mais uma etapa percorrida, gostaria de agradecer a todos aqueles que de alguma forma apoiaram e contribuíram para a minha evolução e aprendizagem ao longo deste ano.

Em primeiro lugar agradeço à Fundação para a Ciência e Tecnologia pelo financiamento deste trabalho, através do projecto PTDC/SAU-TOX/117912/2010, co-financiado por FEDER/Compete e Fundos Nacionais.

Agradeço ao Doutor Paulo Jorge Oliveira por me ter recebido no seu grupo. Por toda a sua disponibilidade, compreensão e apoio ao longo deste ano. Acima de tudo agradeço toda a confiança depositada no meu trabalho, o que fez com que cada desafio fosse possível de ultrapassar. Agradeço também à Doutora Maria Sancha dos Santos por ter aceitado ser minha co-orientadora.

Em seguida, mas não menos importante, agradeço a todos os membros do Mitochondrial Toxicology and Disease Group que sempre contribuíram para um óptimo ambiente de trabalho e companheirismo contribuindo assim para a realização desta tese, bem como para o meu crescimento pessoal. Em especial, gostaria de agradecer:

À Ana Filipa Branco, a quem devo grande parte dos ensinamentos laboratoriais apreendidos ao longo deste ano. Tenho a agradecer também por toda a paciência, companhia, boa disposição e por trazer sempre um novo entusiasmo a cada desafio. A sua dedicação e paixão pela ciência serão sempre um grande exemplo para mim. Agradeço também à Rute Loureiro (Mitosister), pois sem a sua boa disposição e companhia, a realização desta tese não teria sido tão animada.

Agradeço a todos os meus amigos sem o apoio dos quais nada seria possível: Catarina Xavier, Marisa Oliveira, Sara Vieira, Ricardo Leitão, Ana Isabel Santos, Vanessa Machado, Gladys Caldeira, entre tantos...e um muito obrigada à Maria

Manuela Azevedo por ter partilhado comigo bons e maus momentos, por todas as suas palavras positiva nos momentos necessários.

Agradeço de forma muito especial ao João Costa por toda a companhia, carinho e por estar sempre do meu lado em todos os momentos.

Por fim agradeço aos meus pais e irmã, a quem devo todos os sucessos que possa alcançar na vida, agradeço por todo o apoio, educação e compressão.

A todos um muito obrigada!

INDEX

ABBREVIATIONS

ADP	Adenosine diphosphate
AIF	Apoptosis Inducing Factor
ANT	Adenine nucleotide translocator
APAF-1	Apoptosis peptidase activating factor-1
ATP	Adenosine trisphosphate
BCL-2	B-cell lymphoma-2
CR	Caloric restriction
CsA	Cyclosporin A
CypA	Cyclophilin A
Cyt c	Cytochrome c
DAN	Daunorubicin
DIABLO	Direct inhibitor of apoptosis-binding protein with low pI
DISC	Death-inducing signaling complex
DOX	Doxorubicin
DNA	Deoxyribonucleic acid
DTT	Dithiothreitol
FoxO	Forkhead transcription factors
HEPES	N-(2-hydroxyethyl)-1-piperazine-N` -(2-ethanesulfonic acid)
HSP70	Heat-shock protein 70
IgG	Immunoglobulin G
IMS	Mitochondrial intermembrane space
JNK	Jun-N-terminal kinase
MnSOD	Manganese superoxide dismutase
MOMP	Mitochondrial outer membrane permeabilization
MPTP	Mitochondrial permeability transition pore
ΔΨ	Mitochondrial transmembrane electric potential
NADPH oxidase	Nicotinamide adenine dinucleotide phosphate-oxidase
OMM	Outer mitochondrial membrane
OXPHOS	Oxidative phosphorylation
PAGE	Polyacrylamide gel electrophoresis
PAR	Poly(ADP-ribose)
PARP	PAR polymerase

PBS	Phosphate buffered saline
PCD	Programmed Cell Death
PIN 1	Propyl isomerase 1
PKC β	Protein kinase C beta
PMSF	Phenylmethanesulfonylfluoride
PP2A	Type 2 protein serine/threonine phosphatase
PVDF	Polyvinylidene fluoride
RES	Resveratrol
RNA	Ribonucleic acid
ROS	Reactive oxygen species
RTK	Receptor protein tyrosine kinase
SHC	Src homolog and collagen homolog proteins
SMAC	Second mitochondria-derived activator of caspase
SRB	Sulforhodamine B
TNF	Tumor Necrosis Factor
TOM/TIM	Outer membrane translocase/inner membrane translocase
VDAC	Voltage-dependent anion channel
XIAP	X-linked inhibitor of apoptosis protein

ABSTRACT

Doxorubicin (DOX) is a potent and broad-spectrum anthracycline with antineoplastic properties. However, the use of this drug is limited due to a dose-dependent and cumulative myocardial toxicity that devolps to cardiomyopathy. DOX-induced cardiotoxicity is multifactorial, with increased reactive oxygen species production, which ultimately results in cardiomyocyte dysfunction and apoptosis, being hailed as one of the main mechanisms to justify DOX cardiotoxicity. p66Shc protein has been described for its role as a stress response for increased levels of reactive oxygen species (ROS). When oxidative stress increases, p66Shc is translocated to mitochondria promoting higher levels of ROS and causing cell death.

In the present study, we aimed to investigate whether p66Shc signaling is activated during DOX treatment of the cardiomyoblast cell line H9c2 and whether the transcriptional factor FoxO3a, reported to transcriptionally activate target genes responsible for apoptosis and cell cycle arrest, is also involved in the activated redox pathway. Our results demonstrate that after 24h of incubation with DOX, there is an up-regulation of p66Shc protein, although unexpectedly, a decreased ratio between the serine 36-phosphorylated form and total p66Shc was measured. Our results also suggest a physical involvement of p66Shc and FoxO3a that increases upon DOX treatment and FoxO3a translocation to the nucleus, leading to the up-regulation of several proteins involved in DOX cell death including superoxide dismutase-2, p53 and Bim. Hispidin, a PKC β inhibitor, was used in the present study to block DOX toxicity on H9c2 cells, although per se it caused already some cytotoxicity. The results suggest that p66Shc signaling may have a role in the activation of DOX stress/toxicity responses after H9c2 cell treatment and that selective inhibition of this pathway may be a

promising therapeutic approach, as well as a good framework to investigate the persistent DOX cardiotoxicity, an hallmark of this anthracyclin.

Keywords: Cardiotoxicity, Doxorubicin, FoxO3a, H9c2 rat cardiomyoblasts, p66Shc.

RESUMO

Doxorrubicina (DOX) é um composto antracíclico com propriedades anticancerígenas. Contudo, o uso deste composto é limitado devido a uma toxicidade cumulativa e dependente da dose que afecta o miocárdio e se manifesta como cardiomiopatia. A toxicidade induzida pela DOX é multifactorial e um dos principais mecanismos para explicar essa mesma toxicidade baseia-se no aumento de produção de espécies reactivas de oxigénio, que conduz à disfunção dos cardiomiócitos e apoptose. A proteína p66Shc tem sido descrita pelo seu papel ao ao nivel da resposta ao stresse em relação ao aumento dos níveis espécies reactivas de oxigénio. Quando ocorre um aumento do stresse oxidativo, a p66Shc é translocada para a mitocôndria contribuindo para aumentar ainda mais a produção de espécies reactivas de oxigénio e, consequente morte celular.

No presente estudo, tivemos como objectivo investigar se a p66Shc é activada durante o tratamento com DOX da linha celular derivada de cardiomioblastos H9c2 de rato e, se o fator de transcrição FoxO3a, descrito por induzir a transcrição de genes envolvidos em apoptose e na paragem do ciclo celular, também está relacionado com a via redox que poderá estar a ser activada. Os nossos resultados demonstram uma activação da p66Shc após 24 horas de tratamento com DOX, apesar de contrariamente ao esperado, ter-se observado uma diminuição na razão entre a p66Shc fosforilada na serina 36 e a p66Shc total. Os nossos resultados também sugerem uma interacção entre a p66Shc e o FoxO3a, cuja translocaçao para o núcleo aumenta após tratamento com DOX, conduzindo à sobreexpressao de várias proteínas envolvidas na morte celular induzida pela DOX que incluem, a superóxido dismutase-2, p53 e Bim. Apesar de por si só provocar alguma citotoxicidade, o composto Hispidina, um inibidor da PKC β, foi usado no

presente estudo de forma a bloquear a toxicidade induzida pela DOX nas células H9c2. Os resultados sugerem que a sinalização da p66Shc pode ter um papel na activação da resposta ao stresse/toxicidade induzida pela DOX após tratamento das H9c2 e a inibição selectiva desta via pode ser importante para a terapia, bem como base para investigar a persistência cardiotóxica induzida pela DOX, que é um efeito secundário característico desta antraciclina.

Palavras-chave: Cardiotoxicidade, Doxorubicina, FoxO3a, cardiomioblastos H9c2 de rato, p66Shc.

CHAPTER 1- INTRODUCTION

1.1. Doxorubicin as a Chemotherapeutic Agent

Doxorubicin (DOX) is a potent and broad-spectrum anthracyline antibiotic with antineoplastic properties that was first isolated by aerobic fermentation of the pigment-producing *Streptomyces peucetius caesius*. This technique has been performed through solvent extraction, followed by chromatographic purification and crystallization as an hydrochloride form (Arcamone *et al*., 1969). Similarly to others anthracyclines, DOX has a four-ring 7,8,9,10-tetrahydrotetracene-5,12-quinone structure (figure 1) in which the tetracycline ring system represents the chromosphore and includes a quinone structure (Zunino and Capranico, 1990, Minotti *et al*., 2004). When excited at 500 nm DOX presents two emission peaks (550 nm and 590 nm), which provides it with intrinsic fluorescence.

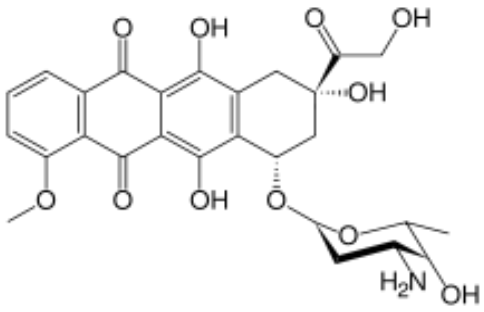

Figure 1. Chemical structure of Doxorubicin (adapted from Wallace, 2007).

DOX is an analogue of Daunorubicin (DAN), a glycoside formed by a tetracycline quinone to which a daunosamine sugar residue is bound. Despite this minor difference, important consequences for the activity of both compounds exist, with DOX being very effective for the treatment of breast cancer, childhood solid tumors, soft tissue sarcomas, and aggressive lymphomas, while DAN shows activity against acute lymphoblastic or myeloblastic leukemias (Weiss, 1992).

DOX has become one of the most widely prescribed antineoplastic compounds due to its cytostatic biological activity, as well as its long half-life in the body and lipophilic properties (Weiss, 1992). Cytotoxicity increases exponentially with both drug concentration and time of exposure. Children and old adults are particularly susceptible to the cardiotoxic effects of anthracycline chemotherapy, and there is no safe concentration range for anthracycline treatment in this population (Zhang *et al.*, 2009).

Currently, DOX is clinically used for the treatment of several types of cancer such as breast, ovarian, transitional cell bladder, bronchogenic lung, thyroid and gastric cancers, as well as soft tissue sarcoma, osteogenic sarcomas, neuroblastoma, Wilms' tumor, malignant lymphoma (Hodgkin's and non-Hodgkin's), acute myeloblastic leukemia, acute lymphoblastic leukemia and Kaposi's sarcoma related to acquired immunodeficiency syndrome (AIDS) (Mross *et al*., 2006).

Despite extensive clinical utilization, the action mechanisms of anthracyclines in cancer cells remain a matter of controversy and different mechanisms have been proposed. Drug–cell membrane interactions, DNA intercalation, topoisomerase interaction, generation of free radicals and apoptosis are some of the well known mechanisms by which DOX has been proposed to act (Mross *et al*., 2006). These different mechanisms are represented in Figure 2.

DOX intercalates into double-stranded DNA, covalent binding to DNA or regulatory proteins (Leonhard *et al*., 1992). Doxorubicin is rapidly taken up into the nucleus of cells where it binds with high affinity to DNA through classical intercalation between base pairs. The structure of the planar anthracycline ring of DOX is capable of intercalating into the DNA double helix in a reversible way, interfering with the correct reading fidelity of both DNA and RNA polymerases. Indeed, hydrophobic interactions, hydrogen bonds to DNA phosphate groups and the insertion of the daunosamine sugar

into the DNA small groove with an affinity to the CpG-complex and transcriptional active sites leads to a stable drug-DNA-complex with a long half-life (Quigley *et al.*, 1980).

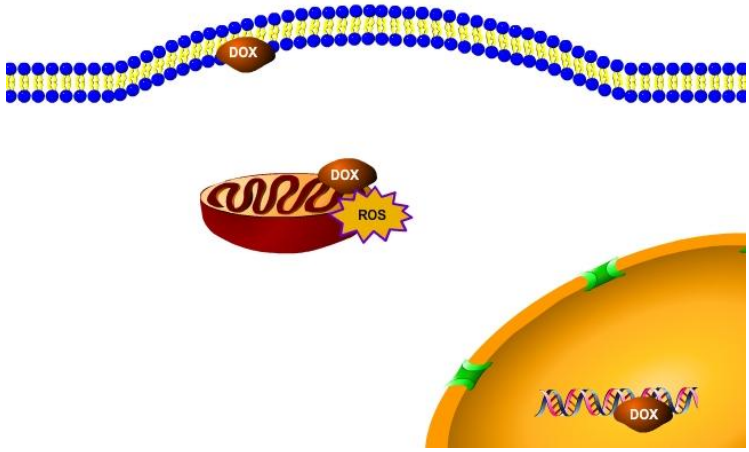

Figure 2. Schematic representation of possible DOX mechanisms as an antineoplastic agent. Doxorubicin can interact with cell membranes, mitochondria and DNA. DOX can interact with cell membrane and it is accumulated in the nucleus where it binds with high affinity to DNA, inhibiting interactions of DNA transcription factors and RNA polymerase. DOX also acts as a topoisomerase II poison where it perturbs the re-ligation step of topoisomerase II. DOX can stimulate ROS production in mitochondria and consequently, disrupt the function of this organelle.

Although DOX may exert its anticancer activity through DNA intercalation, this mechanism is not sufficient to explain the whole spectra of different actions of the anthracyclines. The planar aglycone, without the daunosamine sugar, intercalates with DNA as well, but no antitumor activity was found (Dessypris *et al.*, 1986). DOX also interacts as a topoisomerase II poison since, once intercalated into DNA, the drug disturbs the re-ligation step of topoisomerase II resulting in the formation of the ternary drug-DNA-topoisomerase II 'cleavable complex' (Cutts *et al.*, 2005). There are many early reports of DOX-DNA adducts formed by enzymatic, microsomal or cellular activation of the drug and this was enhanced in tumor cells when treated with pre-activated DOX (Cummings *et al.*, 1991). It is still unclear if the potent antitumor effect

is a direct consequence of the drug-DNA interaction *in vivo* but it appears that drug specificity in addition to DNA binding is important for the antitumor activity of antineoplastic drugs (Tewey *et al.*, 1984).

1.2. Doxorubicin-Induced Cardiac Toxicity

DOX cardiotoxicity is expressed as a dose-dependent and cumulative cardiomyopathy and ultimately in high mortality risk. This risk of cardiotoxicity is higher in individuals with a previous history of cardiomyopathy, or mediastinal irradiation with previous heart disease (Allen, 1992; Papkovsky, 2004). In fact, drug related myocardial toxicity may develop even years after the administration (Bristow *et al.*, 1981). DOX causes numerous morphological alterations in cardiac-like cells, including loss of myofibrils, distension of the sarcoplasmic reticulum, lamin degradation, vacuolization of the cytoplasm and nuclear swelling, as well as mitochondrial depolarization and fragmentation of mitochondrial filaments, besides causing membrane blebbing, a morphological hallmark of apoptosis (Sardao *et al.*, 2009b). As described before, the mechanisms of DOX cardiotoxicity are dose-dependent and a redox cycling mechanism appears to be very important in the context of DOX cardiac toxicity. Initially, a univalent quinone reduction to the corresponding semiquinone free radical occurs, which ultimately involves three different pathways: reduction to the corresponding hydroquinone, covalent DNA adducts or proteins production, or even the transfer of the unpaired electron to another electron acceptor, completing a reduction/oxidation DOX cycle (Monti *et al.*, 1995). This redox cycle generates reactive free radical species, a possibly primary mechanism for the toxicity observed with this agent and with other anthracyclines (Lee *et al*., 1991).

One primary effect of DOX on mitochondrial bioenergetics is an interference with oxidative phosphorylation and inhibition of ATP synthesis (Oliveira and Wallace, 2006). Free radical generated from DOX redox-cycling on mitochondrial NADH dehydrogenase (Complex I) are thought to be responsible for many of the secondary effects of DOX, including lipid peroxidation, the oxidation of both proteins and DNA, and the depletion of glutathione and pyridine nucleotide reducing equivalents in the cell (Davies and Doroshow, 1986).

In the presence of molecular oxygen and a proper electron donor (complex I in mitochondria), DOX forms semiquinone radicals which are rapidly reoxidized in a process which generates superoxide and other reactive oxygen species. DOX is then available to participate in further reduction/oxidation cycles (Davies and Doroshow, 1986; Fang *et al*., 2007). Free radicals resulting from DOX redox cycle are thought to be responsible for many of the secondary effects, including lipid peroxidation, the oxidation of both proteins and DNA, the depletion of glutathione and pyridine nucleotides. Since DOX redox cycling occurs primarily in mitochondria, disruption of mitochondrial function is the main mechanism proposed to explain DOX cardiotoxicity (Doroshow and Davies, 1986; Wallace, 2007). Most of these cellular events can contribute to cardiomyocyte dysfunction and, in some cases death, which has been proposed to be involved in DOX-induced cardiomyopathy (Kumar *et al.*, 2001, Mizutani *et al.*, 2005, Zhang *et al.*, 2009).

DNA damage and signaling pathways involving the tumor suppressor p53 and Bax translocation to mitochondria are early events in DOX-induced cardiac cell death (Sardao *et al.*, 2009a). Shizukuda *et al.*, (2005) have also shown that disruption of the p53 gene reduces DOX-induced cardiotoxicity and attenuates the decline of left ventricle systolic function, apoptosis of cardiac myocytes, and the depletion of

myocardial glutathione and Cu/Zn superoxide dismutase. p53 protein can also act directly as a pro-apoptotic protein. Once translocated to the mitothondria, p53 can activate the mitochondrial dependent pathway of apoptosis, which occurs independently of new gene transcription or protein synthesis (Liu *et al.*, 2008a).

Since mitochondria play a vital role on the energy production of cells, these organelles are quite abundant in cardiac tissue (up to 35% of the cell volume) since energy supply must be kept high to sustain contractile function (Lebrecht *et al.*, 2005; Tokarska-Schlattner *et al.*, 2006). As described above, DOX interferes with cardiac oxidative phosphorylation, including inhibition of both NADH and succinate oxidase of heart mitochondria *in vitro* and *in vivo* (Santos *et al.*, 2002). DOX is also a potent inhibitor of the Mg-dependent FoF1-ATPase of heart and skeletal muscle mitochondria (Davies and Doroshow, 1986, Boucek *et al.*, 1987). Indeed, *in vivo* studies shown that DOX cardiotoxicity decreases in the presence of radical scavengers supporting that oxidative stress is important in this mechanism (Jung and Reszka, 2001).

DOX-induced oxidative stress can also be a part of the mechanism of increased mitochondrial permeability transition pore (MPTP) which has been implicated in mitochondrial and cell dysfunction (Halestrap *et al.*, 1997).

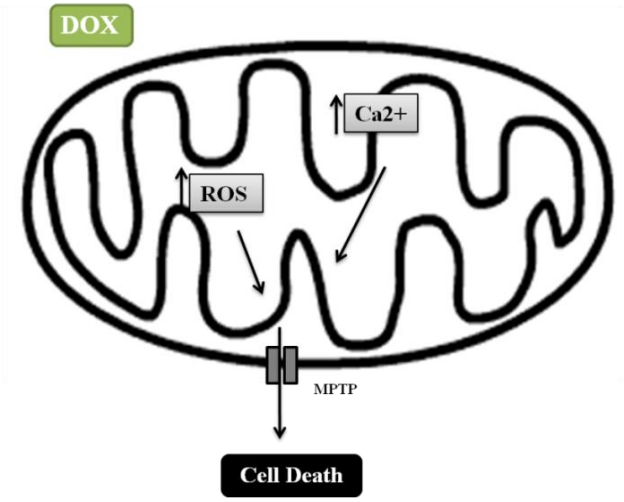

Figure 3. DOX effect on mitochondrial calcium homeostasis and functionality. DOX induces cardiac mitochondrial calcium deregulation due an over-generation of ROS. Disruption of mitochondrial calcium homeostasis by DOX is also associated with MPTP. The opening of MPTP consequently releases pro apoptotic factors, promoting cell death.

It has been reported that DOX inhibits the net accumulation of calcium by isolated cardiac mitochondria and stimulates the release of calcium from the mitochondrial matrix (Sokolove and Shinaberry, 1988; Pereira *et al.*, 2009). However, Cyclosporin A (CsA) reverses that decrease *in vitro* in mitochondrial calcium-loading capacity which indicates that the effect is due to an increased sensitivity to induction of MPTP, since that compound is a specific inhibitor of the MPTP (Broekemeier and Pfeiffer *et al*., 1989). The adenine nucleotide translocator (ANT), an important component of the mitochondrial machinery of ATP synthesis because of its intrinsic activity of adenine nucleotide translocase, is also proposed to be a structural or at least regulatory component of the MPTP (Vieira *et al*., 2000). ANT has a dual role: one acting in both regulation of mitochondrial physiology and a second one as MPTP inductor. Induction of MPTP after DOX treatment occurs through increased oxidation of vicial thiol groups in specific mitochondrial protein (Oliveira *et al*., 2006) and/or through disturbing the adenine nucleotide translocate (ANT) activity and expression in

the heart. In fact, the decrease in the amount of ANT protein in DOX-treated rats (Oliveira and Wallace, 2006) may be a good explanation for both increased MPTP induction and inhibition of respiration.

DOX toxicity persists during an extended period of time, although this phenomenon still unexplored in the literature (Steinherz *et al*., 2001). Some studies in rodent model have reported deleterious alterations in cardiac mitochondrial function, including decreased calcium loading capacity and gene expression profile (Zhou *et al*., 2001; Berthiaume *et al*., 2007; Richard *et al*., 2011) supporting the notion that DOX cardiotoxicity in the myocardium is persistent and irreversible. Indeed, long-term persistence of DOX cardiotoxicity has a large impact in survivors of childhood cancer since it may lead to the appearance of later cardiac alterations during stressful events, including pregnancy, (Bar *et al*., 2003) and may disturb the ability to perform physical activity (Johnson *et al*., 1997). However, the mechanisms for this persistent toxicity are still unknown.

1.3. Prevention of Doxorubicin-Induced Cardiotoxicity

Since ROS overgeneration has been considered a primary mechanism of DOX-induced cardiotoxicity, clinical approaches were designed to attenuate or prevent this cardiotoxicity, consisting mainly of antioxidants and iron chelators. In fact, several compounds with antioxidant properties have been investigated *in vitro* and *in vivo* with some positive outcomes (resumed in figure 4).

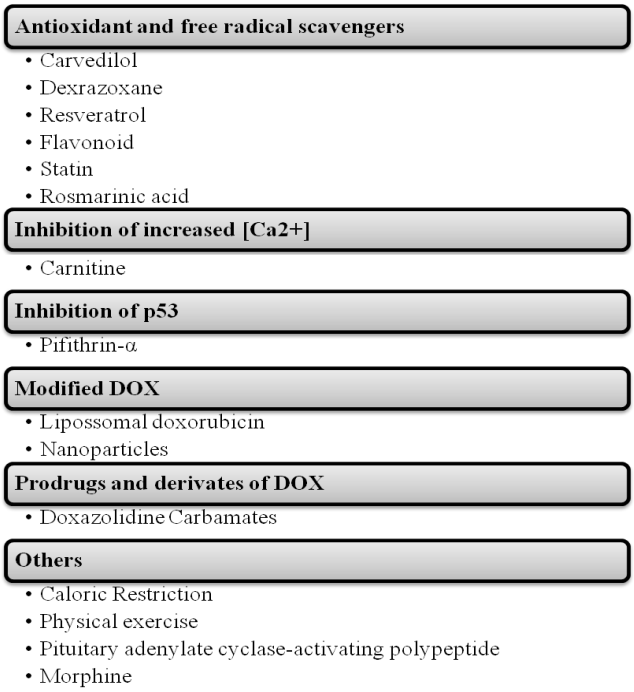

Figure 4. Potential strategies to prevent DOX-induced cardiotoxicity. Some of the strategies to reduced/prevent DOX side effects, as well as cardiomyopathy includes the use of anti-oxidant and free radical scavengers, inhibition of increased calcium concentrations, inhibition of p53, delivery systems for DOX administration, and DOX prodrugs/derivatives (Adapted from Zhang *et al*., 2009).

Carvedilol is clinically used for the treatment of congestive heart failure, mild to moderate hypertension, and myocardial infarction (Fazio *et al*., 1998). This compound is an adrenergic blocking agent with strong antioxidant properties and has been observed to protect against DOX-induced mitochondrial-mediated cardiomyopathy. Carvedilol antioxidant effect is based on its ability to chelate free iron and direct scavenging activity (Oettl *et al*., 2001; Oliveira *et al.*, 2004, Spallarossa *et al.*,2005). Carvedilol also removes iron from its complex with DOX, and thereby reducing hydroxyl radicals and superoxide generation (Lebrecht *et al.*, 2007). Dexrazoxane, the only cardioprotective drug currently available clinically against DOX toxicity, is an intracellular iron chelator which has been proved to protect myocardial mitochondria from genetic and functional lesions induced by

DOX. Resveratrol, a naturally occurring phytoalexin, can act as an intracellular antioxidant and anti-inflammatory agent. Studies with this compound showed an increase in the cellular levels of antioxidant function by directly scavenging reactive oxygen radicals, preventing the formation of cellular reactive oxygen, and/or increasing cellular detoxification mechanisms (Oktem *et al.*, 2010). In particular, RES has been shown to protect against DOX-induced oxidative stress through changes in mitochondrial function, mediated by Sirt1 pathway leading to cardiac cell survival (Danz *et al.*, 2009, Zhang *et al.*, 2011). Some cardioprotective effects have been attributed to opioids, particularly morphine, which has similar effects to a phenomenon known as Ischemic Preconditioning. It has been clearly shown that opioids exert protective effect in the heart and in other organs against stress conditions through specific opioid receptors. Morphine was able to protect heart against the most unwanted effects of DOX. Kelishomi *et al.*, (2008) have demonstrated that morphine exert a very positive protective effect on a high dose of DOX. Sharma *et al.*, (2010) reported that Rosuvastatin pretreatment for 30 days significantly decreases cardiac tissuecaspase-3 activity, DNA fragmentation, and decreases serum lactate dehydrogenase and lipid levels, along with reversal of hemodynamic changes induced by DOX.

Similarly, flavonoids and phenolic acids also seem to have a protective role against DOX-induced cardiotoxicity. Overall, luteolin-7-O-b-D-glucopyranoside showed cardioprotective effect by inhibiting the DOX-induced intracellular level of ROS and calcium overload (Wang *et al.*, 2010). Pifithrin-alpha, a p53 inhibitor, was found to be a protective agent against the cardiotoxic effects induced by DOX administration, confirming DNA damage as an early event in cardiomyocyte death (Liu *et al.*, 2004; Sardão *et al.*, 2009a).

Several other compounds have been studied in order to prevent cardiotoxicity and new approaches are continually being proposed. Recently, formulations of liposome-encapsulated DOX have been approved for the treatment of tumors resistant to conventional anticancer drugs. Nanoparticles, prodrugs and DOX derivatives are also promising vehicles for antitumor drug delivery. Increasing DOX intracellular accumulation, as well as the therapeutic efficacy reduces the cytotoxic effect on off-target cells (Jiang *et al.*, 2011; Ren *et al.*, 2011; Shieh *et al.*, 2011).

L-carnitine is a vitamin-like compound which has been successfully used in several forms of cardiomyopathy (Sayed-Ahmed *et al.*, 1999). *L*-carnitine inhibits DOX-induced ROS generation and NADPH oxidase activation, also reducing cleaved caspase-3 levels and cytosolic cytochrome *c*, and increases Bcl-$x_{L,}$ expression, protecting cardiomyocytes from DOX-induced apoptosis (Chao *et al.*, 2011).Currently, other important mechanisms to protect the heart from DOX toxicity have been considered. Caloric restriction (CR), physical exercise, and endogenous neuropeptides are some of them. CR induces a general attenuation of oxidative damage, inflammation and apoptosis, through interactions with multiple signaling pathways, including activation of AMPK, insulin-like growth factor 1 (IGF-1), Akt and mTOR (Chen *et al.*, 2011). Physical exercise in its various forms has been shown to be an effective intervention and daily exercise seems to antagonize some harmful consequences of DOX treatment (Ascensao *et al.*, 2011; Hydock *et al.*, 2011). Pituitary adenylate cyclase-activating polypeptide (PACAP) is a widely distributed endogenous neuropeptide, also occurring in the cardiovascular system. This neuropeptide inhibits cardiac fibrosis and protects cardiomyocytes against oxidative stress and in vitro

ischemia/reperfusion. PACAP treatment also reduces caspase-3 activation and increased the level of phospho-Bad (Racz *et al.*, 2010).

Future research should continually improve the essential mechanisms and develop new therapeutic strategies in order to prevent the main side effects from doxorubicin administration, as well as premature cardiomyocyte death in pediatric patients who need anthracycline treatment.

1.4. Cell Death Signaling Pathways

Apoptosis is a highly conserved mechanism of programmed cell death (PCD) that was first described in 1972 by Currie and colleagues (Kerr *et al.*, 1972). PDC is an essential process for the elimination of damaged, unwanted or unnecessary cells not only during organism development and homeostasis, but also to maintain the balance between cell proliferation and differentiation. Contrary to other forms of cell death, such as necrosis, apoptosis involves the activation of a signaling cascade that causes cells to maintain membrane integrity through most of the death process. Characteristic apoptotic features include cell membrane blebbing and shrinkage, formation of apoptotic bodies, nuclear envelope breakdown, caspase activation, phosphatidylserine present on the plasma membrane outer leaflet, as well as chromatin condensation and DNA fragmentation (Savill and Fadok *et al.*, 2000). This process is tightly controlled by a complex regulatory network. However, failure of this regulation may lead to pathological disorders such as developmental defects, autoimmune diseases, neurodegeneration or even cancer (Thompson, 1995; Hanahan and Weinberg *et al.*, 2000).

There are two main major apoptotic pathways that can be triggered through a wide range of stimuli: the extrinsic pathway (death receptor pathway) or the intrinsic

pathway (the mitochondrial pathway) as pictured in Figure 5. These two apoptotic signaling pathways are evolutionally conserved, but the precise molecular events involved in the regulation of caspase enzymatic cascades are often specific to cell type and death stimulus.

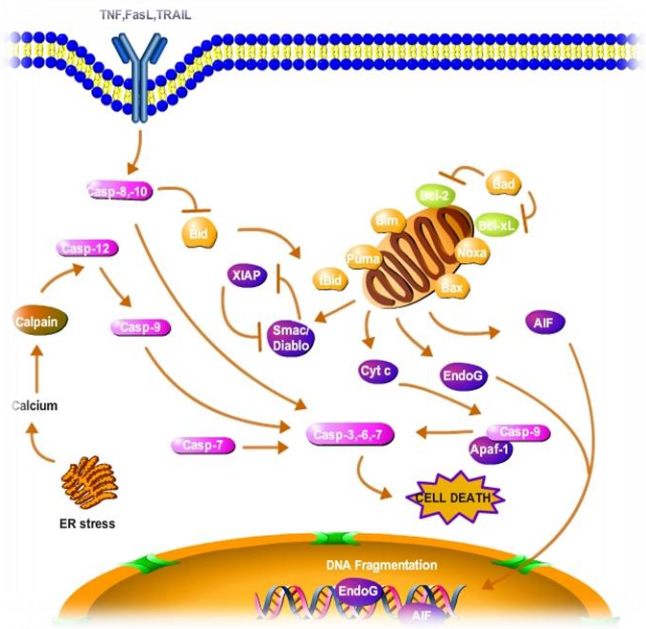

Figure 5. Apoptotic signaling pathways. Apoptosis can result from activation of two biochemical cascades: the extrinsic (death receptor) and the intrinsic (the mitochondrial pathway) pathways. The extracellular apoptotic pathway is initiated at the plasma membrane by specific transmembrane receptors, whereas mitochondrial apoptosis is triggered by intracellular stimuli such as Ca^{2+} overload and high production of ROS. In both, initiator caspases (caspase-8 and -9, respectively) are activated and can catalyze the proteolytic maturation of executioner caspases, such as caspase-7 and -3. Mitochondrial membrane permeabilization is an important event in mitochondrial pathway by activating both caspase-dependent and independent mechanisms that eventually execute cell death. After MMP, the mitochondrial intermembrane space protein cytochrome *c* and other pro-apoptotic factors are released into the cytosol. Cyt c interacts with the adaptor protein apoptotic peptidase activating factor 1 (APAF-1), as well as with procaspase-9 to form the apoptosome. This sequentially activates caspase-9 and executioner caspases, such as caspase-3, in a process known as the caspase cascade. One of the major links between extrinsic and mitochondrial apoptosis is provided by the BCL-2 homology domain 3 (BH3)-only protein BID, which can promote MMP following caspase-8-mediated cleavage. Endoplasmic reticulum (ER) also promotes the activation of caspase-12 with subsequent activation of caspase-9 and -3 promoting cell death (adapted from Hotchkiss *et al.* 2006).

Caspases are cysteine-dependent aspartate-directed proteases responsible for propagating the apoptotic signaling cascade. Apoptotic caspases comprise a protein family synthesized as inactive zymogens containing a prodomain followed by p20 and p10 subunits, where zymogens can be cleaved during apoptosis. Based on their function, caspases are classified into three groups: Inflammatory caspases (involved in inflammation and not in apoptosis), apoptotic initiator caspases (with long prodomains containing either a death effector domain (DED) (caspase-8 and -10) or a caspase activation and recruitment domain (CARD) (caspase-2, -9), and apoptotic effector caspases (executioner class known as caspase-3, -6,-7) (Stennicke and Salvesen, 2000).

1.4.1. Extrinsic Apoptotic Pathways

The extrinsic pathway (receptor-mediated death pathway) is modulated by cell surface death receptors, such as Fas, tumor necrosis factor receptor (TNFR), or TRAIL receptors by their respective ligands. Death receptor ligands characteristically initiate signaling via receptor oligomerization, which in turn results in the recruitment of specialized adaptor proteins and activation of caspase cascades. Binding of FasL induces trimerization, and recruitment of the adaptor protein Fas-associated death domain and caspase-8, forming a death-inducing signaling complex (DISC). Autoactivation of caspase-8 at the DISC can directly cleave and activate caspase-3, or alternatively, it can cleave Bid, a pro-apoptotic Bcl-2 family protein. When cleaved, tBid translocates to mitochondria, inducing cytochrome c release and activation of effector caspases, including caspase-6, -3 and -7 in order to carry out the apoptotic cell death program. FasL and TNF-α may also activate JNK via ASK1/MKK7, inhibiting Bcl-2 and promoting apoptosis (Jin and El-Deiry, 2005; Van Herreweghe *et al.*, 2010).

Although cardiomyocytes are usually resistant to Fas-induced apoptosis, recently studies indicate that cardiomyocyte apoptosis caused by DOX can be executed through a Fas mediated pathway. Similarly, Kalivendi *et al.*, 2005) showed that DOX treatment of rat cardiomyocytes increased mitochondrial ROS production, activated the calcium/calcineurin signaling pathway, and consequently activated nuclear factor-activated T cell-4 (NFAT4), leading to up-regulation of Fas/FasL.

1.4.2. Intrinsic Apoptotic Pathways

The intrinsic pathway is initiated following intrinsic signals including DNA damage induced by irradiation or chemicals, and exposure to certain chemotherapeutic agents. This pathway is characterized by permeabilization of the outer mitochondrial membrane (OMM), which leads to the release of pro-apoptotic factors from the IMS into the cytosol. Mitochondrial integrity and the intrinsic pathway are controlled by the evolutionarily conserved B-cell lymphoma-2 (BCL-2) protein family. The pro-apoptotic Bcl-2 proteins, Bad, Bid, Bax and Bim translocate to mitochondria following death stimuli, promoting the release of cytochrome c to the cytoplasm. Consequently, cytosolic cytochrome c binds to apoptosis protease-activating factor 1 (APAF-1) and procaspase-9, generating an intracellular DISC-like complex known as “apoptosome”, where caspase-9 is activated, and subsequently process caspase-3. The two pathways of apoptosis, extrinsic/death receptor and intrinsic/mitochondrial, converge on caspase-3, and subsequently on other proteases and nucleases conducting the terminal events of programmed cell death (Jin and El-Deiry *et al*., 2005; Parsons and Green, 2010).

As described in Figure 6, cytochrome *c* is required for formation of the apoptosome and activation of caspase-9, thus, without MOMP and the release of cytochrome *c* from the IMS, caspase-9 activation and subsequent activation of

downstream effector caspases does not occur. However, another protein, second mitochondria-derived activator of caspase/direct IAP-binding protein with low pI (Smac/DIABLO) also contributes to caspase activation by neutralizing inhibitor of apoptosis proteins (IAPs) which binds to and prevents caspase-9 activity, as well as their downstream effectors (Brenner and Mak *et al.*, 2009). Following an apoptotic stimuli, the effector molecules Bak and Bax undergo conformational changes that trigger the formation of homo-oligomers in the OMM. Bak and Bax homo-oligomers form pores in the OMM through where IMS proteins, including cytochrome c, SMAC/DIABLO, the Apoptosis-Inducing Factor (AIF), Endonuclease G (EndoG) and Omi/HtraA2 (Pradelli *et al.*, 2010), translocate to the cytosol and initiate the apoptotic signaling process. Besides the translocation during apoptosis, translocation and oligomerization of Bax are central events. However, the mechanism for recruitment of Bax to intracellular organelles is not fully understood. Activated following DNA damage, p53 induces the transcription of Bax, Noxa and Puma. Emerging experimental evidence has shown that BH3-only proteins, such as Bid and Bim, could activate Bax directly or indirectly (Liu *et al.*, 2011).

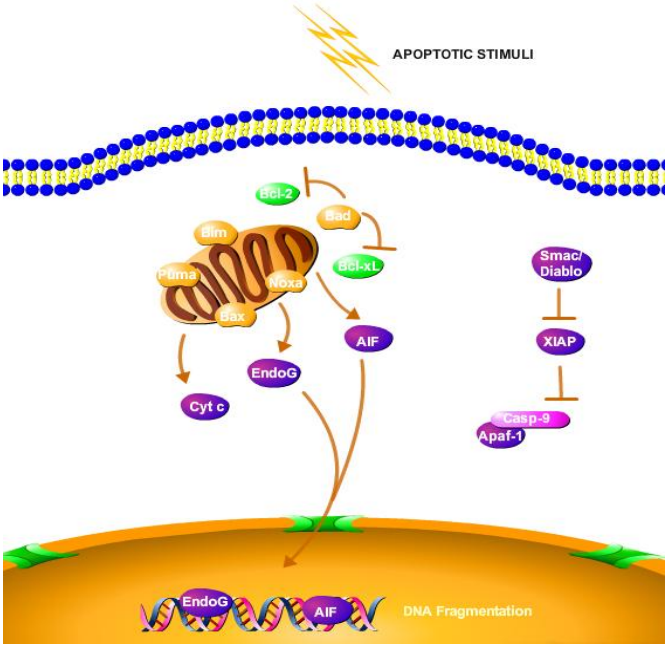

Figure 6. The Mitochondrial role in apoptosis. ROS and calcium overload are two possible apoptotic stimuli that can lead to mitochondrial membrane permeabilization (MMP). After MMP, the mitochondrial intermembrane space (IMS) protein cytochrome *c* (Cyt *c*) and other pro-apoptotic factors such as Apoptosis Inducing Factor (AIF) and Endonuclease G (EndoG) are released into the cytosol. AIF and EndoG can trigger cell death without activating the caspase cascade. On the other hand, cytochrome c interacts with the adaptor protein apoptotic peptidase activating factor 1 (APAF-1), as well as with procaspase-9 to form the apoptosome. This sequentially activates caspase-9 and executioner caspases, such as caspase-3, ending with cell death. Second mitochondria-derived activator of caspase/direct inhibitor of apoptosis-binding protein with low pI (Smac/DIABLO) is also a proapoptogenic mitochondrial protein that is released to the cytosol in response to diverse apoptotic stimuli. In the cytosol, Smac/DIABLO interacts and antagonizes inhibitors of apoptosis proteins (IAPs), allowing the activation of caspases and consequent apoptosis.

Mitochondrial permeability mechanisms, as well as release of cytochrome c during apoptosis are not yet completely understood. However, Bcl-xl, Bcl-2, and Bax seem to also interact with the voltage-dependent anion (VDAC), which affect or regulate Cyt c release.

Several studies have shown that DOX-induced cardiomyocyte apoptosis is associated with increased expression and activation of p53 tumor suppressor protein.

DNA lesions induced by ROS or directly by DOX activated ERK1/2, followed by increased phosphorylation of p53. p53 downstream genes such as Bax, are then expressed inducing the intrinsic apoptosis pathway (L'Ecuyer *et al.*, 2006, Liu *et al.*, 2008b).

1.4.3. Caspase-Independent Mechanisms

Intermembrane mitochondrial proteins, such as EndoG and AIF have been suggested as the main effectors in nuclear DNA fragmentation independently of caspase recruitment (Gupta, 2001). EndoG is compartmentalized in the IMS of healthy cells (Lee *et al.*, 2005). Mammalian EndoG is synthesized as an inactive 32 kDa pro-peptide. The mitochondrial signal peptide is cleaved off by an unknown proteinase upon entering the mitochondria and the mature active 27 kDa EndoG can be released from mitochondria during apoptosis (Lee *et al.*, 2005). When released from mitochondria, this protein migrates to the nucleus where it attacks nuclear DNA being another protein with an important function in both cell life and death (Burhans and Weinberger, 2007).

AIF is a flavoprotein with a molecular mass of 57 kDa consisting of three structural domains: FAD-binding domain, NAD-binding domain and C-terminal domain. This protein has NADH oxidase activity and is normally contained in the mitochondrial intermembrane space or loosely associated with the inner mitochondrial membrane (Susin *et al.*, 1999; Sevrioukova, 2011). AIF was one of the first proteins shown to be released from mitochondria during apoptosis. AIF translocation from mitochondria into nucleus promotes apoptosis and seems to play a crucial role during caspase-independent apoptotic cell death (Cande *et al.*, 2004). AIF can translocate to the cytoplasm with the thought MPTP complex (Daugas *et al.*, 2000) or through pores formed by pro-apoptotic Bcl-2 family members Bax, Bak, and Bid (Landshamer *et*

al.,2008). When released from mitochondria, AIF acts as death effector, migrating to the nucleus in a PARP-dependent manner, inducing chromatin condensation and large-scale DNA fragmentation resulting in 50 kbp fragments in a caspase-independent manner, as seen in Figure 7 (Susin *et al.*, 2000).

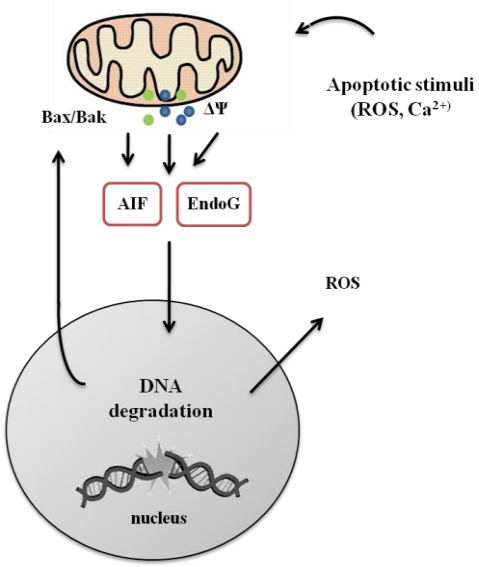

Figure 7. Caspase-independent mechanisms. The pro-apoptotic proteins AIF and EndoG are released from mitochondria due an apoptotic stimulus (ROS or DOX, for example). Translocation from mitochondria to the nucleus promotes apoptosis and seems to play a crucial role in apoptotic cell death. Once in the nucleus, AIF and EndoG induce chromatin condensation and large-scale DNA fragmentation, increasing ROS production. Due to DNA fragmentation, p53 can be activated and act as a transcription factor promoting an increase in Bax and Bak expression. Bax/Bak is translocated to mitochondrial membranes producing Bax clusters, which interfere with mitochondrial integrity and cell death.

Two isoforms have been described for their role in AIF translocation: PARP-1, whose activation leads to excessive consumption of cytoplasmic NAD and AMP generation, contributing to mitochondrial depolarization and, consequently, translocation of AIF (Formentini *et al*., 2009; Vosler *et al*., 2009), as well as PARP-2, that contributes to nuclear translocation of AIF via PAR accumulation (Li *et al*., 2010). However, none of the AIF effects can be prevented by addition of Z.VAD.fmk, a

caspase inhibitor, which can be used to confirm that AIF acts through caspase-independent mechanism (Susin *et al*., 2000).

1.4.4. The Apoptotic Role of p66Shc

Src homolog and collagen homolog proteins (Shc) are widely known to serve as adaptor proteins in receptor protein tyrosine kinase (RTK) signaling with three main isoforms: p66Shc, p45Shc and p52Shc. p66Shc is a 66 kDa proto-oncogene, known as receptor tyrosine kinase signaling mediator and recently identified to be as sensor to oxidative stress-induced apoptosis and as a longevity protein in mammals (Ravichandran, 2001). This isoform is transcribed from a promoter in the first intron of Shc locus. It contains four functional domains, a SH2 domain (~100 amino acids) at the COOH-terminal that mediates the formation of multiprotein complexes during signaling and a PTB binding domain, which is separated by a collagen homology (CH1) domain, enriched in proline and glycine residues and contains the essential tyrosine phosphorylation sites (Yoshida *et al.*, 2004). This isoform also carries a cytochrome c-binding region within the CH2-PTB domains which is primarily implicated in mitochondrial regulation of oxidative stress (figure 8) (Giorgio *et al.*, 2005).

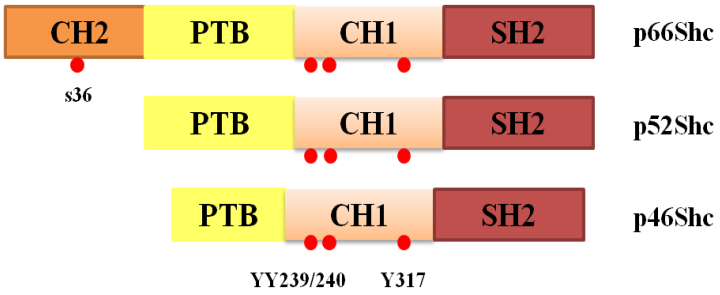

Figure 8. Schematic organization of Shc protein. All the Shc isoforms contains three functional domains: a SH2 domain at the COOH-terminal, a PTB binding domain, which is separated by a collagen homology (CH1) domain. p66Shc also contains a CH2-PTB domain that can be phosphorylated on serine 36 (adapted from Yoshida *et al*., 2010).

Several hypotheses have been proposed in order to describe the signaling pathways involving p66Shc. One idea proposes that p66Shc is translocated to mitochondrial intermembrane space in response to oxidative stress promoted by the activation of the protein kinase C (PKC β), a critical regulator of cell proliferation, survival, and cell death. PKC β seems to induce the phosphorylation of p66Shc on Ser 36 which is then recognized by the prolyl isomerase Pin1 that catalyzes its cis-trans isomerization. Subsequently, p66Shc is dephosphorylated by type 2 protein serine/threonine phosphatase (PP2A) and imported in the mitochondria where it would bind to cytochrome c and act as a oxireductase, increasing ROS levels and promoting apoptosis (Figure 9) (reviewed in Raffaello and Rizzuto, 2011). ROS are not only the final result of the oxidative stress accumulated during aging, but they are believed to play a significant role regulating different signaling pathways.

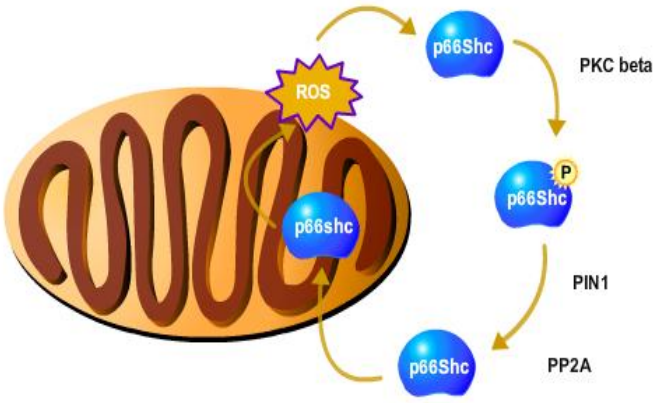

Figure 9. Protein p66Shc signaling pathway. Upon some cellular stress (ROS, Ca^{2+}) PKC β is activated and phosphorylates p66Shc on Ser 36. This modification allows the recognition and the binding of Pin1 that isomerizes p66Shc. As a consequence, p66Shc is dephosphorylated by PPA2 and imported into mitochondria where it binds to cytochrome c and acts as an oxidoreductase. Thus, activation of p66Shc induces ROS overgeneration and ageing (adapted from Raffaello and Rizzuto, 2011). Nevertheless, more recent results appear to suggest that p66Shc does not neter the mitochondrial matrix.

More recent data appears to suggest that p66Shc does not enter mitochondria, remaining associated with the outer membrane, thus excluding interaction with cytochrome c in the IMS (Lebiedzinska *et al*., 2010; Wieckowski *et al*., 2009).

p66Shc is primarily expressed in epithelial cells (Migliaccio *et al.*, 1997), hematopoietic cell lines and peripheral blood lymphocytes, and its expression varies in breast (Stevenson and Frackelton, 1998, Jackson *et al.*, 2000) and prostate cancer cell lines (Veeramani *et al.*, 2008). The expression of these adaptor proteins, especially p66Shc, is regulated by steroid hormones that play a distinct role in the regulation of tumor development, cancer cell proliferation, progression, and metastatic processes of major types of cancers (Henderson and Feigelson, 2000). For example, there is a direct correlation between the protein level of p66Shc and prostate cancer cell proliferation, demonstrating the importance of p66Shc adaptor protein in the tumorigenicity of human prostate cancer (Lee *et al.*, 2004, Veeramani *et al.*, 2008). In ovarian carcinoma cell lines, p66Shc protein level positively correlates with ErbB-2 expression, a prognostic marker for ovarian cancer (Kumar *et al.*, 2011).

Accumulation of oxidative cellular damage caused by ROS is apparently an important component of ageing (Vigneron and Vousden, 2012). In agreement, mutations and deletions of both nuclear and mitochondrial DNA are common phenomena in aged mammals (Lee and Wei, 2007). The oxidative stress theory of ageing, from which the mitochondrial theory of ageing resulted, is based around the idea of a vicious cycle, in which somatic mutations of mitochondrial DNA (mtDNA) triggers respiratory chain dysfunction leading to increased ROS production and in turn to the accumulation of further mtDNA mutation (reviewed in Raffaello and Rizzuto, 2011). It has been shown that mitochondria not only represent the major source of ROS production but are also the major targets of their damaging effects. One functional role

of Shc proteins is in regulation of redox signaling, thus playing a prominent role in oxidative stress-induced apoptosis and in life span. Indeed, despite the fact that p66Shc expression decreases in mice with advanced age (Pinton and Rizzuto, 2008). However, the amount of p66Shc phosphorylated at Ser 36, significantly increases with age, resulting in higher free radical production and, subsequently accumulation of oxidative damages (Lebiedzinska *et al.*, 2009).

On the other hand, Zhang *et al.*, (2010) have found overexpression of p66Shc in senescent cells, which was consistent with prior observations that an increased expression of p66Shc is associated with cellular senescence in bovine fibroblasts (Favetta *et al*., 2004).

The increased ROS production by mitochondria, as a response to p66Shc phorphorylation and possible translocation, seems to increase the probability of mitochondrial permeability transition pore opening, and consequently, release of pro-apoptotic cofactors into the cytoplasm (Orsini *et al*., 2004). This explains how p66Shc is connected with oxidative damages, apoptosis and ageing.

Some authors described that cytosolic p66Shc is phosphorylated and translocated to mitochondria through the interaction with TOM/TIM (transporter outer membrane/transporter inner membrane) import complex and mitochondrial heat shock protein mtHsp70, where it associates to cytochrome c acting as an oxidoreductase, thus generating ROS (Orsini *et al.*, 2004). Moreover p66Shc was also shown to be an essential downstream target of p53 stress induced elevation of oxidants, cytochrome c release, and apoptosis (Trinei *et al*., 2002). Mitochondrial respiration generates hydrogen peroxide (H_2O_2) through dismutation of superoxide anion, by directly transferring electrons from cytochrome c to molecular oxygen (Giorgio *et al.*, 2007) which in turn, induces opening of MPTP and cellular apoptosis. Intracellular ROS

levels and oxidation-damaged DNA are significantly reduced in p66Shc-/- primary cultures and shows enhanced resistance to apoptosis, whereas overexpression of p66Shc increases the sensitivity to apoptosis. Overexpression of p66Shc increases ROS production while its ablation is sufficient to decrease their levels (Trinei *et al.*, 2002). p66Shc knockout mice are resistant to oxidative stress, showing a 30% increase in average lifespan (Hu *et al.*, 2007).

Although several aspects of p66Shc signaling are still unexplored, one attractive hypothesis is that an over-activation of p66Shc signaling may result in long-term persistence of mitochondrial stress.

1.4.5. FoxO Transcription Factors and p66Shc

Forkhead transcription factors are a superfamily of proteins firstly found in *Drosophila Melanogaster* and whose primary function is to act as transcription factors in the nucleus and bind as monomers to their cognate DNA targeting sequences (Carlsson *et al*., 2002). This protein superfamily shares a conserved 100-residue DNA binding domain, the forkhead (FKH) domain, as seen in Figure 10 (Kaestner *et al*., 2000). In mammals four isoforms of the FoxO transcription factor family can be found: FoxO1, FoxO3, FoxO4 and FoxO6. All of them belong to the most divergent subfamily because of sequence differences within their DNA-binding domains (Wijchers *et al*., 2006).

FoxO proteins can regulate several mechanisms including apoptosis, cell cycle transitions, DNA repair, cell differentiation, glucose metabolism, longevity, as well as oxidative stress (Barthel *et al*., 2005; Greer and Brunet, 2005). For example, FoxO proteins are involved in transactivation of Bim, a gene that encodes a member of the pro-apoptotic BH3-only subgroup of BCL-2 family proteins during apoptosis (Stahl *et*

al., 2002). However, FoxO proteins can induce cell death through mitochondria-dependent and independet mechanisms (Modur *et al*., 2002).

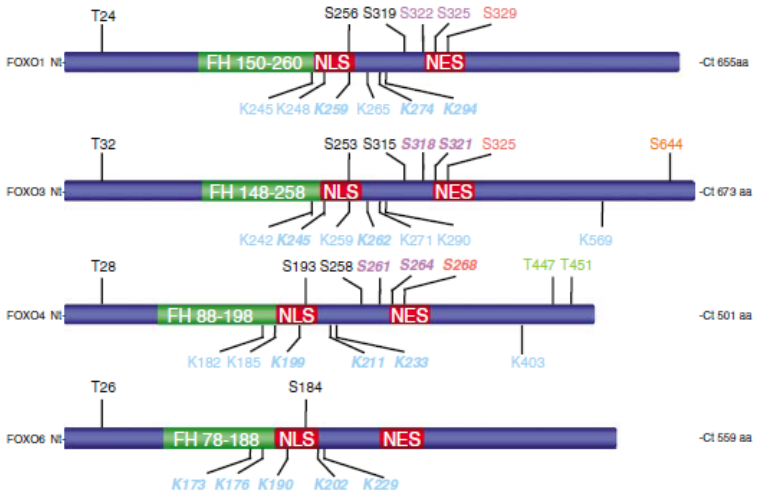

Figure 10. FoxO family structure and sites of phosphorylation. The subfamily members FoxO1, FoxO3, FoxO4 and FoxO6 as FoxO transcription factors are regulated by phosphorylation and acetylation in response todifferent stimuli: insulin, growth factors or stress stimuli. According with their post-translational modifications, FoxO subcellular localization is different. Other effects include FoxO degradation, DNA-binding ability, transcriptional activity, or protein–protein interactions (adapted from Greer and Brunet, 2005).

FoxO isoforms are also involved in signaling as a response to growth factor stimulation and oxidative stress through PI3K/Akt signaling pathway (Biggs *et al*., 1999). For instance, FoxO1, FoxO3 and FoxO4, are critically regulated by Akt-dependent phosphorylation at three specific sites in response to growth factor and insulin stimulation (Thr 32, Ser 253 and Ser 315 for human FoxO3). Furthermore, some other signaling pathways can directly regulate FoxO activity: the stress-activated Jun-N-terminal kinase (JNK), the mammalian ortholog of the Ste20-like protein kinase (MST1) and the deacetylase Sirt1 (Brunet *et al*., 2004; Essers *et al*.,2004; Lehtinen *et al*., 2006). In response to insulin or growth factors, FoxO is exported from the nucleus to the cytoplasm in an Akt-dependent phosphorylation process. When phosphorylated,

FoxO factors will remain in the cytoplasm and transcriptional function is repressed (Brunet *et al*., 1999; Essers *et al*., 2004). In the presence of growth factors or insulin, FoxO-dependent transcription is inhibited promoting cellular proliferation and survival, but also rendering the cell sensitive to oxidative damage (Figure 11). However, upon oxidative or nutrient stress stimuli several proteins can induce the phosphorylation, acetylation and monoubiquitination of FoxO factors at a number of regulatory sites by factors such as AMPK (AMP-dependent kinase), JNK (Jun-N-terminal kinase), MST1 and CBP (CREB binding protein (Brunet *et al*., 1999). FoxO factors translocate to the nucleus binding to the deacetylase Sirt1 and promoting gene transcription (Figure 11).

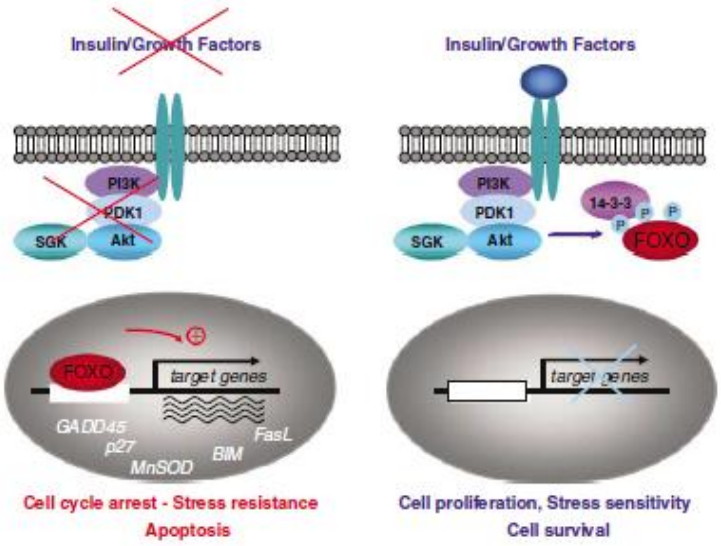

Figure 11. Regulation of FoxO factors in the presence or absence of insulin or growth factors. In the presence of insulin or growth factors, FoxO factors are negatively regulated. The PI3K-Akt/SGK is activated and promotes FoxO phosphorylation on three conserved residues promoting their export from the nucleus through binding with the chaperone 14-3-3 and FoxO sequestration on the cytoplasm. This negative regulation allows cells to become more sensitive to ROS, but also leads to proliferation and cell survival (A). In the absence of insulin or growth factors FoxO factors are translocated into the nucleus where they promote gene transcription of key target genes involved in apoptosis and cell cycle arrest: MnSOD (manganese superoxide dismutase), Bim (pro-apoptotic Bcl2-.interacting mediator of cell death), FasL (Fas ligand), p27 (cyclin-dependent kinase inhibitor) and GADD45 (growth arrest- and DNA damage-inducible gene 45 α). Adapted from Greer and Brunet, 2005.

Some FoxO downstream targets include the manganese superoxide dismutase (MnSOD), FasL, p53 and the pro-apoptotic Bcl2-interacting mediator of cell death Bim (Nemoto and Finkel *et al*., 2002). Genes involved in cell-cycle arrest, the growth arrest and DNA damage-inducible gene 45 α (Gadd45 α) and the cyclin-dependent kinase inhibitor (p27), were also reported as being downstream targets for FoxO factors (Van der Horst *et al*., 2004). Depending on the post-translational modification (phosphorylation, acetylation and mono/polyubiquitination) the subcellular localization of FoxO is altered, as well as protein stability, DNA binding properties, and transcriptional activity (Rena *et al*., 2002).

One of FoxO isoforms, FoxO3a is particularly highly expressed in brain, spleen, heart, and ovaries. Loss of FoxO3a transcriptional activity leads progenitor cells or tumor cells resistant to the cytostatic effects of extracellular effectors such as TGFβ, which may contribute to tumor development (Gomis *et al*, 2006).

Recently, a link between p66Shc and FoxO3a has been suggested. In this mechanism, phosphorylation on serine 36 seems to play a crucial role regulating FoxO3a phosphorylation (Nemoto and Finkel, 2002). p66Shc may act in a redox-dependent pathway that sensitizes cells to pro-apoptotic stimuli by activating Akt, phosphorylating/inactivating FoxO transcription factors, and preventing the induction of free radical scavenging genes (Kisielow *et al*., 2004). However, this is a different mechanism from the Akt-FoxO inactivation pathway recruited by trophic factor.

Chahdi and Sorokin (2008), reported that FoxO3a phosphorylation requires p66Shc phosphorylation in an Akt-independent mechanism, and that both p66Shc and FoxO3a are physically interacting in a model of SV40-transformed human mesangial cells (HMCs). For instance, p66Shc phosphorylated on serine 36 seems to FoxO3a phosphorylation and cytoplasmatic localization appears to occur. The importance on

this interaction is more evident when oxidative stress no longer stimulates phosphorylation of FoxO3a in p66Shc deficient cells.

1.5. Investigating DOX-Induced Cardiotoxicity - H9c2 as a Model for Cardiac Cells

In vivo models of DOX-induced cardiomyopathy and *in vitro* studies using different cell lines have been widely reported in the literature (L'Ecuyer *et al*., 2001). The myoblastic cell line H9c2 (Kimes and Brandt, 1976) has been extensively used as an *in vitro* model to study morphological and biochemical alterations induced by DOX treatment (Sardão *et al*., 2007). This cell line retains both skeletal and cardiac tissues properties, showing similar electrophysiological and biochemical properties to adult cardiomyocytes (Hescheler *et al*., 1991). H9c2 cells have been considered as a proper model to study molecular responses of the cardiomyocyte to oxidative damage, intracellular DOX degradation, DNA damage induced by DOX, p53 activation or even to study the protective effect of different compounds such as carvedilol and resveratrol, known for their cardioprotective function (Oliveira *et al.*, 2004; Danz *et al.*, 2009; Kweon *et al.*, 2010). Sardao *et al.*, (2009b) reported that DOX treatment causes morphological alterations in mitochondrial, nuclear, and fibrous protein structures in H9c2 cells. Also DOX treatment results in increased mitochondrial apoptotic signaling in H9c2 cells which is secondary to p53 activation and occurs through Bax-mediated effects (Sardao *et al.*, 2009a).

CHAPTER 2 – OBJECTIVES

A major limitation of doxorubicin administration is a dose-related cardiomyopathy, which can lead to congestive heart failure which is thought to occur due to several mechanisms including the overgeneration of reactive oxygen species (Mross *et al*., 2006). One of the critical aspects of DOX-induced cardiotoxicity is a dose-dependent and persistent toxicity which can lead to the development of a characteristic cardiomyopathy occurring often decades after treatment.

Our hypothesis for the present work is that DOX causes an activation of the p66Shc signaling pathway which leads to a progressive deterioration of mitochondrial function. The signaling mechanism of p66Shc on doxorubicin-induced cell death has never been explored before, and so our work is very relevant for the mechanisms of DOX toxicity and its implication in clinical therapies.

In the present work we investigate p66Shc signaling, including phosphorylation on serine 36, using as a model the myoblastic cell line, H9c2. In this particular research, we intend to investigate the initial step of what we believe is a feedback loop that leads to the progression and persistence of DOX-induced cardiotoxicity. Hence, we investigated whether DOX activates p66Shc signaling in H9c2 myoblasts.

The role of the Forkhead transcription factor (FoxO3a) family, reported as an inducer for the transcriptional activity of target genes responsible for apoptosis and cell cycle arrest, has also been studied in our cell model. Since FoxO3a is highly expressed in heart (Salih and Brunet, 2008), a possible link between p66Shc protein and FoxO3a was studied. We also hypothesize that p66Shc is physically interacting with FoxO3a in a stress-dependent pathway contributing for the mitochondrial dysfunction and cell death during DOX treatment.

CHAPTER 3 – MATERIAL & METHODS

3.1. Reagents

Dulbecco`s modified Eagle`s medium (DMEM), penincilin, streptomycin, fetal bovine serum (FBS) and Trypsin were purchased from Gibco-Invitrogen (Grand Island, NY). Hispidin, doxorubicin, dithiothreitol (DTT), Phenylmethanesulfonyl fluoride (PMSF), protease inhibitor cocktail (leupeptin, antipain, chymostatin, and pepstatin A), sulforhodamine B (SRB) were obtained from Sigma (St. Louis, USA). Goat polyclonal anti-p53 antibody were purchased from Santa Cruz (Santa Cruz, CA). Mouse monoclonal anti-AIF, rabbit monoclonal anti-Bax, rabbit monoclonal anti-Bim, rabbit anti-Akt and rabbit anti-phospho Akt (Ser 473) antibodies were purchased form Cell Signaling (Danvers, MA). Rabbit polyclonal anti-FoxO3a, rabbit polyclonal anti-FoxO3a (phospho Ser 253) and rabbit polyclonal anti-Superoxide dismutase 2 were purchased from Abcam (Cambridge, UK). Mouse monoclonal anti-SHC was purchased from BD Biosciences (Woburn, MA). Mouse monoclonal anti-Shc/p66 (Ser 36) was purchased from Calbiochem (Merck, Darmstadt, Germany). Mouse polyclonal Cytochrome c was purchased from BD Farmingen (San Diego, CA). Secondary antibody Fluorescein (FITC) anti-Mouse IgG and alkaline phosphatase (AP)-conjugated were purchased from Jackson ImmunoResearch Laboratories, Inc. (Cambridgeshire, UK). DOX was dissolved in miliQ water at a stock solution of 25 mM.

3.2. Cell Culture and Treatments

The H9c2 cell line was purchased from America Tissue Type Collection (Manassas, VA; Catalog # CRL – 1446). Cells were cultured in DMEM medium supplemented with 1,5 g/L sodium bicarbonate, 10% fetal bovine serum, 100U/ml of penincilin and 100 µg/ml of streptomycin in 150 cm^2 tissue culture flasks at 37 ºC in a humidified atmosphere of 5% CO_2. H9c2 cells were treated with 0.5 µM and 1 µM DOX for 24

hours or 48 hours, according to the assay. In the experiments performed with Hispidin, the compound was added to the cells in a concentration of 5 µM or 10 µM four hours prior to DOX treatment. For immunocytochemistry, cells were seeded on glass coverslips at a density of $3.5x10^5$ cells/well in six well plates containing coverslips (final volume of 2 ml per well). For sulforhodamine B assay cells were also seeded at $3.5x10^5$ cells/well in 24well-plates at a final volume of 1 ml per well.

3.3. Cytotoxicity and Cell Density Evaluation by Sulforhodamine B (SRB) Assay

The sulforhodamine B (SRB) assay, a colorimetric method used for cell density determination, is based on the measurement of cellular protein content (Houghton *et al*., 2007). The dye binds to basic aminoacids of cellular proteins mass which is related to cell number. H9c2 cells ($3.5x10^3$ cells/well) were seeded in 24 well plates and at specific time points, the incubation media was removed and cells were fixed in 1% acetic acid in ice-cold methanol for at least 30 minutes. Cells were then incubated with 0.5 % (wt/vol) SRB dissolved in 1% of acetic acid for 1h at 37ºC. The unbound dye was removed with 1% acetic acid solution. Dye bound to cell proteins was extracted with 10 mM Tris base solution, pH 10, and the optical density of the solution was determined at 540 nm. Results were expressed as a percentage of time zero (first time point harvested after cell attachment, 24 hours after seeding). This assay was performed in order to evaluate the cytotoxic effects of DOX and Hispidin.

3.4. Collection of Total, Cytosolic, Mitochondrial and Nuclear Extracts from H9c2 Cells

To obtain total cellular extracts, H9c2 cells were harvested by trypsinization after treatments and washed once with PBS. In order to collect total cells (attached and floaters), two centrifugation steps were performed for 5 minutes at 1000xg. Cellular

pellet was resuspended in collecting buffer (20 mM HEPES/NaOH, pH 7.5, 250 mM Sucrose, 10 mM KCl, 2 mM MgCl2, 1 mM EDTA) supplemented with 2 mM dithiothreitol (DTT), 100 µM phenylmethylsulfonyl fluoride (PMSF) and a protease inhibitor cocktail (containing 1 µg/ml of leupeptin, antipain, chymostatin and pepstatin A) and ruptured by 30 passages 27-gauge needle. The cell suspension was then kept at -80 ºC until used. For subcellular fractionation, cells were harvested as described above and resuspended in homogenization buffer (250 mM sucrose, 20 mM K+ Hepes pH 7.5, 10 mM KCl, 1.5 mM MgCl2, 0.1 mM EDTA, 1 mM EGTA) supplemented with 1 mM DTT, 100 µM PMSF and protease inhibitor cocktail (containing 1 µg/ml of leupeptin, antipain, chymostatin and pepstatin A). Cells were incubated on homogenization buffer for 15 min on ice. Cells were then transferred to a pre-cooled tissue homogenizer and homogenized 30 times using a tight pestle. The homogenized cells were centrifuged at 217xg for 5 min at 4ºC. The pellet was discarded and the supernatant was centrifuged again at 14000 xg for 15 min at 4º C. The pellet, containing the mitochondrial fraction was resuspended in 50 µl of homogenization buffer. Mitochondrial fractions were stored at -80 ºC until used. For cytosolic and nuclear extraction, the K266-100 Nuclear/Cytosol Fractionation kit from Biovision was used. Protein contents were determined using the Bradford assay (Bradford M.M, 1976).

3.5. Western Blott Analysis

After denaturation at 95°C for 5 min in a Laemmli buffer (from BioRad), equivalent amounts of proteins (25 µg) were separated by electrophoresis in 8% or 12% SDS-polyacrylamide gels (SDS-PAGE) and electrophoretically transferred to apolyvinylidene difluoride (PVDF) membrane for 90 min at 100 V. After blocking membranes with 5% milk in TBST (50 mM Tris-HCl, pH 8; 154 mM NaCl and 0.1% Tween 20) for 2 hours at room temperature, membranes were incubated overnight at

4°C with the respective antibodies (Table 1). Membranes were washed and incubated with the secondary goat anti-mouse IgG (1:2500) and goat anti-rabbit IgG (1:2500) antibodies. Membranes were incubated with the ECF detection system (from GE Healthcare, Piscataway, NJ) and imaged with Versa Doc imaging system (Bio-Rad, Hercules, CA). Densities of each band were calculated with Quantity One Software (Bio-Rad). Membranes were also stained with Ponceau reagent to confirm equal protein loading in each lane.

Table 1 - Primary and secondary antibodies used for Western Blotting experiments.

PRIMARY ANTIBODIES	DILUITION	HOST	SUPPLIER
AIF	1:1000	Mouse	Cell signaling (#4642)
Akt	1:1000	Rabbit	Cell Signaling (#9272)
Akt-p (Ser 473)	1:1000	Rabbit	Cell Signaling (#9271)
Bax	1:2000	Rabbit	Cell Signaling (#2772)
Bim	1:1000	Rabbit	Cell Signaling (#2819)
Cyt c	1:1000	Mouse	BD Farmigen (#556433)
FoxO3a	1:1000	Rabbit	Abcam (#ab4709)
FoxO3a-p (Ser 253)	1:1000	Rabbit	Abcam (#ab47285)
p53	1:1000	Rabbit	Cell signaling (#2524)
p66Shc	1:1000	Mouse	BD Biosciences (#610879)
p66Shc-p (Ser 36)	1:1000	Mouse	Calbiochem (#566807)
SOD2	1:5000	Rabbit	Abcam (#ab13533)

3.6. Immunocytochemistry (ICC)

H9c2 cells were seeded on glas coverslips in six-well plates and incubated with 0.5 µM DOX and 1 µM DOX. Thirty minutes before the treatment was over, cells were incubated with Mitotracker Red (125 nM) at 37 ºC in the dark. Cells were then washed with cold PBS and fixed with 4% paraformaldehyde for 15 minutes at room temperature. Cells were rinsed with PBS, blocked with 1% milk in PBS-T during one hour at 37 ºC cells and probed with the respective antibody solution overnight at 4°C (Table 2). After that, cells were incubated with the respective secondary antibody (FITC-conjugated anti-mouse or anti-rabbit antibody) for 2 hours at 37 ºC. Between the primary and the secondary antibodies, cells were rinsed 3 times with PBST during 5minutes each. Coverslips were mounted on glass slides. Cells were observed under a Zeiss LSM 510Meta confocal microscope. Images were obtained through LSM Image Browser.

Table 2 - Primary antibodies used for Immunocytochemistry experiments.

PRIMARY ANTIBODIES	DILUITION	HOST	SUPPLIER
p66Shc	1:250	Mouse	BD Biosciences (#610879)
FoxO3a	1:250	Rabbit	Abcam (#ab47409)

3.7. Caspase-3 and 9-like Activity

The activity of caspase-3 and -9 was analyzed in total cellular extracts collected with the following conditions: control, 1 µM DOX, 5 µM Hispidin and10 µM Hispidin. Cells were also treated with 5 µM and 10 µM of Hispidin and four hours later DOX was

added for 24 and 48 hours more, respectively. After treatment, cells were harvested by tripsinization and washed once with PBS. Floating cells were also collected and combined with adherent cells. In order to collect total cells, two centrifugation steps were performed for 5 minutes at 1,000xg. Cellular pellet was ressuspended in collecting buffer (HEPES/NaOH, pH 7.5, 250 mM Sucrose, 100 mM KCl, 2mM MgCl2, 1 mM EDTA) supplemented with 2 mM DTT, 100 µM PMSF and a protease inhibitor cocktail (containing 1µg/ml of leupeptin, antipain, chymostatin and pepstatin A) and kept at -80ºC. Protein contents were assayed using the Bradford method. Caspase-3 and -9 like activity was evaluated following the cleavage of the colorimetric substrate Ac-LEHD-pNA (purchased from Clabiochem). Extracts containing 25 µg and 50 µg of total protein were incubated in a reaction buffer, for caspase-3 and -9-like activity, respectively. Reaction Buffer containing 25 mM Hepes (pH 7.4), 10% Sucrose, 10 mM DTT, 0.1%, CHAPS and 100 µM caspase-3 or -9 substrate for 2 hours at 37 ºC was added. Caspase activity was determined following the detection of the chromosphore p-NA after cleavage from the labeled substrate Ac-LEHD-pNA. The method was calibrated with known concentrations of p-nitroanilide (purchased from Calbiochem) and the results are expressed as % pNa released.

3.8. Nuclear Chromatin Condensation

Nuclear morphology of cells was studied by using the cell-permeable DNA dye Hoechst 33342. Cells with homogeneously stained nuclei were considered to be normal, whereas the presence of chromatin condensation in non-mitotic cells was indicative of apoptosis. After Hispidin or DOX treatment, cells were washed twice with PBS, fixed with 2 ml of ice cold absolute methanol and stained with 1 µg/ml of Hoecsht 33342 for 30 minutes at 37ºC in the dark. Nuclear morphology changes were detected by using an epifluorescence Nikon Eclipse TE2000U microscope (UV filter). Two hundred cells

from several randomly chosen fields were counted and the number of apoptotic cells was expressed as a percentage of the total number of cells.

3.9. Imunoprecipitation (IP)

H9c2 cells were harvested by trypsinization and washed once with PBS. Floating cells were also collected. In order to collect total cells, two centrifugation steps were performed for 5 minutes at 1000xg. Cellular pellet was resuspended in collecting buffer (20 mM HEPES/NaOH, pH 7.5, 250 mM Sucrose, 10 mM KCl, 2 mM MgCl2, 1 mM EDTA) supplemented with 100 µM phenylmethylsulfonyl fluoride (PMSF), a protease inhibitor cocktail (containing 1 µg/ml of leupeptin, antipain, chymostatin and pepstatin A), N-Ethylmaleimide (NEM) 10 mM, Orthovanadate (NaVO 4) 10 mM, 10% SDS and 1% Triton X – 100). Antibody-immobilized beads were prepared by incubating p66Shc or Mouse IgG antibodies with 30 µl of Protein G PLUS-Agarose beads (Santa Cruz Biotechnology, CA), overnight at 4 ºC. The immobilized antibodies were incubated with 1 mg protein during 2 hours at 4 ºC, and the beads were washed five times (1 min centrifugations, 3 300 x g) at 4 ºC with wash buffer, supplemented as described for the lysis buffer. The final pellet, containing the immunoprecipitated p66Shc bound to the antibody-immobilized beads, was used for Western Blot analysis.

2.10. Statistical Analysis

Data are expressed as means±SEM for the number of experiments indicated in the legends of the figures. Double comparisons were performed by t-test. Multi comparisons were performed using one-way analysis of variance (ANOVA) followed by a Bonferroni post-hoc test. Significance was accepted with p value <0.05.

CHAPTER 4 - RESULTS

4.1. Doxorubicin Treatment Induces p66Shc Protein Upregulation

Alterations in p66Shc protein content induced by DOX treatment were analyzed by both immunocytochemistry and Western Blot assays (Fig. 12). For immunocytochemistry experiments (Fig. 12 A), control and DOX treated cells were fixed and labeled with an antibody against p66Shc. The results demonstrate an increase in p66Shc nuclear fluorescence intensity when cells were treated with DOX (both 0.5 and 1 µM) for 24 hours (data not shown) and 48 hours (Fig. 12 A). For Western Blot, H9c2 cells were treated with 0.5 and 1 µM DOX for 24 and 48 hours and total cellular extracts were collected, as described in the material and methods section. For total cellular extracts treated with DOX during 24 hours, an increase in p66Shc protein content is only statistically significant at 1 µM DOX, although a significant increase occurs for both DOX concentrations after 48 hours of incubation.

Cytosolic and nuclear fractions were also analyzed (Fig. 12 B). No changes were seen in cytosolic fractions during 24 hours treatment, but a significant increase occurs for 48 hours treatment at 1 µM DOX. Interestingly, p66Shc content increases within the nucleus for both time points used when cells were treated with 1 µM DOX. Phosphorylation of p66Shc on serine 36 was also analyzed in total cellular extracts by Western Blot. A significant decrease was observed for cells treated with 1 µM DOX during 48 hours (Fig. 13 A), but no changes occured for 24 hour treatment. Cytosolic and nuclear fractions were also analyzed. A significant decrease for 1 µM occurred after 24 and 48 hours treatment, in cytosolic fractions (Fig. 13B). A significant decrease also occurred after 24 hours treatment for 0.5 µM DOX. In nuclear fractions (Fig. 13C) a significant decrease was observed after 24 and 48 hours treatment for 1 µM DOX.

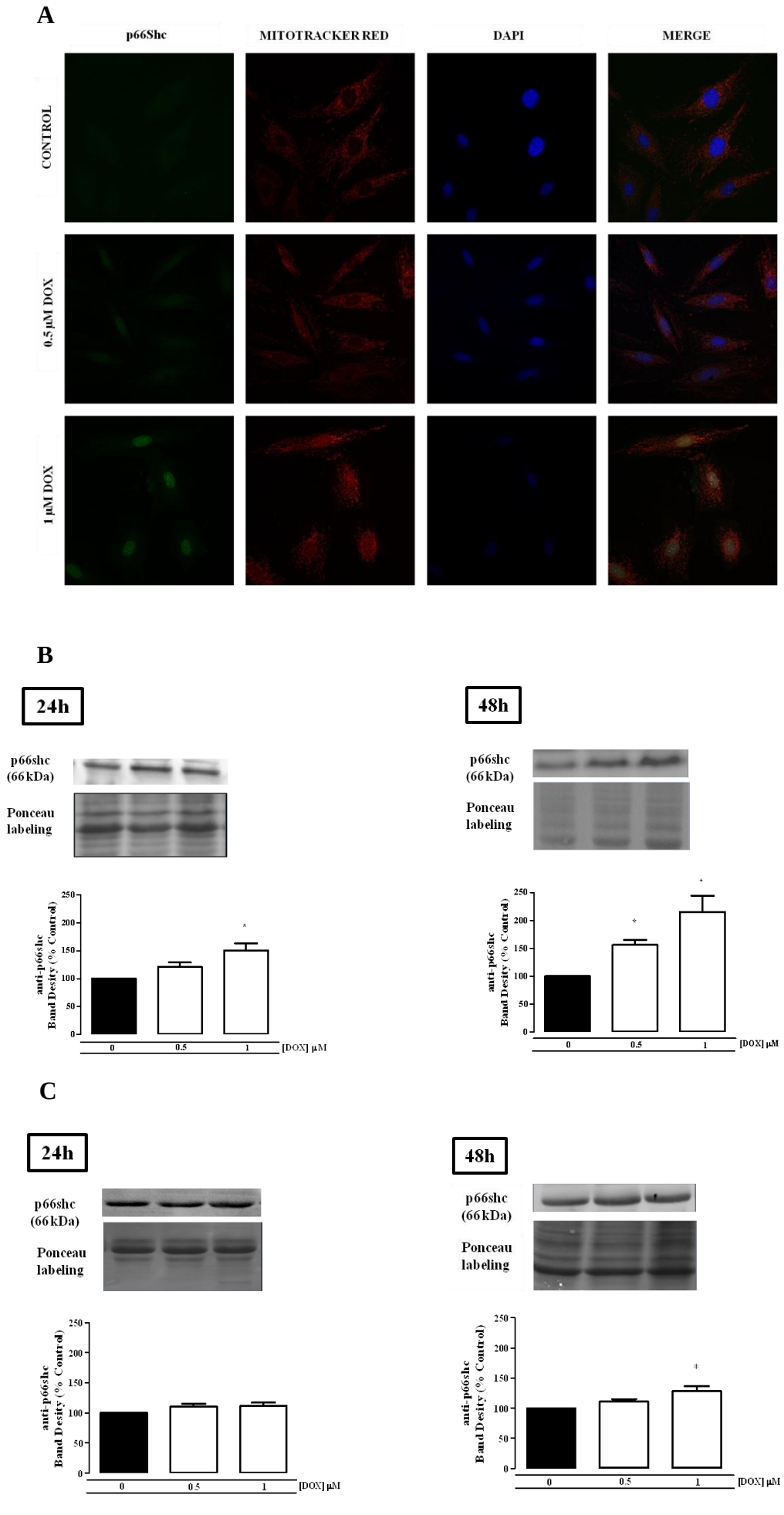
A
p66Shc
MITOTRACKER RED
DAPI
MERGE
CONTROL
0.5 µM DOX
1 µM DOX
B
24h
48h
p66shc (66kDa)
Ponceau labeling
anti-p66shc Band Desity (% Control)
[DOX] µM
C
24h
48h
p66shc (66kDa)
Ponceau labeling
anti-p66shc Band Desity (% Control)
[DOX] µM

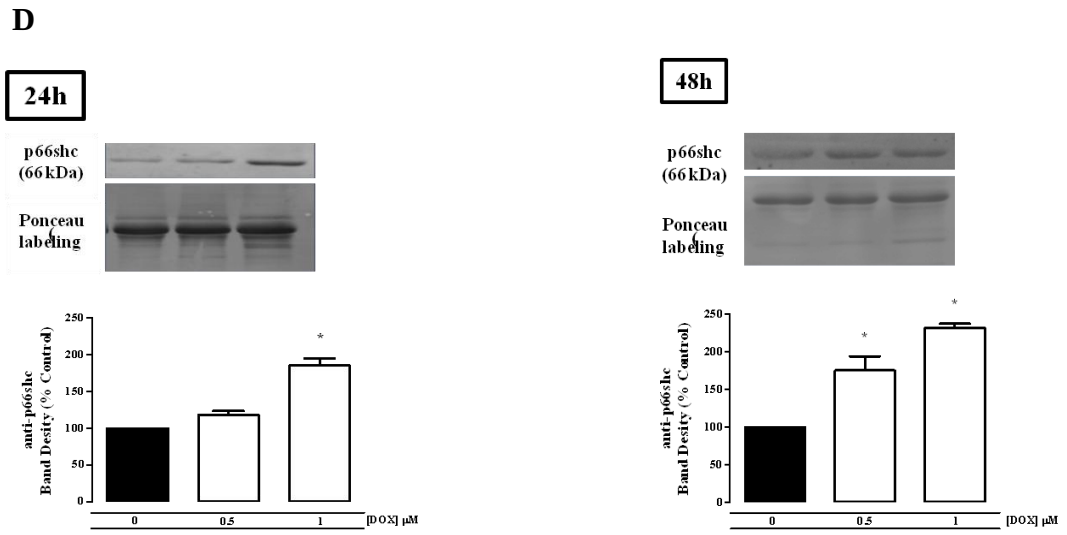

Figure 12. DOX treatment increases p66Shc content in H9c2 cells. (A) Confocal microscopy images of nuclei showing H9c2 cells treated with 0.5 and 1 µM DOX during 48 hours. After treatment, cells were incubated with mitotracker Red (red), fixed and labeled with an antibody against p66Shc (green). Cells were also counterstained with DAPI (blue), as described in the material and methods section. Confocal microscopy images show an increase in p66Shc in mitochondrial and nuclear compartments after DOX treatment. p66Shc content in total cellular extracts (B), cytosolic (C) and nuclear fractions (D) identified by Western Blot analysis as a protein band of 66 kDa. Cells were collected after treatment with 0.5 and 1 µM DOX for 24 and 48 hours treatment, as described in material and methods section. Images are representative experiments of four independent experiments. Ponceau labeling shows the loading of equal protein amount in each lane. Densitometric analysis of p66Shc protein, expressed as % of control. Data are expressed as means±SEM of four different experiments. Statistical analysis: *p < 0.05 compared with control for the respective time point.

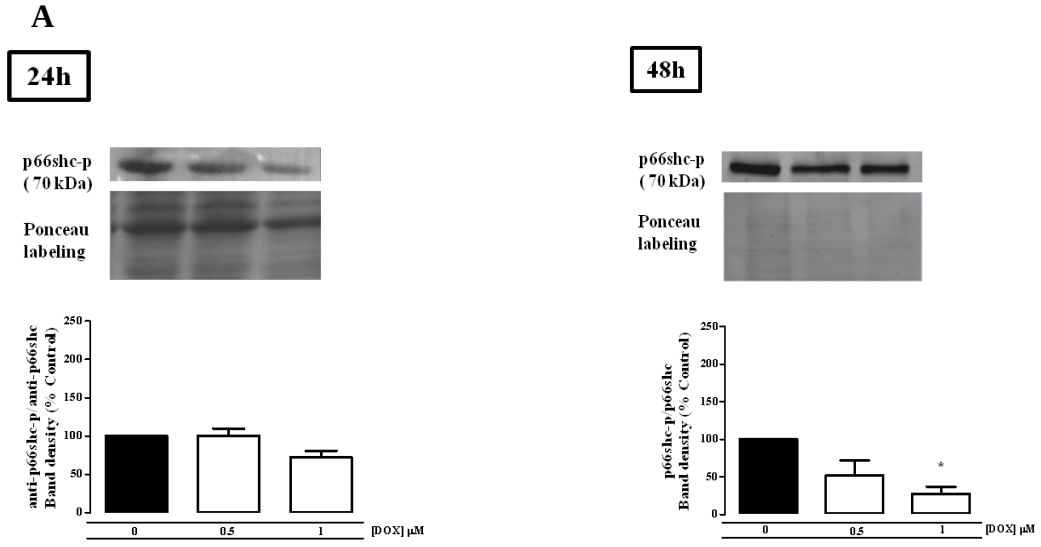

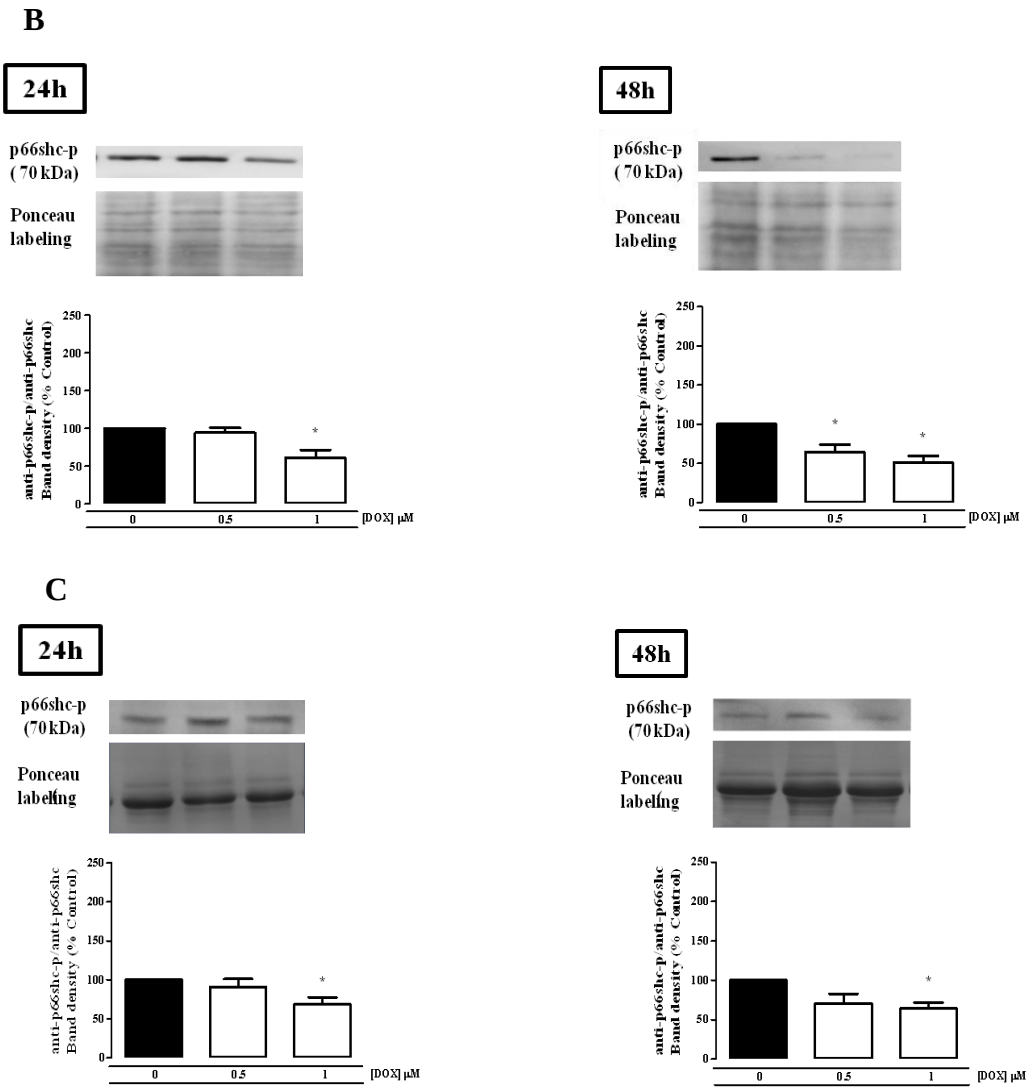

Figure 13. Serine 36-phosphorylated p66Shc content in whole cell extracts. p66Shc-p content in total cellular extracts (A), cytosolic (B) and nuclear fractions (C), identified by Western Blot as a70 kDa band. Cells were collected after treatment with 0.5 and 1 µM DOX during 24 and 48 hours, as described in the material and methods section. Images are representative experiments from four different experiments. Ponceau labeling shows the equal protein amount in each lane. B) Densitometric analysis of p66Shc-p protein, expressed as % of control. Data are expressed as means±SEM of four different experiments. Statistical analysis: * $p < 0.05$ compared with control.

4.2. p66Shc, but not the Serine 36- phosphorylated Form, Translocates to Mitochondria after DOX Treatment

The presence of p66Shc in mitochondrial fractions, after DOX treatment was analyzed by Western Blot (Fig. 14 B). The results demonstrate an increase in p66Shc

content in mitochondrial fractions isolated from H9c2 cells treated with 0.5 and 1µM DOX for 24 and 48 hours. However, no changes are observed for cells treated with 0.5 µM DOX during 24 hours. Mitochondrial fractions revealed a decreased content in the ratio between p66Shc phosphorylation on serine 36 and p66Shc after DOX treatment (Fig. 14 B).

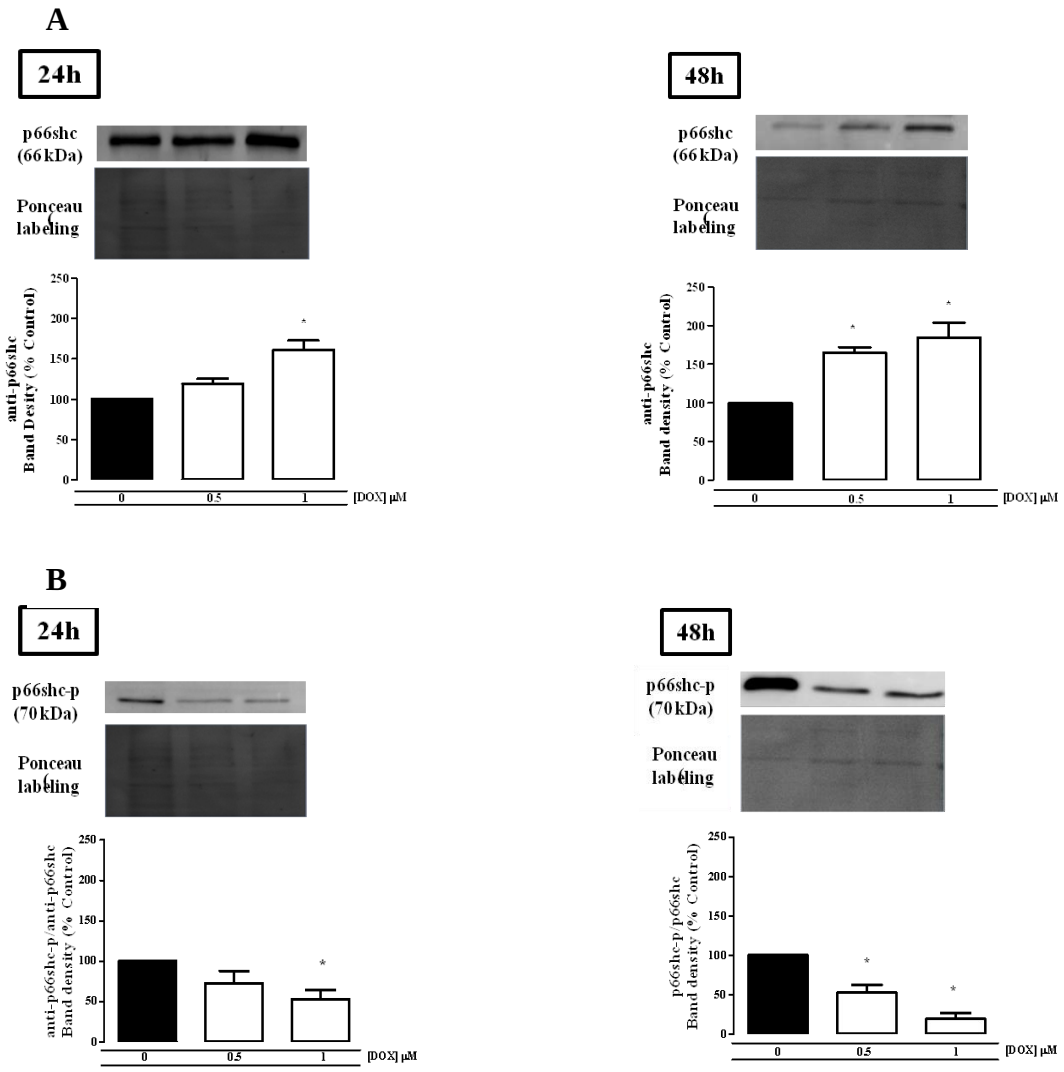

Figure 14. DOX induces p66Shc translocation to mitochondria. p66Shc (A) and p66Shc-p (B) content in mitochondrial fractions, identified by Western Blot as a band of 66 and 70 kDa, respectively. Mitochondrial fractions were collected from H9c2 cells after 24 and 48 hours treatment with 0.5 and 1 µM DOX, as described in the methods section. Western Blot images are representative of four different experiments. Ponceau labeling shows equal protein amount on each lane. B) Densitometric analysis of p66Shc and p66Shc-p protein, expressed as % of control. Data are expressed as means±SEM of four different experiments. Statistical analysis: * $p < 0.05$ compared with control.

4.3. Doxorubicin Treatment Promotes an Increase of Transcriptional Factor FoxO3a in H9c2 Cells

One of the Forkhead family members, the transcriptional factor FoxO3a, is translocated from cytosol to the nucleus as an oxidative stress response (Biggs *et al.*, 1999). through PI3K/Akt signaling. After DOX treatment, total cellular extracts, cytosolic and nuclear fractions were collected and analyzed by Western Blot for content in FoxO3a (Fig. 15). H9c2 cells were treated with 0.5 and 1 µM DOX for 24 and 48 hours and collected, as described in material and methods section. For total cellular extracts, an increase in FoxO3a was observed after treatment during 24 and 48 hours for both DOX concentrations (Fig.15 A). No changes were observed in cytosolic fractions during 24 hour treatment, but a significant decrease occurs for 48 hours treatment with 1 µM DOX (Fig. 15 B). For nuclear fractions, a significant increase in both time points and DOX concentration occurs (Fig. 15 C), with an higher increase detected for 48 hours

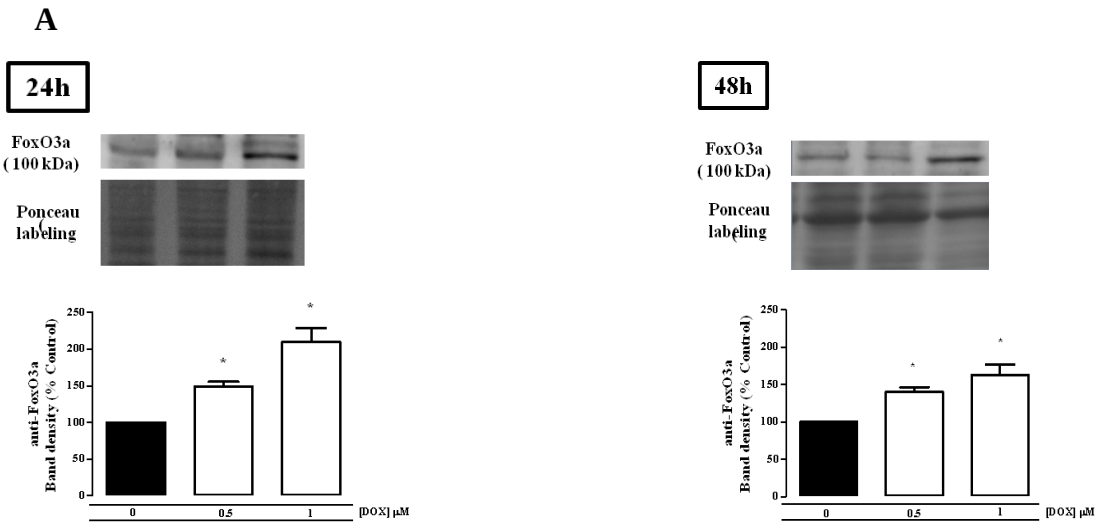

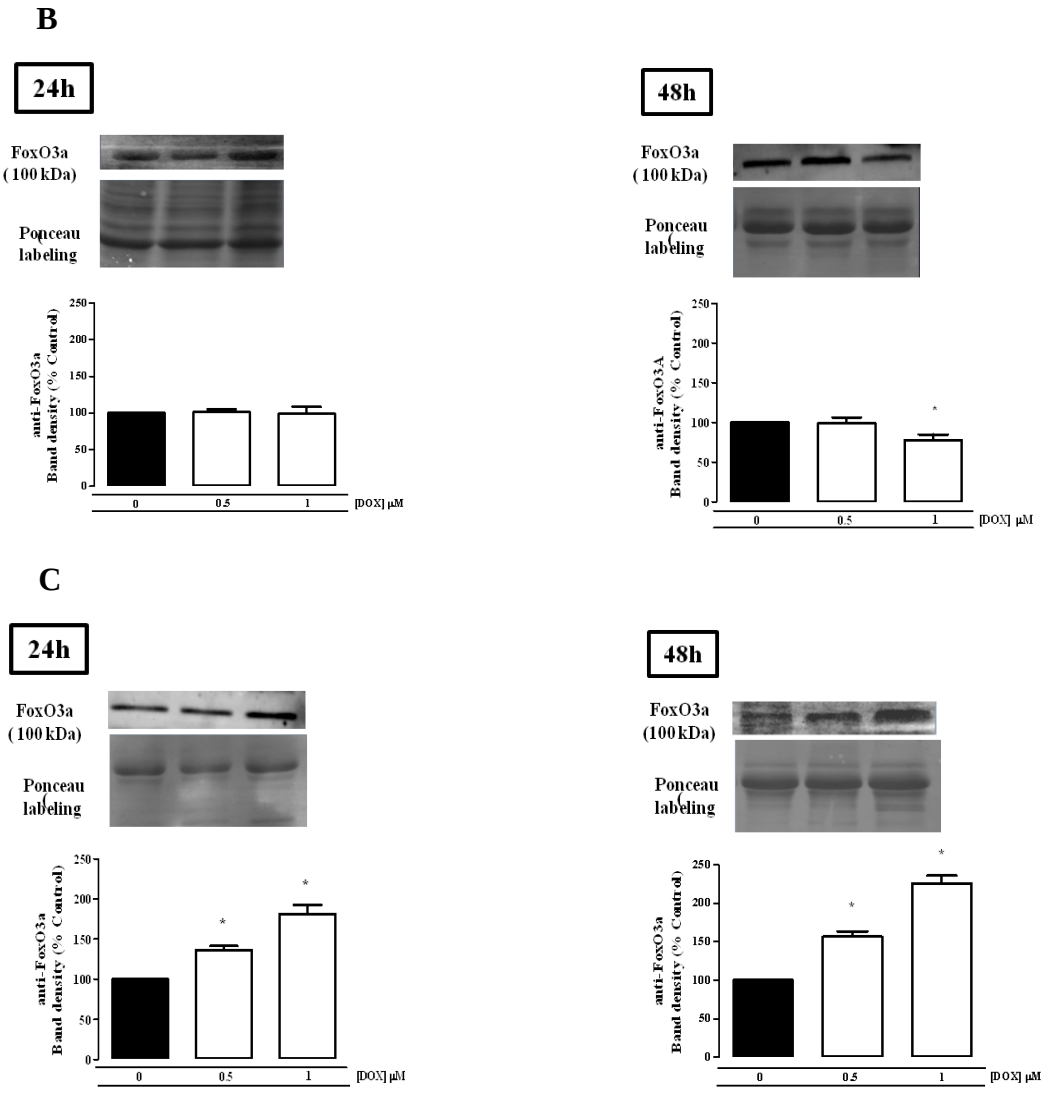

Figure 15. FoxO3a increased in total cellular extracts, cytosolic and nuclear fractions after DOX treatment. FoxO3a content in total cellular extracts (A), cytosolic (B) and nuclear fractions (C), identified by Western Blot as a 100 kDa band. Cells were collected from H9c2 cells after 24 and 48 hours treatment with 0.5 and 1 µM DOX, as described in material and methods section. Western Blot images are representative from four different experiments. Ponceau labeling shows equal protein amount in each lane. Graph represents the densitometric analysis of FoxO3a, expressed as % of control. Data are expressed as means±SEM of four different experiments. Statistical analysis: * $p < 0.05$ compared with control.

4.4. FoxO3a Phosphorylation Decreases after Doxorubicin Treatment

As previously reported, PI3K/Akt signaling pathway mediates the translocation of FoxO3a to the nucleus. After an oxidative stress injury, Akt is phosphorylated and

induces FoxO3a phosphorylation. When phosphorylated, FoxO3a remain in the cytosol and do not promote the upregulation of several important genes involved in apoptosis and cell arrest (Brunet *et al*., 1999; Essers *et al*., 2004). The effect of DOX treatment on FoxO3a phosphorylation on serine 253 was also analyzed. H9c2 cells were treated with 0.5 and 1 µM DOX for 24 and 48 hours. Western blot analysis shows no changes for cells treated during 24 hours, but a significant decrease occurs in total cellular extracts when cells were treated with 1 µM DOX for 48 hours (Fig. 16 A). The same was observed in cytosolic factions for the same time points and concentrations (Fig. 16 B). In H9c2 cells nuclear fractions no significant differences were observed (when compared with non treated cells) (Fig.16 C).

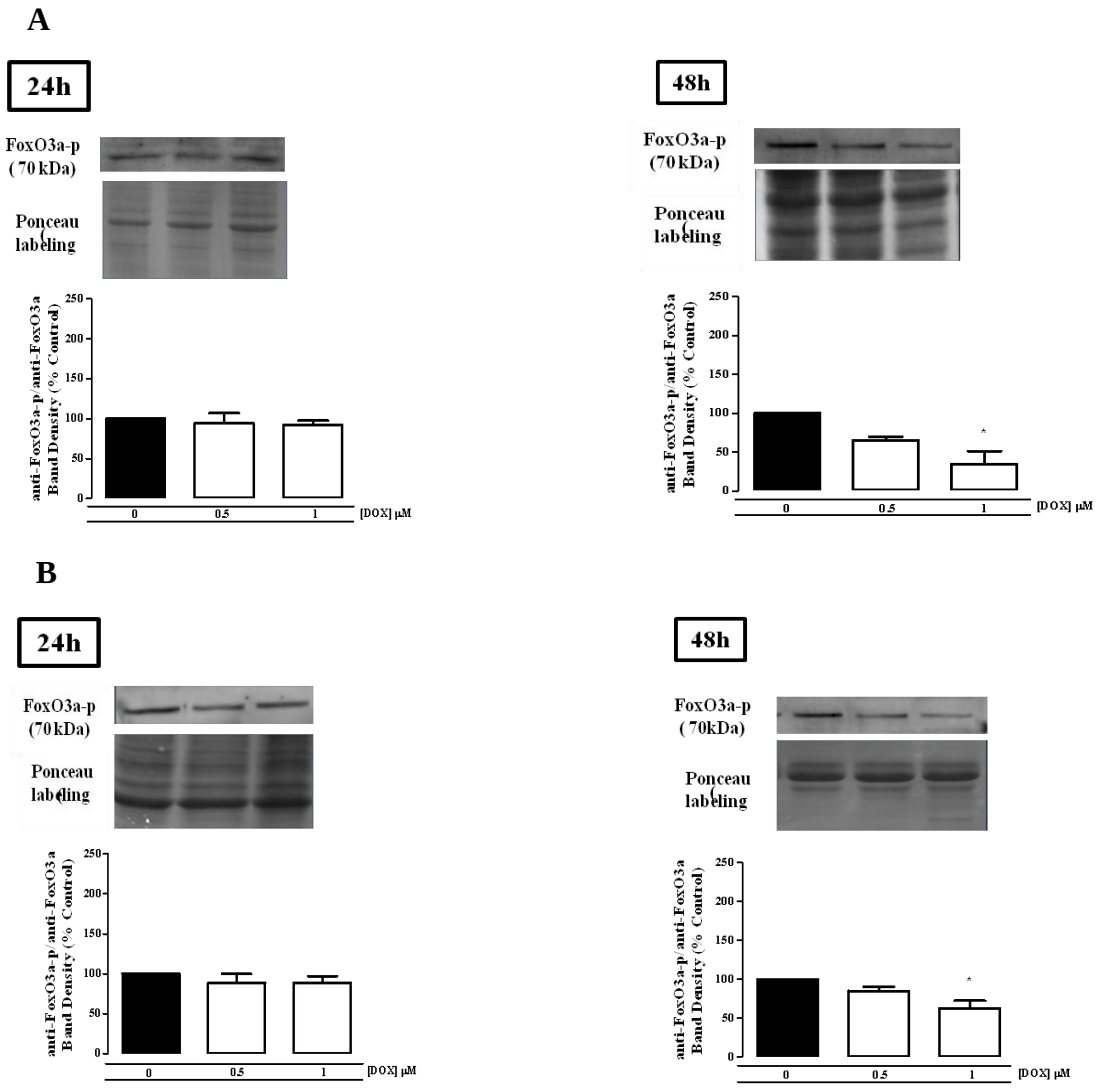

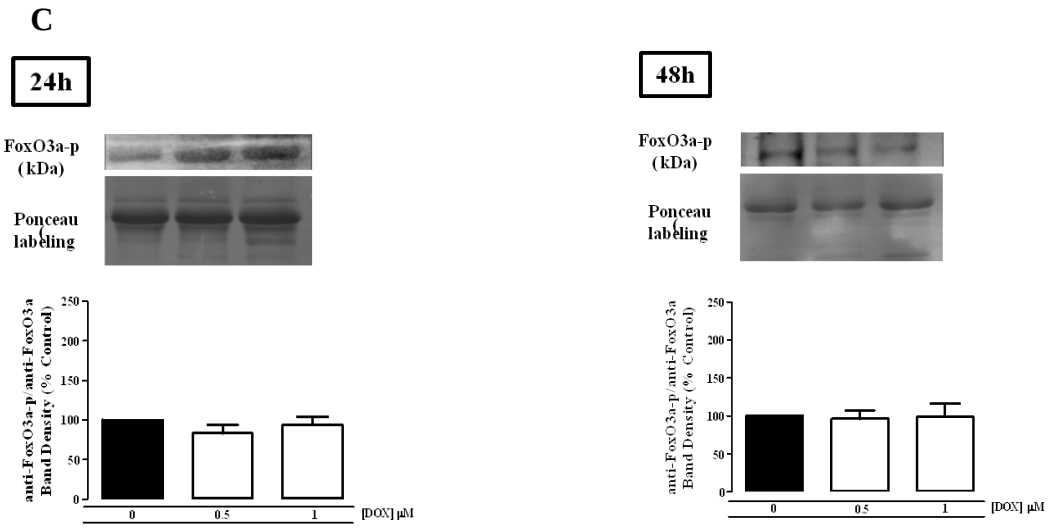

Figure 16. FoxO3a phosphorylation in the cytosolic content decreases after Doxorubicin treatment. FoxO3a-p content in total cellular extracts (A), cytosolic (B) and nuclear fractions (C), identified by Western Blot as a band of 70 kDa. Cells were collected from H9c2 cells after 24 and 48 hours treatment with 0.5 and 1 µM DOX, as described in material and methods section. Western Blot images are representative of four different experiments. Ponceau labeling shows the equal protein amount in each lane. Graph represents the densitometric analysis of FoxO3a-p, expressed as % of control. Data are expressed as means±SEM of four different experiments. Statistical analysis: * $p < 0.05$ compared with control.

4.5. FoxO3a Downstream Targets are Upregulated by DOX Treatment

p53, SOD2 and Bim protein are some of the FoxO3a downstream targets that have been described in the literature (Nemoto S and Finkel T. *et al.*, 2000). After DOX treatment, total cellular extracts were collected and the three FoxO3a downstream targets were analyzed by Western Blot (Fig. 17). H9c2 cells were treated with 1 µM DOX for 24 and 48 hours. The results show a significant increase for 24 and 48 hours treatment for all of the FoxO3a downstream targets analyzed (when compared with non treated cells).

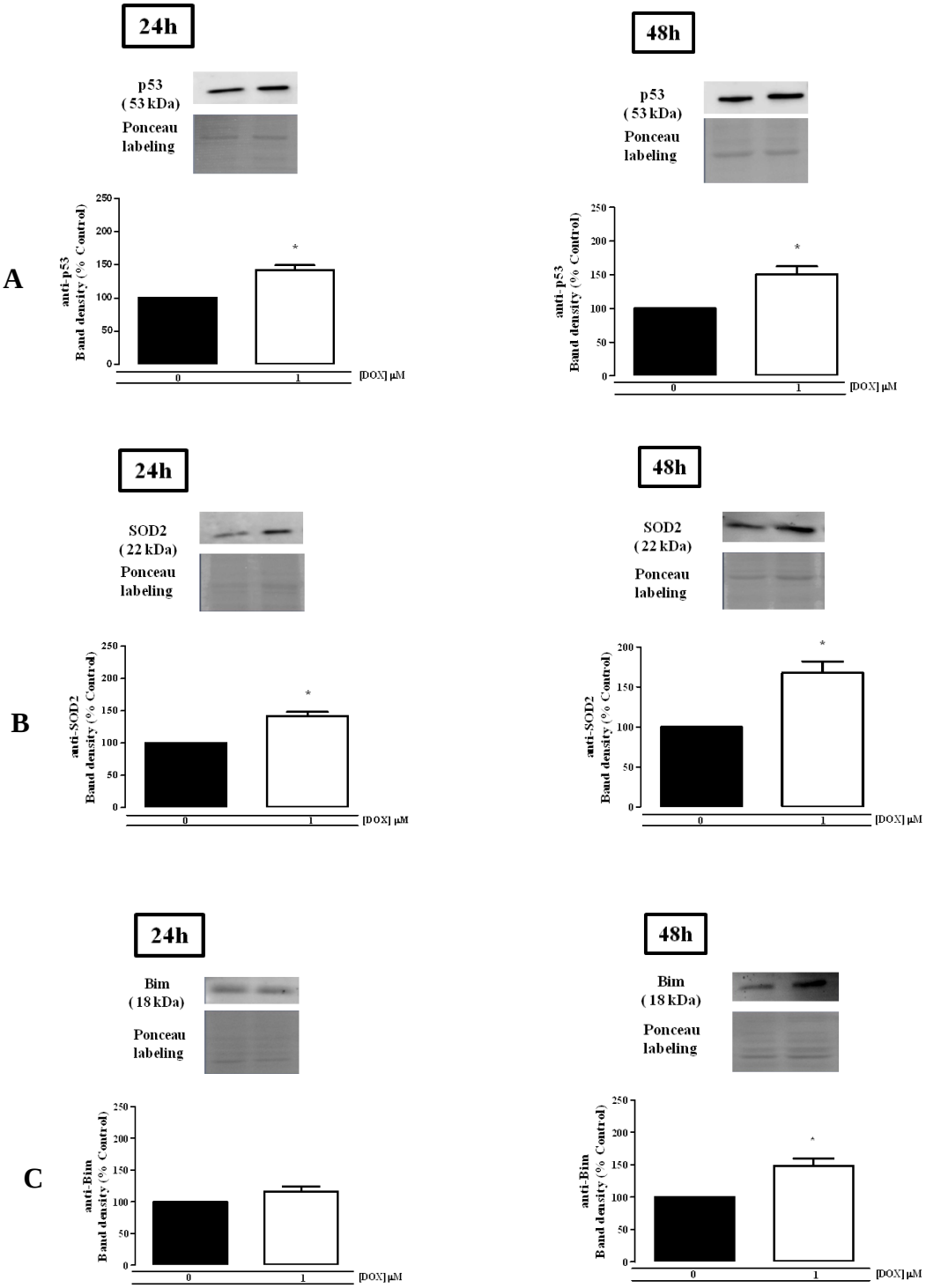

Figure 17. FoxO3a downstream targets are upregulated by DOX treatment. p53 (A), SOD2 (B) and Bim (C) content in total cellular extracts, identified by Western Blot as a band of 53, 22 and 18 kDa, respectively. Cells were collected from H9c2 cells after 24 and 48 hours treatment with 1 µM DOX, as described in the methods section. Western Blot images are representative of four different experiments. Ponceau labeling shows the equal protein amount in each lane. Graph represents the densitometric analysis of p53,SOD2 and Bim expressed as % of control. Data are expressed as means±SEM of four different experiments. Statistical analysis: * $p < 0.05$ compared with control.

4.6. Doxorubicin Caused p66Shc-FoxO3a Nuclear Interaction and Decreased Akt in Total Cellular Extracts

Due to the observed increase in p66Shc protein content in the nuclear fractions of H9c2 cells, a possible interaction with FoxO3a was hypothesized. This possible binding was analyzed by immunocytochemistry (Fig.18) and immunoprecipitation (Fig. 19). For immunocytochemistry experiments, control and treated cells were fixed and labeled with an antibody against p66Shc (red fluorescence) and against FoxO3a (green fluorescence). H9c2 cells were treated with 0.5 and 1 μM DOX during 24 and 48 hours, as previously described. An increase in FoxO3a content was detected as nuclear fluorescence intensity in treated cells (both 0.5 and 1 μM) for 24 hours (data not shown) and 48 hours (Fig. 18). For immunoprecipitation (IP) experiments, cells were treated with 1 μM DOX for 24 and 48 hours, and appropriately collected, as described in the material and methods section. Cell extracts from H9c2 cells were immunoprecipitated with anti-p66Shc or IgG control followed by immunoblotting with anti-FOXO3a or anti-p66Shc (positive control) (Fig. 19). The results confirm the p66Shc and FoxO3a binding after 24 and 48 hours with increased binding after DOX treatment (Fig. 19).

The presence of Akt, a regulator of cell death and survival (Brazil and Hemings, 2001; Brunet and Greenberg, 2001), was also analyzed in total cellular extracts treated with 1 μM DOX during 24 and 48 hours. Akt has been reported for its role in regulating FoxO3a translocation to the nucleus. As seen in Figure 20, Western Blot assay results demonstrate no changes for cells treated during 24 hours, but a significant increase was detected for 48 hours treatment (when compared with non treated cells). Phosphorylation of Akt on serine 473 is responsible to induce phosphorylation of FoxO3a and so, this transcriptional factor remains in the cytosol. Phosphorylation of Akt was also analyzed for cells treated with 1 μM DOX. In this case, a significant increase for both time points was detected (Fig. 21).

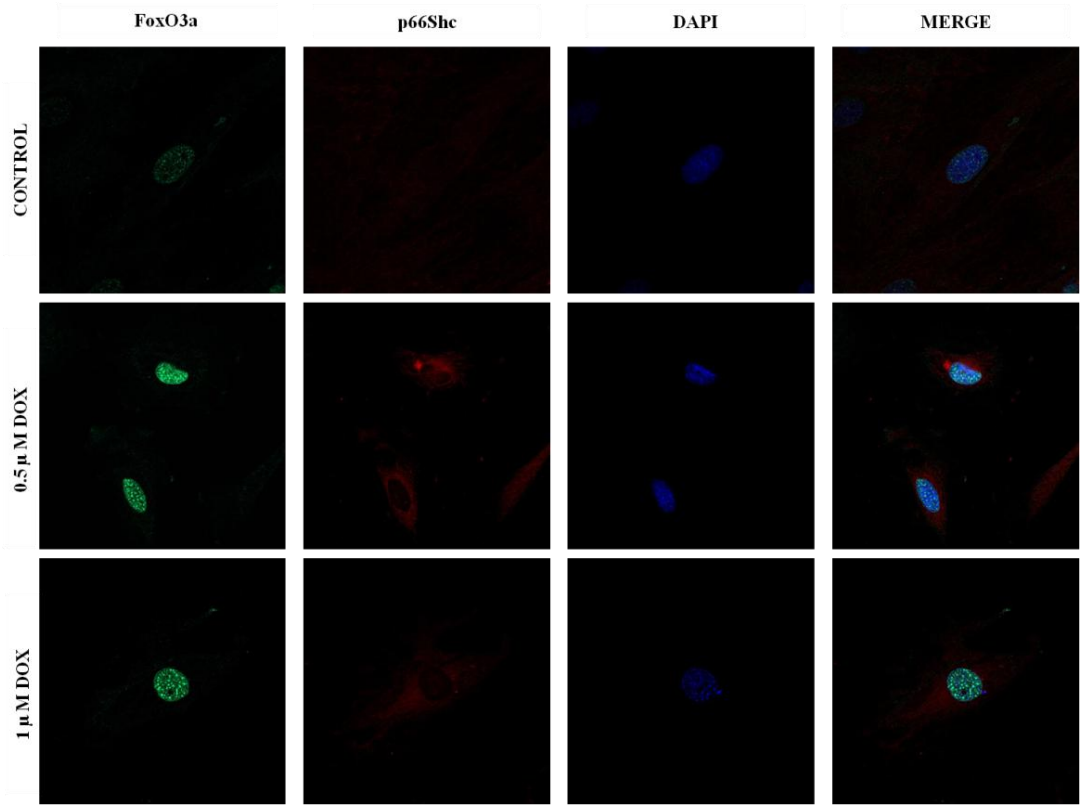

Figure 18. FoxO3a content increases in nuclear fractions from H9c2 cells after DOX treatment. Confocal microscopy images of H9c2 cells treated with 0, 0.5 and 1 µM DOX during 48 hours. After treatment, cells were fixed and labeled with an antibody against p66Shc (red) and FoxO3a (green) andcounterstained with DAPI (blue), as described with material and methods section. Confocal microscopy images illustrate an increase of FoxO3a in nuclear labeling after H9c2 cells treatment with DOX. However, an increase in p66Shc content was not detected as expected. Data are representative of three different experiments.

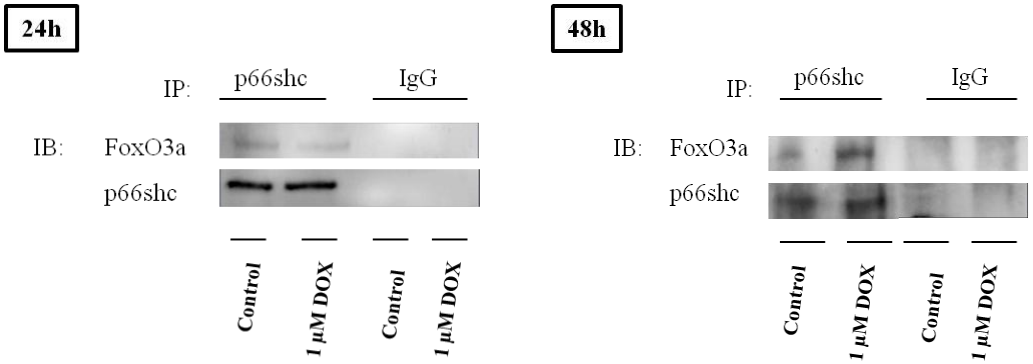

Figure 19. p66Shc interacts with FoxO3a in H9c2 cells. Cell extracts from H9c2cells were immunoprecipitated with anti-p66Shc or IgG control followed by immunoblotting with anti-FOXO3a or anti-p66Shc (positive control). Data are representative of three different experiments.

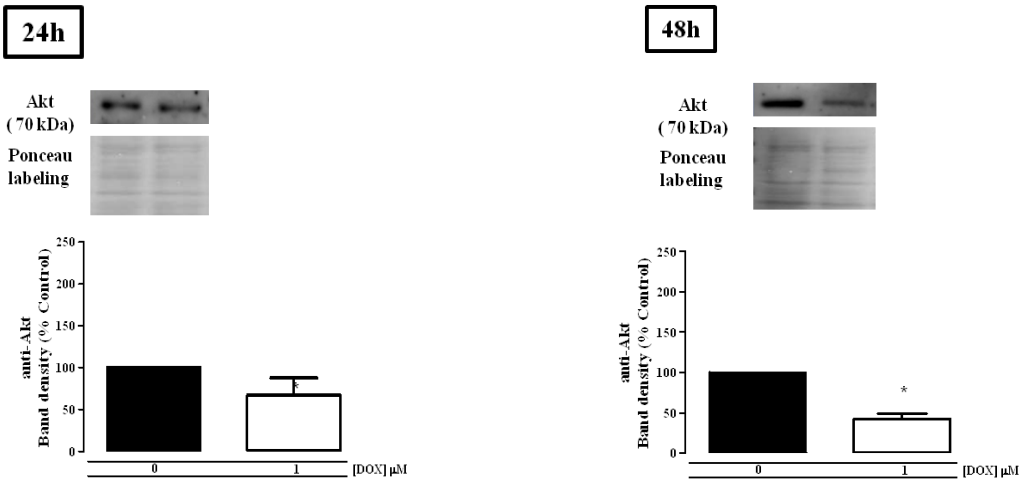

Figure 20. Akt content in H9c2 cells after DOX treatment. Akt content in total cellular extracts, identified by Western Blot as a 70 kDa band. Cells were collected from H9c2 cells after 24 and 48 hours treatment 1 µM DOX, as described in the methods section. Western Blot images are representative of four different experiments. Ponceau labeling shows the equal protein amount in each lane. Graph represents the densitometric analysis of Akt, expressed as % of control. Data are expressed as means±SEM of four different experiments. Statistical analysis: * $p < 0.05$ compared with control.

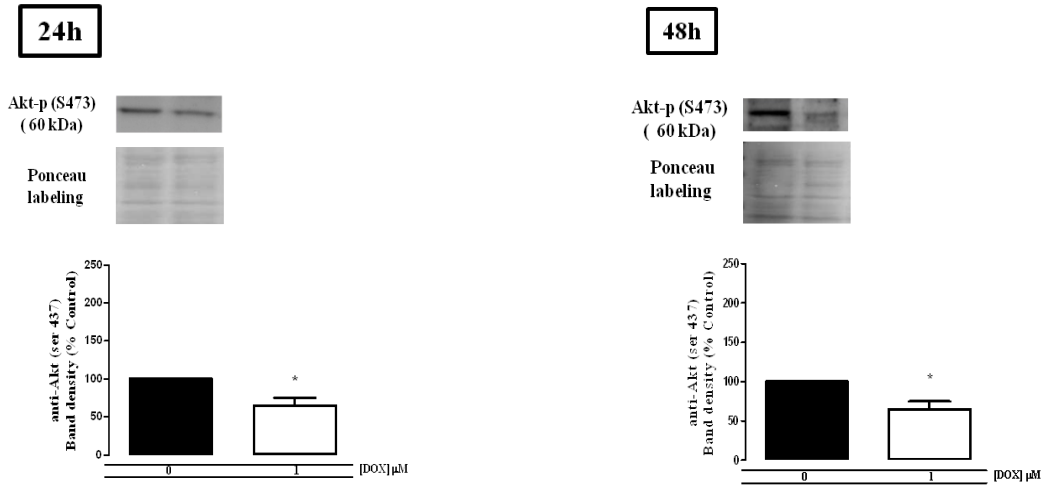

Figure 21. Akt phosphorylation on serine 473 content in H9c2 cells after DOX treatment. Akt phosphorylation content in total cellular extracts, identified by Western Blot as a 60 kDa band. Cells were collected from H9c2 cells after 24 and 48 hours treatment with 1 µM DOX, as described in the methods section. Western Blot images are representative of four different experiments. Ponceau labeling shows the equal protein amount in each lane. Graph represents the densitometric analysis of Akt-p, expressed as % of control. Data are expressed as means±SEM of four different experiments. Statistical analysis: * $p < 0.05$ compared with control.

4.7. Effect of PKC β Inhibitor on Doxorubicin-Induced Cytotoxicity and Mitochondrial Dysfunction

The p66Shc signaling pathway has not been clearly established. However, the most acceptable model proposes that p66Shc is translocated to mitochondrial spaces in response to oxidative stress promoted by the activation of the protein kinase C (PKC β). PKC β seems to induces the phosphorylation of p66Shc on Ser 36 which is then recognized by the prolyl isomerase Pin1 that catalyzes its cis-trans isomerization. Subsequently, p66Shc is dephosphorylated by type 2 protein serine/threonine phosphatase (PP2A) and imported in the mitochondria (Raffaello and Rizzuto, 2011). Since PKC β mediates the primary step for p66Shc activation, the effect of Hispidin, a PKC β inhibitor (Jang *et al*., 2010) was studied.

The effect of Hispidin, a PKC β inhibitor (Jang *et al.*, 2010), on DOX-induced cytotoxicity treatment was analyzed by using the SRB assay (Fig. 22 A). Caspase-3 and -9 like activities were also evaluated by following the cleavage of the colorimetric substrates Ac-DEVD-pNA and Ac-LEHD-pNA, respectively (Fig. 22 B and C). The concentration of Hispidin used was based on preliminary experiments where the toxic threshold of Hispidin on H9c2 cells was evaluated (data not shown). After four hours pre-incubation with 5 µM or 10 µM Hispidin, H9c2 cells were incubated with 1 µM DOX for 24 hours or 48 hours more. The results demonstrate that Hispidin treatment did not prevent cell death or caspase-3 and -9 activation induced by DOX treatment (Fig. 22 B and C). Caspase-3 activation also increases with Hispidin treatment for both time points and concentrations, but caspase-9 activation was only significantly higher for cells treated with DOX (48 hours treatment) and Hispidin (for both time points). Indeed, capase-9 activation decreases when cells were treated with Hispidin and DOX simultaneously for both time points (when compared with cells only treated with DOX).

A

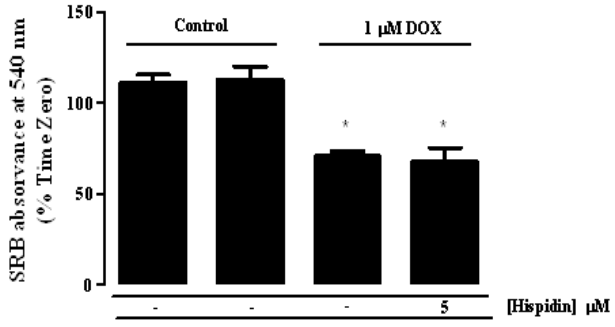

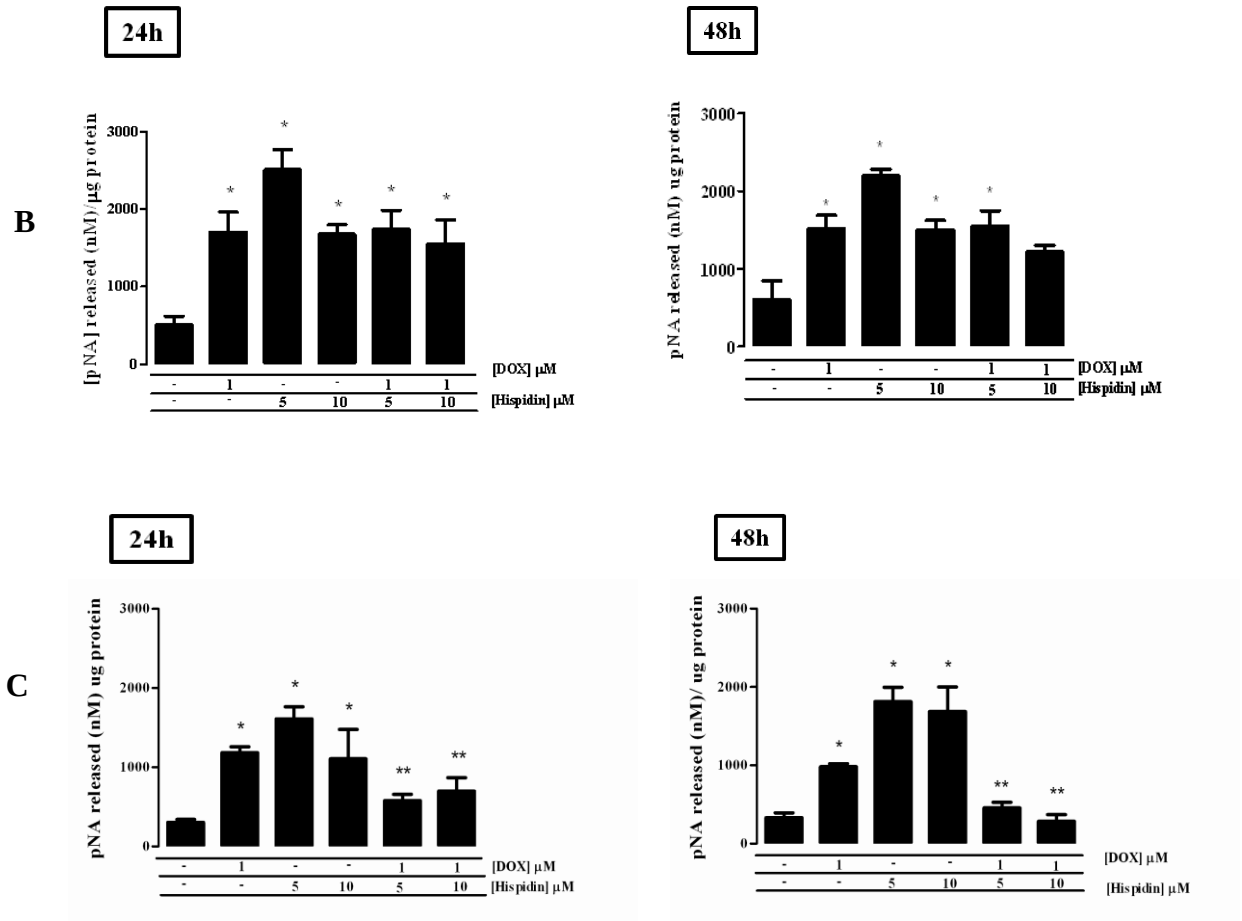

Figre 22. Effect of Hispidin treatment on cell mass and caspase -3 and -9 activity.. **(**A) The effect of Hispidin on DOX-induced cell death was analyzed by using the sulforhodamine B dye-binding assay. Cell treatment was performed as described in the material and methods section. Data represent the means±SEM of three different experiments. Caspase-3 (B) and -9 (C) -like activities were measured after 24 and 48 hours treatment by following the cleavage of colorimetric substrates Ac-DEVD-pNA and Ac-LEHD-pNA, respectively. The caspase-like activity was expressed as concentration of pNA released per µg protein. The results were calibrated with known concentrations of pNA. Data are expressed as means±SEM of four different experiments. Statistical analysis: * $p < 0.05$ vs control (no DOX added) and ** $p < 0.05$ vs DOX treatment.

4.8. Hispidin Treatment Decreases p66Shc Content Total Cellular Extracts

The presence of p66Shc content in total cellular extracts (Fig. 23 A) and mitochondrial fractions (Fig. 23 B), after DOX treatment, were analyzed by Western Blot. p66Shc content increases with DOX treatment (Fig. 12). Cells were

treated with 5 and 10 µM Hispidin during 24 and 48 hours. Cells treated during 24 hours shown an increase in p66Shc content (compared with non treated cells), but for 48 hours the same does not occur and no significant changes were observed (compared with non treated cells). The same occurs for cells treated with Hispidin and pre-incubated with DOX, but a significant decrease is observed for 48 hours treatment. p66Shc content in mitochondrial fractions increases for both time points when cells were treated with DOX, but for cells treated with 5 and 10 µM Hispidin, a significant increase was also detected. When cells were treated with Hispidin and DOX a significant decrease was also detected (when compared with DOX treated cells).

A

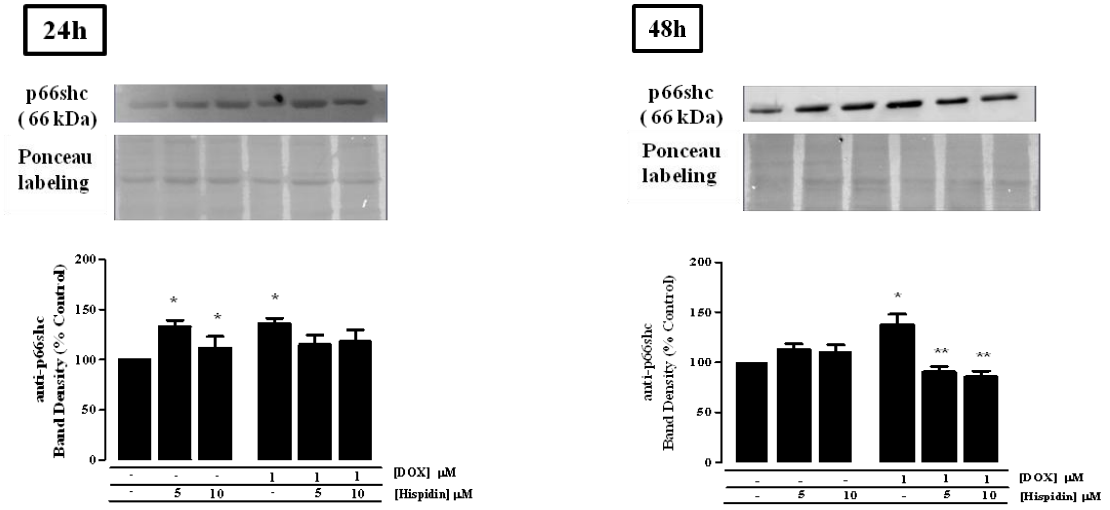

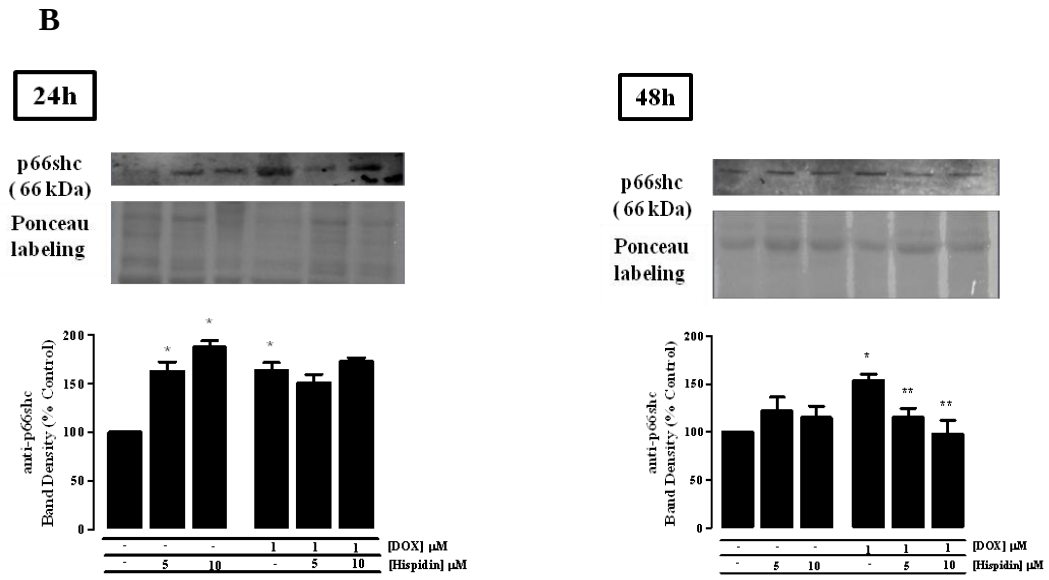

Figure 23. Hispidin treatment decreases p66Shc protein content in total cellular extracts and mitochondrial fractions of H9c2 cells. p66Shc content in total extracts (A) an mitochondrial fractions (B), identified by Western Blot as a band of 66 kDa, respectively. Cells were collected as described in the material and methods section. Images are representative of four independent experiments. Ponceau labeling shows the loading of equal amount of protein in each lane. Graph represents the densitometry analysis of p66Shc expressed as % of control. Data are expressed as means ± SEM of four different experiments. Statisctical analysis: *p < 0.05 compared with control for the respective time point and **p < 0.05 vs DOX treatment.

4.9. Hispidin Treatment Prevents DOX-Induced Decrease in the Serine 36-Phosphorylated Form of p66Shc

Phosphorylation of p66Shc on serine 36 in total extracts (Fig. 24 A) and mitochondrial fractions (Fig. 24 B), was analyzed by Western Blot, after DOX treatment. As previously described (Fig. 13), p66Shc-p content decreases with DOX treatment. Cells were treated with 5 and 10 µM Hispidin during 24 and 48 hours. For both total extracts and mitochondrial fractions when cells were treated during 24 and 48 hours no significantly changes were observed (for all used concentrations). The same occurs for cells treated with Hispidin and pre-incubated with DOX.

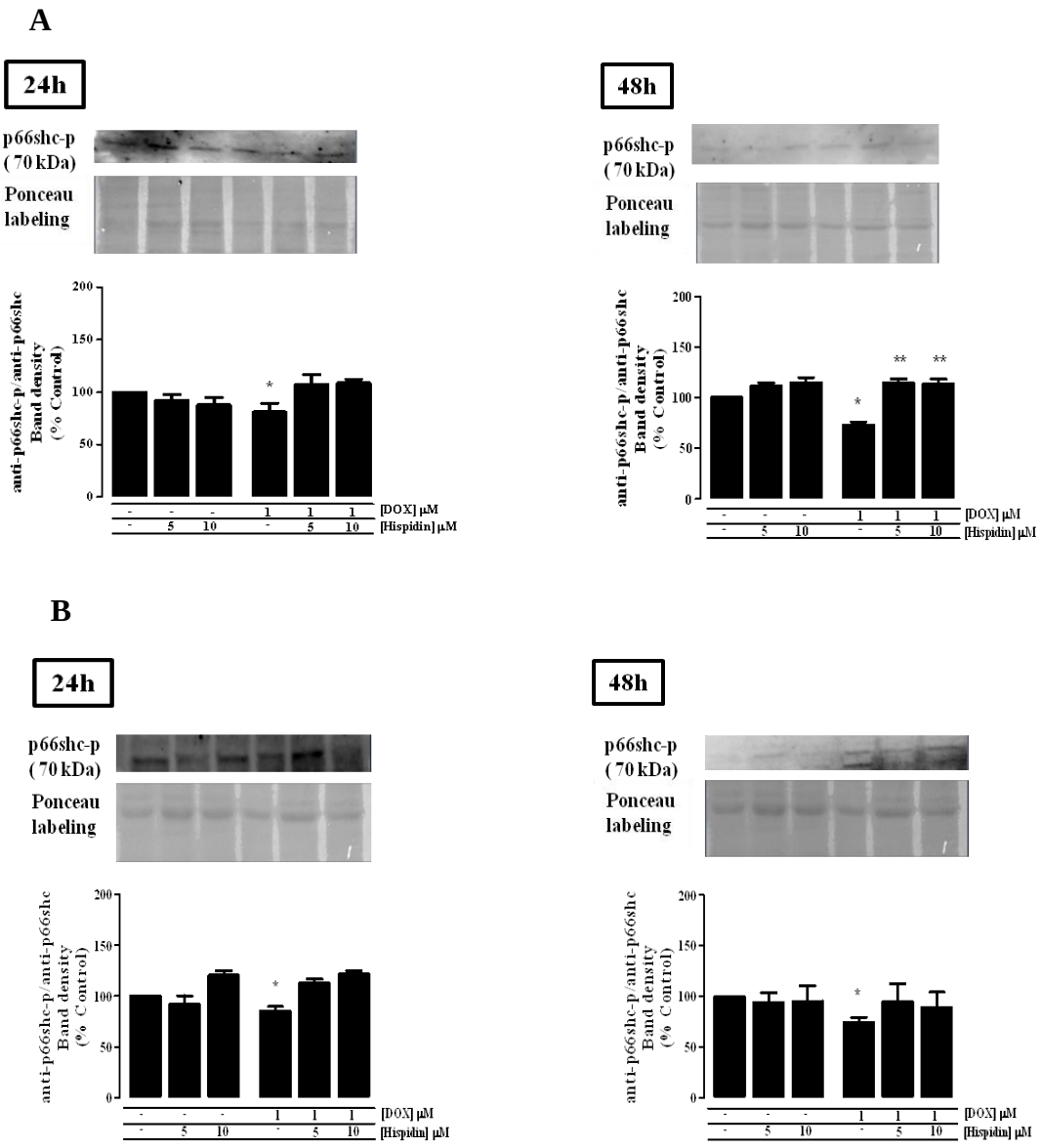

Figure 24. p66Shc phosphorylation content in total cellular extracts and mitochondrial fractions of H9c2 cells after Hispidin treatment. p66Shc-p in total extracts (A), and mitochondrial fractions (B), identified by Western Blot as a band of 70 kDa, respectively. Cells were collected as described in the material and methods section. Images are representative of four independent experiments. Ponceau labeling shows the loading of equal amount of protein in each lane. Graph represents the densitometry analysis of p66Shc-p expressed as % of control. Data are expressed as means ± SEM of four different experiments. Statisctical analysis: *$p < 0.05$ compared with control for the respective time point and **$p < 0.05$ vs DOX treatment.

4.10. Effects of PKC β Inhibition on Pro-Apoptotic Proteins

Content in p53, Bax (Fig. 25), cytochrome c (Fig. 26) and AIF (Fig. 27) in total cellular extracts, was analyzed by Western Blot, after DOX treatment. Cells were treated with 5 µM and 10 µM Hispidin during 24 and 48 hours. The results demonstrate an increase in the content of p53 in total cellular extracts from H9c2 cells treated with Hispidin (both concentrations). However, a significant increase in Bax concentration caused by Hispidin treatment per se as only detected when cells were treated with 10 µM Hispidin for 24 and 48 hours.

The next objective was to identify whether Hispidin could alter the effects of DOX on pro-apoptotic proteins p53, Bax, cytochrome c and AIF. H9c2 cells were also pre-incubated with Hispidin for 24 and 48 hours, followed by 1 µM DOX treatment during 24 and 48 hours more. In this, no significant differences were observed (compared with cells treated only with DOX) in p53 content. Although a decrease in DOX-induced p53 up-regulation was noticeable for 48 hours. Pre-incubation with Hispidin partly decreased DOX-induced Bax increase.

After DOX treatment, cytochrome c release from mitochondria was analyzed by Western Blot. To this propose total cellular extracts and isolated mitochondrial fractions were probed against a cytochrome c antibody. An increase of cytochrome c in total cellular extracts (Fig. 26 A) after treatment with 1 µM DOX for 24 and 48 hours. The same occurs when cells were treated with 10 µM Hispidin. However, cells pre-incubated with Hispidin and treated with DOX showed a small decrease in Cyt c content (when compared with cells treated with DOX). Mitochondrial fractions (Fig. 26 B) treated with the same experimental conditions were also analyzed. The results shown an increase when cells were treated with Hispidin, but a decrease was observed for cells treated with DOX (24 and 48 hours treatment), as

expected. After 48 hours treatment with Hispidin and DOX, a significant decrease in cytochrome c loss in mitochondria was detected (when compared with cells treated with DOX). As previously reported, AIF content in total cellular extracts does not change with DOX treatment. The same was observed when cells were treated with Hispidin or with both compounds during 24 hours. However, when cells were treated with Hispidin (10 µM) and DOX simultaneously during 48 hours, AIF total content increased (Fig. 27 A). Mitochondrial fractions of H9c2 cells were also analyzed. After 24 hours treatment, a significant decrease was detected for cells treated with DOX, 5 or 10 µM Hispidin. The results were similar for 48 hours (Fig. 27 B). It is also noticeable that Hispidin blurred the decrease of AIF in mitochondrial fractions.

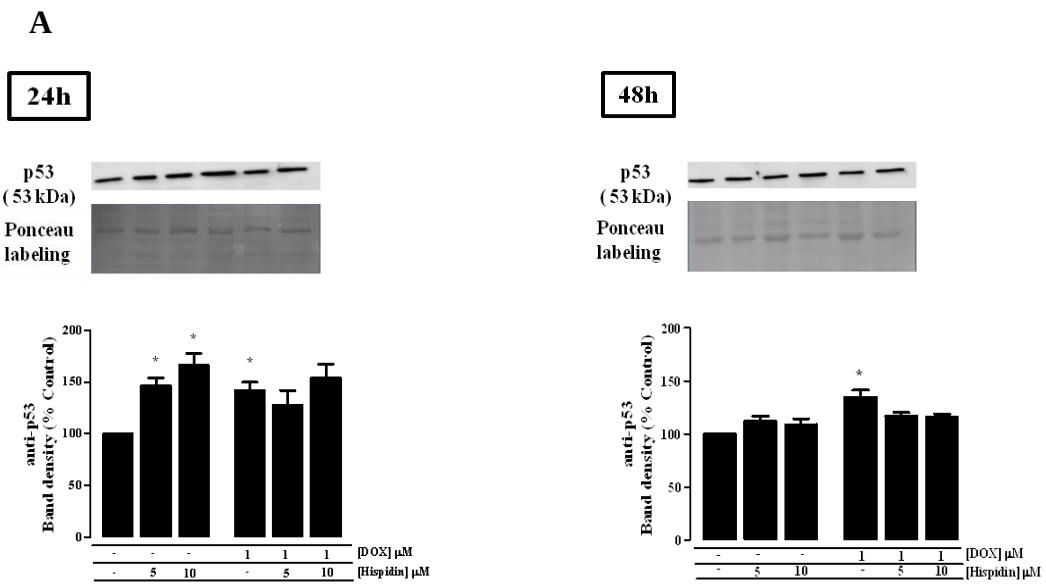

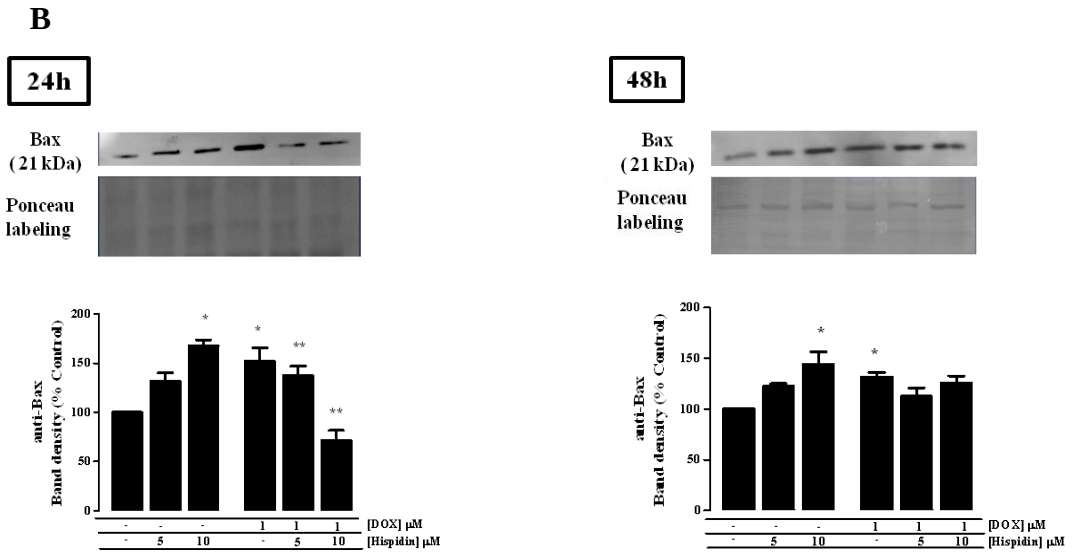

Figure 25. p53 and Bax protein content in total cellular extracts. p53 (A) and Bax (B) content in total extracts, identified by Western Blot as a band of 53 and 21 kDa, respectively. Total extracts were collected as described in the material and methods section. Images are representative of four independent experiments. Ponceau labeling shows the loading of equal amount of protein in each lane. Graph represents the densitometry analysis of p53 and Bax expressed as % of control. Data are expressed as means ± SEM of four different experiments. Statisctical analysis: *p < 0.05 compared with control for the respective time point and **p < 0.05 vs DOX treatment.

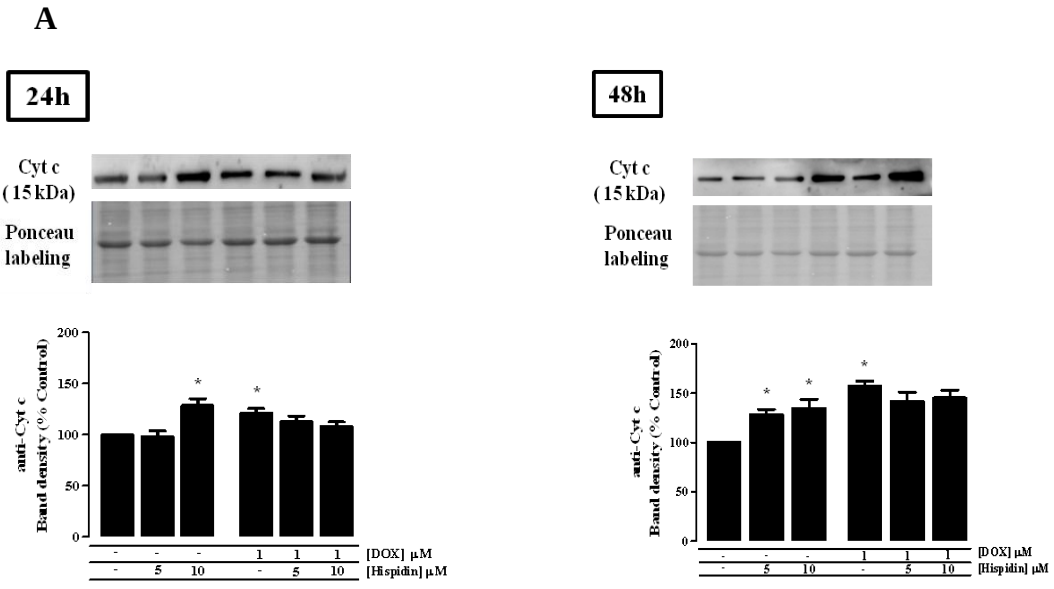

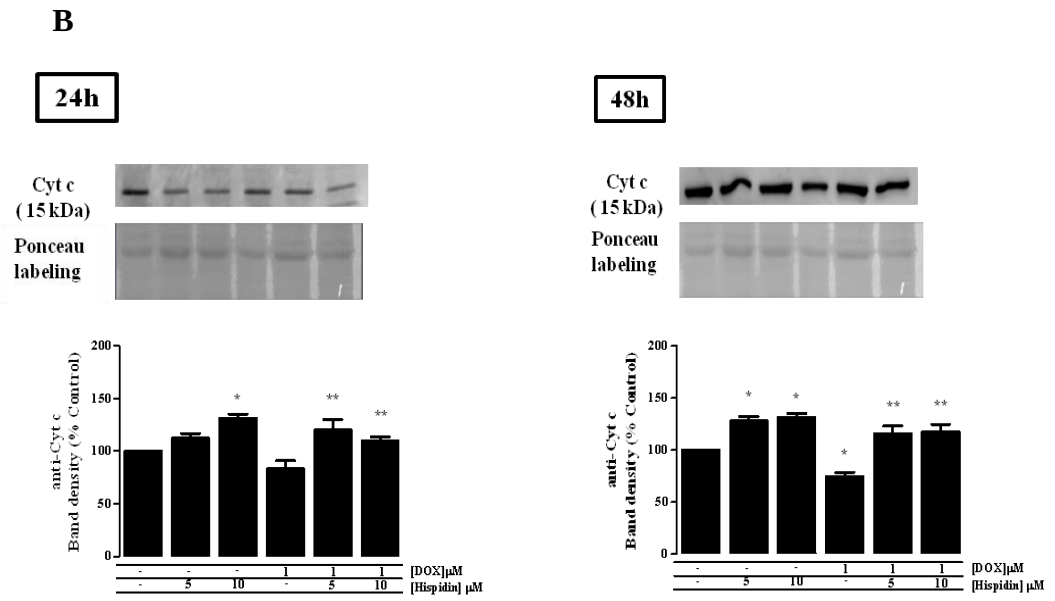

Figure 26. Cyt c protein content in total cellular extracts and mitochondrial fractions of H9c2 cells. Cyt c in total extracts (A), and mitochondrial fractions (B), identified by Western Blot as a band of 15 kDa, respectively. Cells were collected as described in the material and methods section. Images are representative of four independent experiments. Ponceau labeling shows the loading of equal amount of protein in each lane. Graph represents the densitometry analysis of Cyt c expressed as % of control. Data are expressed as means ± SEM of four different experiments. Statisctical analysis: *p < 0.05 compared with control for the respective time point and **p < 0.05 vs DOX treatment.

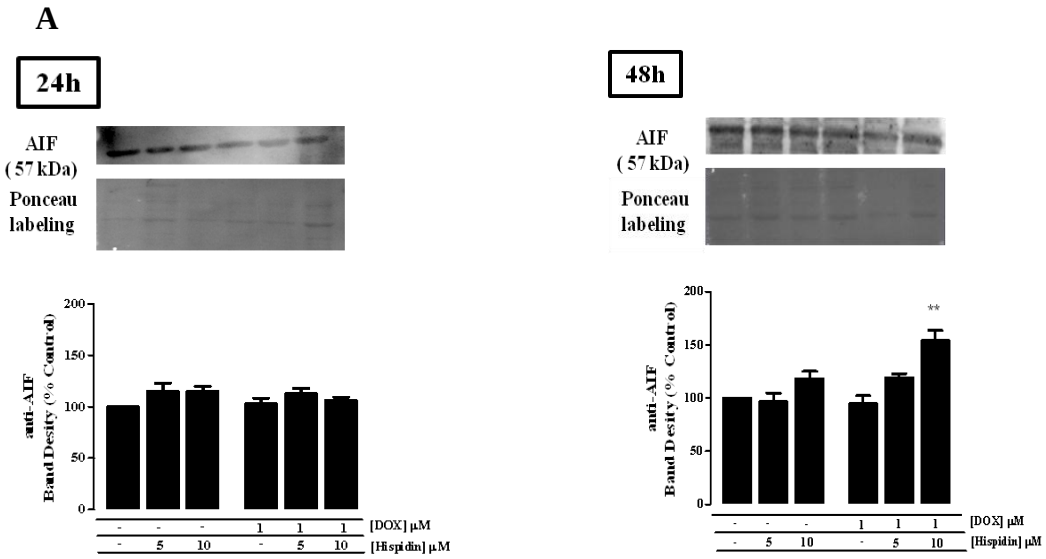

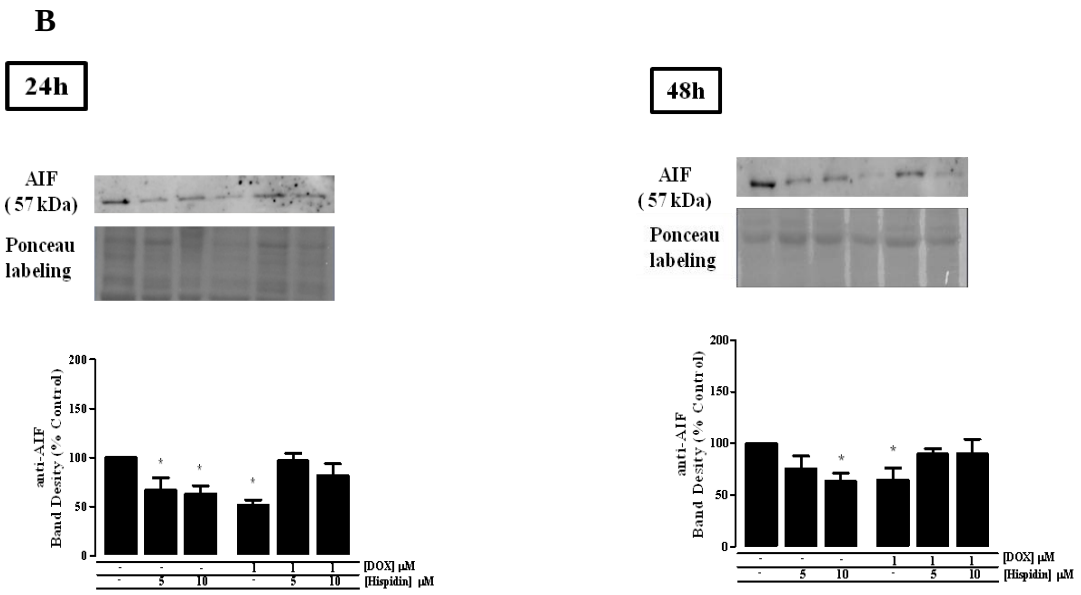

Figure 27. AIF content in total extracts and mitochondrial fractions. AIF content in total extracts (A) and mitochondrial fractions (B), identified by Western Blot as a band of 57 kDa. Cells were collected as described in the material and methods section. Images are representative of four independent experiments. Ponceau labeling shows the loading of equal amount of protein in each line. Graph represents the densitometry analysis of AIF expressed as % of control. Data are expressed as means ± SEM of four different experiments. Statisctical analysis: *p < 0.05 compared with control for the respective time point and **p < 0.05 vs DOX treatment.

4.11. Superoxide Dismutase-2 Content Increases with PKC β Inhibition by Hispidin

Superoxide dismutase-2 (SOD2) content in total cellular extracts was analyzed by Western Blot, after treating cells with DOX (Fig. 28). SOD2 content increased when cells were treated with 5 µM and 10 µM Hispidin during 48 hours, but during 24 hours treatment a significant decrease is only observed at 5 µM Hispidin. Cells treated with DOX only also showed an increase in SOD2 quantity for both time points. However, no changes in SOD2 quantity are observed for cells treated with Hispidin and pre-incubated with DOX during 24 hours.

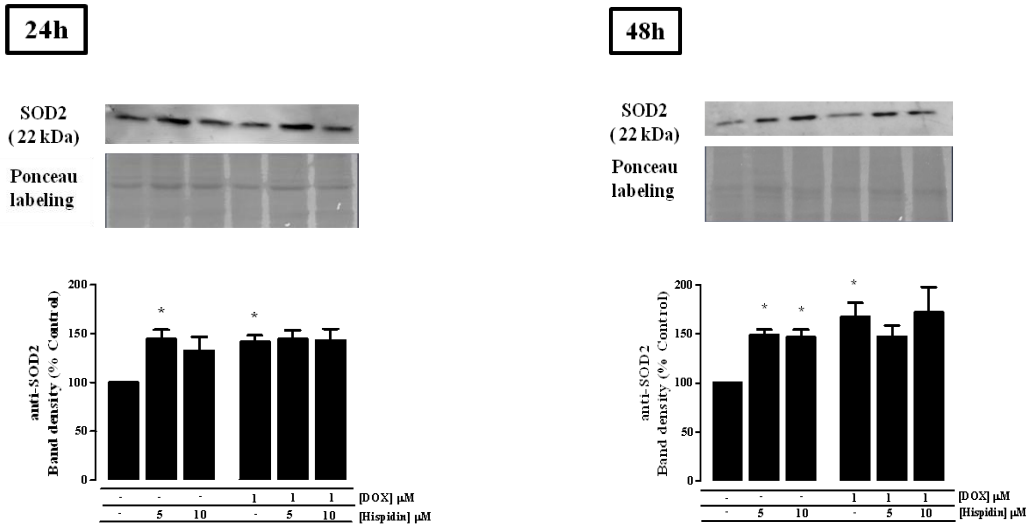

Figure 28. SOD2 protein content in total cellular extracts of H9c2 cells. SOD2 expression in total extracts, identified by Western Blot as a band of 22 kDa, respectively. Total extracts were collected as described in the material and methods section. Images are representative of four independent experiments. Ponceau labeling shows the loading of equal amount of protein in each lane. Graph represents the densitometry analysis of SOD2 expressed as % of control. Data are expressed as means ± SEM of four different experiments. Statisctical analysis: *p < 0.05 compared with control for the respective time point.

4.12. PKC β Inhibition by Hispidin Treatment Induces Chromatin Condensation in H9c2 Cells

Nuclear morphological changes typical of apoptosis were also measured by epifluorescence observation of cells treated with Hispidin. After treatment with different concentrations of Hispidin (5 and 10 µM), H9c2 cells were also treated with 1µM DOX during 24 and 48 hours. The results showed a significant increase in the number of nuclei showing condensed chromatin for both time points (Fig. 29). DOX-induced increase in apoptotic nuclei was not inhibited by Hispidin treatment.

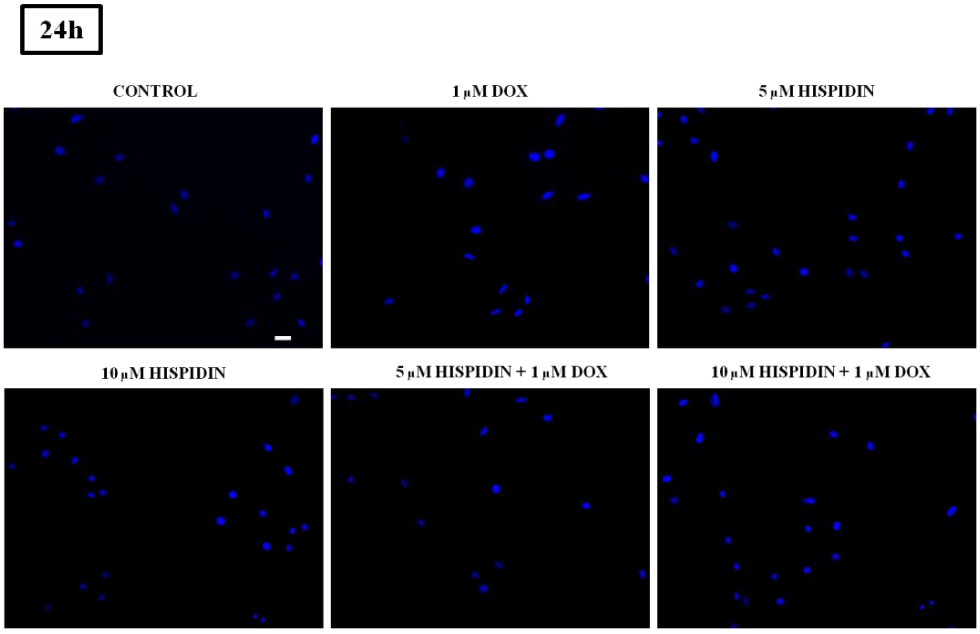
24h
CONTROL
1 μM DOX
5 μM HISPIDIN
10 μM HISPIDIN
5 μM HISPIDIN + 1 μM DOX
10 μM HISPIDIN + 1 μM DOX

A

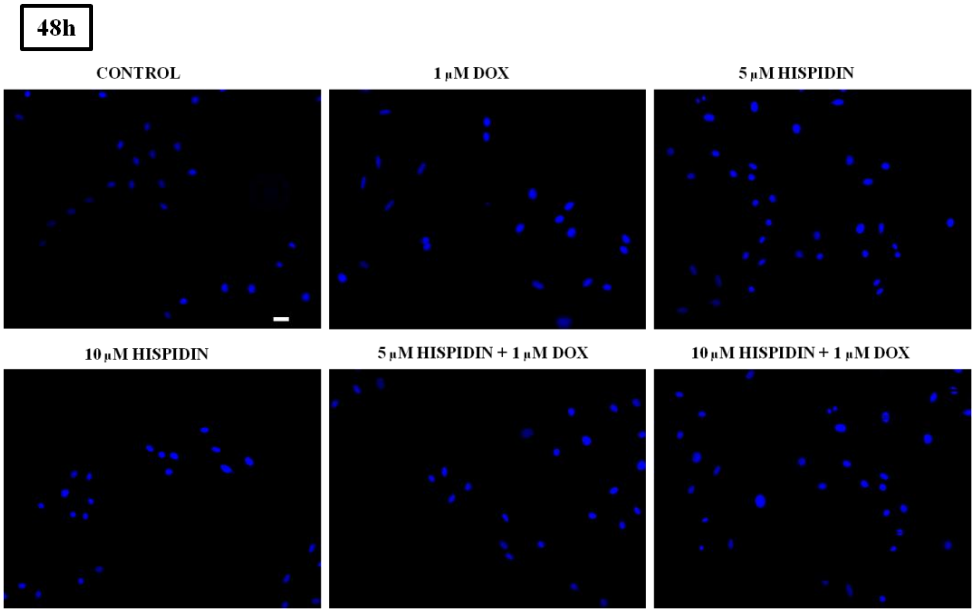
48h
CONTROL
1 μM DOX
5 μM HISPIDIN
10 μM HISPIDIN
5 μM HISPIDIN + 1 μM DOX
10 μM HISPIDIN + 1 μM DOX

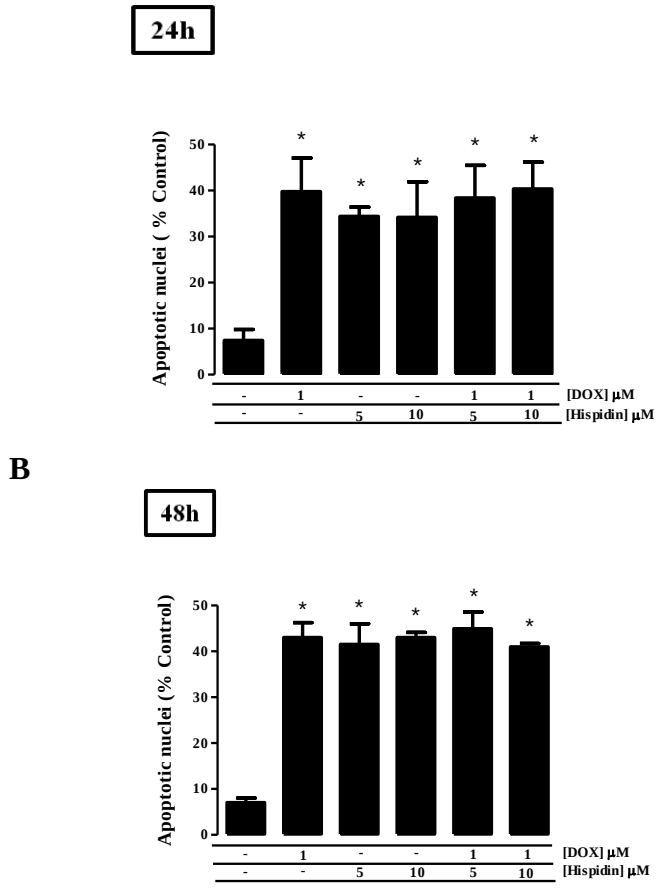

Figure 29. Determination of apoptotic cells by Hoescht nuclear labeling. (A) Epifluorescence microscopy images of nuclei showing H9c2 cells treated with Hispidin or pre-incubated with Hispidin and then treated with 1 µM DOX during 24 and 48 hours. Changes in nuclear morphology characteristic of apoptosis were detected in Hoescht 33342 stained cells. Scale bar represents 40 µm. (B) The number of apoptotic nuclei were counted and expressed as the percentage of total cells counted (approximately 200 cells per coverslip). Data represents the mean±SEM of five different experiments. * $p < 0.05$ vs control.

CHAPTER 5 - DISCUSSION

DOX-induced cardiotoxicity is due to a multifactorial process involving reactive free radical species as a possible primary mechanism for the toxicity observed with this agent and with other anthracyclines (Lee *et al*., 1991). Other mechanisms also proposed p53/Bax pathway translocation to mitochondria as early events in DOX-induced cardiac cell death (Sardao *et al.*, 2009a).

The first objective of the present study was to investigate the initial step that induces p66Shc activation and translocation to mitochondria upon DOX treatment. DOX is responsible for an increase in ROS levels (Mross *et al*., 2006), which we thought to be responsible for p66Shc activation and translocation to mitochondria. Western Blot confirmed the presence and increase in p66Shc content in total cellular extracts (Fig. 12 B) and mitochondrial fractions (Fig. 14 A), suggesting that DOX is activating the p66Shc pathway, in H9c2 cells. Immunocytochemistry also confirmed the presence and increase in p66Shc content, but interestingly an increase was also observed in nuclear fractions during 24 and 48 hours treatment (Fig. 12 A).

p66Shc phosphorylation on serine 36 is a critical step on p66Shc activation (Raffaello and Rizzuto, 2011). This process is induced by protein kinase C (PKC β), which is then recognized by the prolyl isomerase Pin1 that catalyzes its cis-trans isomerization. Subsequently, p66Shc is dephosphorylated by type 2 protein serine/threonine phosphatase (PP2A) and imported in the mitochondria (Raffaello and Rizzuto, 2011).

However, total cellular extracts of H9c2 cells showed a significant decrease in Serine 36-phosphorylated p66Shc (Fig. 13 A), which is also significant in mitochondrial fractions (Fig. 14 B). The decreased phosphorylation is actually unexpected unless increased p66Shc dephosphorylation is enhanced with DOX. More experiments are needed to demonstrate this point. As previously described, an increase in p66Shc

content was observed in nuclear fractions of H9c2 cells after 24 and 48 hours treatment (Fig. 12 D). Data suggested an involvement/binding with another protein. Indeed, some authors reported the physical binding of p66Shc and FoxO3a, a transcriptional factor, in part in a mechanism independent of Akt activation.

FoxO3a is involved in apoptosis, cell cycle transitions, DNA repair, cell differentiation, and oxidative stress (Barthel *et al*., 2005; Greer and Brunet, 2005). FoxO isoforms are regulated as a response to growth factor stimulation and oxidative stress through PI3K/Akt signaling pathway (Biggs *et al*., 1999). In response to several stimulis (insulin or gowth factors), FoxO factors are exported from the nucleus to the cytoplasm in an Akt-dependent phosphorylation process. Akt phosphorylation induces FoxO phosphorylation, remaining in the cytoplasm and their transcriptional function is repressed.

The presence of FoxO3a in H9c2 cells was analyzed by Western Blot (Fig. 15) and immunocytochemistry (Fig. 18). Both experiments confirmed an increase in FoxO3a content after DOX treatment during 24 and 48 hours. FoxO3a is being translocated from the cytoplasm (Fig. 15 B) to the nucleus (Fig. 15 C), suggesting that FoxO3a is involved in DOX-induced cell death. Furthermore, FoxO3a phosphorylation on serine 253 was also analyzed (Fig. 16). Western Blot experiments demonstrate a significant decrease in FoxO3a phosphorylation on serine 253, suggesting once more that FoxO3a does not remain in the cytoplasm, but instead it is being translocated to the nucleus where it contributes for DOX-induced cell death, as described before (Greer and Brunet, 2005). Once in the nucleus, FoxO3a promotes the up regulation of downstream targets involved in several pathways. Superoxide dismutase-2, p53 and the pro-apoptotic Bcl2-interacting mediator of cell death Bim are some of the FoxO downstream targets that can be up-regulated (Nemoto S and Finkel T. *et al*., 2002).

Results shown in Figure 17 revealed an increase of all downstream targets described before, showing that FoxO3a participates in the stress response to DOX treatment of H9c2 cells. Furthermore, the possible binding between p66Shc and FoxO3a was investigated by immunocytochemistry (Fig.18) and immunoprecipitation (Fig.19). Both experiments confirmed the presence of FoxO3a in H9c2 cells, also confirmed previously by Western Blot analyzes. Immunoprecipitation assay revealed that p66Shc is clearly binding to FoxO3a, and this interaction increases after 1 µM DOX treatment during 48 hours, although, no significant interaction is observed after 24 hours treatment. Since PI3K/Akt signaling pathway represents an essential signaling pathway in FoxO3a regulation, Akt content in H9c2 cells was also analyzed (Fig. 20). Western Blot results demonstrated a significant decrease in Akt content after DOX treatment with 1 µM DOX during 48 hours. The same was observed in the ratio of Akt S 473/ Akt after DOX treatment with 1 µM DOX during 48 hours (Fig. 21). Akt is a key survival component, which means that a decrease in Akt may contribute to DOX-induced loss of cells. FoxO proteins are regulated by phosphorylation-dependent nuclear/cytoplasmic shuttling as a result of the activity of Akt and JNK kinases (Biggs *et al*., 1999). Indeed, Akt directly phosphorylates FoxO3a (at the Tyr 32, Ser 253 and Ser 315) and targets them to bind the 14-3-3 nuclear export protein (Brunet *et al*., 2002). This binding would exclude FoxO3a factors from the nucleus, leading to their cytoplasmic accumulation and subsequent degradation (Calnan and Brunet, 2008). The results support the hypothesis that FoxO3a factors are being translocated to the nucleus where they act as transcriptional factors contributing for DOX-induced stress response, including cell death.

The second objective of the present study was to investigate the effects of Hispidin, a protein kinase C (PKC β) inhibitor, in p66Shc activation and signaling. As

previously described, PKC β is involved in p66Shc phosphorylation on serine 36, in a mechanism responsible for p66Shc activation and translocation to mitochondria (Raffaello and Rizzuto, 2011). The results demonstrate that Hispidin induces caspase-3 activation for both time points (24 and 48 hours) and concentrations, but caspase-9 activation only significantly higher for cells treated with DOX (48 hours treatment) and 5 μM Hispidin (for both time points) (Fig. 22 B and Fig. 22 C). Hispidin indirectly prevents p66Shc activation, and so the increased levels of ROS induced by DOX treatment may activate other mechanisms that will lead to caspase activation. The differences observed between caspase-3 and -9 are due to the executioner function of caspase-3 which does not need to be activated through caspase-9.

The results suggest that Hispidin is an effective compound in inhibiting p66Shc activation. p66Shc decreases significantly with Hispidin treatment (Fig. 23) and the ratio between the serine 36-phosphorylated form of p66shc and p66Shc total form (Fig. 24) and are similar to non treated cells. Hispidin might possess antioxidant effects against free radicals as already described in the literature (Jang *et al*., 2010), therefore inhibiting p66Shc activation.

p53 tumor suppressor plays a central role in the regulation of oxidative stress-induced apoptosis (Vogelstein *et al*., 2000). Currently, p66Shc has been reported as a downstream target for p53, as an essential for its function in increasing intracellular oxidants, cytochrome c release and apoptosis (Trinei *et al*., 2002). H9c2 cells treated with Hispidin (5 and 10 μM), showed a significant increase in p53 content after 24 hours treatment, but the same does not occur for 48 hours treatment. After 48 hours treatment, only cells treated with DOX showed increased levels of p53 (Fig. 25). Sardão *et al*., (2009a) reported the role of p53 and Bax in H9c2 cells treated with DOX, as an

important component for DOX-induced cell death. Bax was the first p53 regulating gene to be recognized as involved in the apoptotic process (Miyashita *et al*., 1994; Miyashita *et al*., 1995). The results suggest that Bax, as well as p53 signaling pathway may be connected with p66Shc protein, perhaps in a redox mechanism. Cytochrome c results showed an increase in total cellular extracts (Fig. 26 A) of H9c2 cells when treated with 10 µM Hispidin or DOX during 24 and 48 hours. Interestingly, an increase was also observed for cells treated with 5 µM Hispidin, suggesting that Hispidin is not capable of inhibiting Cyt c release form mitochondria, contributing to cell death (Fig. 26 B).

The apoptosis inducing factor (AIF) is released from mitochondria to the nucleus due to an oxidative stress injury where it promotes chromatin condensation and large-scale DNA fragmentation (Susin *et al.*, 2000). AIF signaling pathway has been reported as a mechanism that occurs independently of caspase activation (Cande *et al*., 2004). H9c2 cells were treated as previously described during 24 and 48 hours, and no changes were detected in total cellular extracts (Fig. 27 A). Mitochondrial fractions (Fig. 27 B) of H9c2 cells revealed a decrease in AIF content when cells were treated with 5 and 10 µM Hispidin and also for cells treated only with DOX for 24 hours. However, cells treated during 48 hours do not show the same results. Indeed, AIF release only occurs for cells treated with DOX, suggesting that AIF release from mitochondria may be involved with p66Shc activation. This is even more evident when cells were pre-incubated with Hispidin and four hours later treated with DOX, because one more time no changes were observed.

The Manganese superoxide dismutase converts superoxide generated by the respiratory chain into hydrogen peroxide, and acts in ROS detoxification (Li *et al*., 1995). p66Shc has been reported as a repressor of Superoxide dismutase (Koch *et al*.,

2008). This link is observed when SOD2 content increased after Hispidin treatment during 24 and 48 hours treatment (Fig. 28). However, is not sufficient to inhibit SOD2 after DOX treatment confirming once more that p66Shc regulates SOD2 levels in a redox mechanism.

Moreover, despite the good results of Hispidin in inhibiting p66Shc activation is not sufficient to counteract DOX-induced cell death (Fig. 29), suggesting that this protein may not be essential in that mechanisms but interferes with important key steps for mitochondria function, compromising cell death.

CHAPTER 6 - CONCLUSION

6.1. Final Conclusion

This work presents a major contribution to understand the underling mechanism of DOX-induced cardiotoxicity. Despite all negative aspects involving in DOX therapy, this compound is still a very effective anticancer drug.

The first aim of the present work was to investigate if DOX causes activation of the p66Shc signaling pathway which leads to a progressive deterioration of mitochondrial function. Our data indicate that p66Shc is being activated upon DOX treatment, leading to an increase in p66Shc in mitochondrial fractions. However, the ratio between p66Shc phosphorylation on serine 36 and p66Shc decreases, suggesting that in our cell model other mechanisms might be involved on p66Shc activation. Our results also suggest that inhibiting the activation of p66Shc signaling can also contribute to prevent DOX-induced cell death. It is very likely that p66Shc activation is involved in the up-regulation of several proteins normally associated with DOX toxicity, including p53.

In fact, a second goal of this work was to investigate a possible interaction between p66Shc and the transcriptional factor FoxO3a in a stress-dependent pathway contributing for the mitochondrial dysfunction and cell death during DOX treatment was also investigated. Our results point that p66Shc and FoxO3a are translocated to the nucleus promoting cell death.

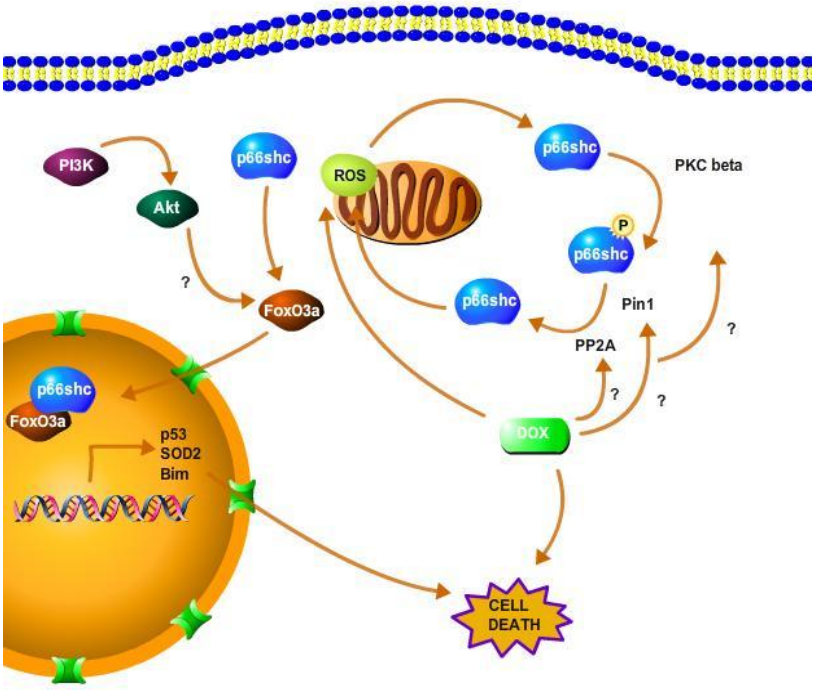

Figure 30. A new mechanism to explain DOX-induced cardiotoxicity. p66Shc and FoxO3a are physically interacting, and upon DOX treatment they are translocated to the nucleus promoting cell death.

6.2. Future Perspectives

In our study, we suggest that p66Shc activation and FoxO3a are important in contributing to cell death after DOX treatment. However, certain limitations are associated with the use of a cell line as a model, and so the results obtained should be confirmed using an in vivo model. Furthermore, PI3K/Akt pathway should be analyzed in more detail in order to clarify this contribution in FoxO3a regulation and cell survival. Following this, a PI3K and Akt inhibitor should be used.

In this work, the effect of a PKC β inhibitor, Hispidin, was assessed. Despite of all good results demonstrating an efficient inactivation of p66Shc, more experiments should be performed about the selectivity of this inhibitor. Indeed, a p66Shc knockdown or knockout would provide us useful information about this protein and its role in

mitochondria dysfunction, and also it would increase the validity of our results. In order to identify whether DOX-induced stress participates in the activation of the p66Shc, we will use N-acetylcystein (NAC), the GSH precursor, which we have demonstrated already to inhibit cell death caused by DOX (Sardão *et al*., 2009a), and observe if NAC inhibits the DOX-induced p66Shc up-regulation.

CHAPTER 7 - REFERENCES

Allen A.(1992). The cardiotoxicity of chemotherapeutic drugs. *Semin Oncol* 19**(5)**:529-542.

Arcamone F, Cassinelli G, Fantini G, Grein A, Orezzi P, Pol C and Spalla C.(1969). Adriamycin, 14-hydroxydaunomycin, a new antitumor antibiotic from S. peucetius var. caesius. *Biotechnol Bioeng* 11**(6)**:1101-1110.

Ascensao A, Lumini-Oliveira J, Oliveira PJ and Magalhaes J.(2011). Mitochondria as a target for exercise-induced cardioprotection. *Curr Drug Targets* 12**(6)**:860-871.

Bar J, Davidi O, Goshen Y, Hod M, Yaniv I and Hirsch R.(2003). Pregnancy outcome in women treated with doxorubicin for childhood cancer. *Am J Obstet Gynecol* 189 **(3)**: 853-857.

Berthiaume J and Wallace KB.(2007). Persistent alterations to the gene expression profile of the heart subsequent to chronic Doxorubicin treatment. *Cardiovasc Toxicol* 7 **(3)**: 178-191.

Biggs WHI, Meisenhelder J, Hunter T, Cavenee WK and Arden KC.(1999). Proc. Natl. Acad. Sci. USA, 96, 7421–7426.

Boucek RJ, Olson RD, Brenner DE, Ogunbunmi EM, Inui M and Fleischer S.(1987). The major metabolite of doxorubicin is a potent inhibitor of membrane-associated ion pumps. A correlative study of cardiac muscle with isolated membrane fractions. *J Biol Chem* 262**(33)**:15851-15856.

Bradford, MM.(1976). A rapid and sensitive method for the quantitation of727 microgram quantities of protein utilizing the principle of protein-dye binding. *Anal728 Biochem* 72:248-254

Brazil, DP and Hemmings B. A.(2001). Ten years of protein kinase B signalling: a hard Akt to follow. *Trends Biochem. Sci.* 26:657-664.

Brenner D and Mak TW.(2009). Mitochondrial cell death effectors. *Curr Opin Cell Biol* 21**(6)**:871-877.

Bristow MR, Minobe WA, Billingham ME, Marmor JB, Johnson GA, Ishimoto BM, Sageman WS and Daniels JR.(1981). Anthracycline-associated cardiac and renal damage in rabbits. Evidence for mediation by vasoactive substances. *Lab Invest* 45**(2)**:157-168.

Broekemeier KM and Pfeiffer DR.(1989). Cyclosporin A-sensitive and insensitive mechanisms produce the permeability transition in mitochondria. *Biochem Biophys Res Commun* 163**(1)**:561-566.

Brunet A, Bonni A, Zigmond MJ, Lin MZ, Juo P, Hu LS, Anderson MJ, Arden KC, Blenis J and Greenberg ME.(1999). Akt promotes cell survival by phosphorylating and inhibiting a Forkhead transcription factor.*Cell* 96:857–868.

Brunet A, Datta SR and Greenberg ME.(2001). Transcription-dependent and independent control of neuronal survival by the PI3K-Akt signaling pathway. *Curr Opin Neurobiol* 11:297–305.

Brunet A, Sweeney LB, Sturgill JF, Chua KF, Greer PL, Lin Y, Tran H, Ross SE, Mostoslavsky R and Cohen HY.(2004). Stress-dependent regulation of FOXO transcription factors by the SIRT1 deacetylase. *Science* 303:2011–2015.

Burhans WC and Weinberger M.(2007). Yeast endonuclease G: complex matters of death, and of life. *Mol Cell* 25**(3)**:323-325.

Calnan DR and Brunet A.(2008). The FoxO code. *Oncogene* 27:2276-88

Cande C, Vahsen N, Garrido C and Kroemer G.(2004). Apoptosis-inducing factor (AIF): caspase-independent after all. *Cell Death Differ* 11**(6)**:591-595.

Carlsson P, Mahlapuu M.(2002). Forkhead transcription factors: key players in development and metabolism. *Developmental Biology* 250**(1)**:1–23.

Chahdi A and Sorokin A.(2008). Endothelin-1 Couples βPix to p66Shc: Role of βPix in Cell Proliferation through FOXO3a Phosphorylation and p27kip1 Down-Regulation Independently of Akt. *Molecular Biology of the Cell* Vol. 19, 2609–2619**.**

Chao HH, Liu JC, Hong HJ, Lin JW, Chen CH and Cheng TH.(2011). L-carnitine reduces doxorubicin-induced apoptosis through a prostacyclin-mediated pathway in neonatal rat cardiomyocytes. *Int J Cardio*.146 **(2)**: 145-152.

Chen K, Xu X, Kobayashi S, Timm D, Jepperson T and Liang Q.(2011). Caloric restriction mimetic 2-deoxy-glucose antagonizes doxorubicin-induced cardiomyocyte death through multiple mechanisms. *J Biol Chem* 286**(25)**:21993-2006

Cummings J, Anderson L, Willmott N and Smyth JF.(1991). The molecular pharmacology of doxorubicin in vivo. *Eur J Cancer* 27**(5)**:532-535.

Cutts SM, Nudelman A, Rephaeli A and Phillips DR.(2005). The power and potential of doxorubicin-DNA adducts. *IUBMB Life* 57**(2)**:73-81.

Danz ED, Skramsted J, Henry N, Bennett JA and Keller RS.(2009). Resveratrol prevents doxorubicin cardiotoxicity through mitochondrial stabilization and the Sirt1 pathway. *Free Radic Biol Med* 46**(12)**:1589-1597.

Daugas E, Susin EA, Zamzami N, Ferri K, Irinopoulos T, Larochette N, Prevost MC, Leber B, Andrews D, Penninger J and Kroemer G.(2000). Mitochondrio-nuclear redistribution of AIF in apoptosis and necrosis. *FASEB J.* 14:729–739.

Davies KJ and Doroshow JH.(1986). Redox cycling of anthracyclines by cardiac mitochondria. I. Anthracycline radical formation by NADH dehydrogenase. *J Biol Chem* 261**(7)**:3060-3067.

Dessypris EN, Brenner DE and Hande KR.(1986). Toxicity of doxorubicin metabolites to human marrow erythroid and myeloid progenitors in vitro. *Cancer Treat Rep* 70**(4)**:487-490.

Doroshow JH and Davies KJ.(1986). Redox cycling of anthracyclines by cardiac mitochondria. II. Formation of superoxide anion, hydrogen peroxide, and hydroxyl radical. *J Biol Chem* 261**(7)**:3068-3074.

Essers MA, Weijzen S, de Vries-Smits AM, Saarloos I, de Ruiter ND, Bos JL and Burgering BM.(2004). FOXO transcription factor activation by oxidative stress mediated by the small GTPase Ral and JNK. *Embo J* 23:4802–4812.

Fang J, Nakamura H and Iyer AK (2007). Tumor-targeted induction of oxystress for cancer therapy. *J Drug Target* 15**(7-8)**:475-486.

Favetta LA, Robert C, King WA and Betts DH.(2004). Expression profiles of p53 and p66Shc during oxidative stress-induced senescence in fetal bovine fibroblasts. *Exp Cell Res* 299, 36–48.

Fazio S, Palmieri EA, Ferravante B, Bone F, Biondi B and Sacca L.(1998). Doxorubicin-induced cardiomyopathy treated with carvedilol. *Clin Cardiol*. 21:777–9.

Formentini L, Macchiarulo A, Cipriani G, Camaioni E, Rapizzi E, Pellicciari R, Moroni F and Chiarugi A.(2009). Poly(ADP-ribose) catabolism triggers AMP-dependent mitochondrial energy failure. *J Biol Chem* 284**(26)**:17668-17676.

Giorgio M, Migliaccio E, Orsini F, Paolucci D, Moroni M, Contursi C, Pelliccia G, Luzi L, Minucci S, Marcaccio M, Pinton P, Rizzuto R, Bernardi P, Paolucci F and Pelicci PG.(2005). Electron transfer between cytochrome c and p66Shc generates reactive oxygen species that trigger mitochondrial apoptosis. *Cell* 122**(2)**:221-233.

Giorgio M, Trinei M, Migliaccio E and Pelicci PG.(2007). Hydrogen peroxide: a metabolic by-product or a common mediator of ageing signals? *Nat Rev Mol Cell Biol* 8**(9)**:722-728.

Gomis RR, Alarcon C, Nadal C, Van Poznak C, Massague J.(2006). C/EBPbeta at the core of the TGFbeta cytostatic response and its evasion in metastatic breast cancer cells. *Cancer Cell* 10:203–214.

Greer EL and Brunet A.(2005). FoxO transcription factors at the interface between longevity and tumour supression.*Oncogene* 24:7410-7425.

Gupta S.(2001). Molecular steps of death receptor and mitochondrial pathways of apoptosis. *Life Sci*. 69: 2957-2964.

Halestrap AP, Connern CP, Griffiths EJ and Kerr PM.(1997). Cyclosporin A binding to mitochondrial cyclophilin inhibits the permeability transition pore and protects hearts from ischaemia/reperfusion injury. *Molecular and Cellular Biochemistry* 174: 167–172.

Hanahan D and Weinberg RA.(2000). The hallmarks of cancer. *Cell* 100**(1)**:57-70.

Henderson BE and Feigelson HS.(2000). Hormonal carcinogenesis. *Carcinogenesis* 21: 427-433.

Hescheler J, Meyer R, Plant S, Krautwurst D, Rosenthal W and Schultz G (1991).Morphological, biochemical, and electrophysiological characterization of a clonal cell (H9c2) line from rat heart. *Circ Res* 69:1476-1486.

Hotchkiss RS and Nicholson DW.(2006). Apoptosis and caspases regulate death and inflammation in sepsis. *Nat Rev Immunol* 6**(11)**:813-822.

Houghton P, Fang R, Techatanawat I, Steventon G, Hylands PJ and Lee CC.(2007). The sulphorhodamine (SRB) assay and other approaches to testing plant extracts and derived compoundsfor activities related to reputed anticancer activity. *Methods* 42:377–387.

Hu Y, Kang C, Philp RJ and Li B.(2007). PKC delta phosphorylates p52ShcA at Ser29 to regulate ERK activation in response to H2O2. *Cell Signal* 19**(2)**:410-418.

Hydock DS, Lien CY, Jensen BT, Schneider CM and Hayward R.(2011). Exercise preconditioning provides long-term protection against early chronic doxorubicin cardiotoxicity. *Integr Cancer Ther* 10**(1)**:47-57.

Jackson JG, Yoneda T, Clark GM and Yee D.(2000). Elevated levels of p66 Shc are found in breast cancer cell lines and primary tumors with high metastatic potential. *Clin Cancer Res* 6**(3)**:1135-1139.

Jang SJ, Jo Lee JS, Lee JH, Kwon DS, Lee KE, Lee SY, and Hon EK (2010). Hispidin Produced from *Phellinus linteus* Protects Pancreatic β-cells from Damage by Hydrogen Peroxide. *Arch Pharm Res Vol 33, No 6, 853-861.*

Jiang W, Lionberger R and Yu LX.(2011). In vitro and in vivo characterizations of PEGylated liposomal doxorubicin. *Bioanalysis* 3**(3)**:333-344.

Jin Z and El-Deiry WS.(2005). Overview of cell death signaling pathways. *Cancer Biol Ther* 4**(2)**:139-163.

Johnson D, Perrault H, Fournier A, Leclerc JM, Bigras JL and Davignon A. (1997). Cardiovascular responses to dynamic submaximal exercise in children previously treated with anthracycline. *Am Heart J* 133 **(2)**:169-173.

Jung K and Reszka R.(2001). Mitochondria as subcellular targets for clinically useful anthracyclines. *Adv Drug Deliv Rev* 49**(1-2)**:87-105.

Kaestner, K. H., Knochel, W. and Martinez, D. E. (2000). Unified nomenclature for the winged helix/forkhead transcription factors. *Genes Dev.* 14:142-146

Kalivendi SV, Konorev EA, Cunningham S, Vanamala SK, Kaji EH, Joseph J and Kalyanaraman B.(2005). Doxorubicin activates nuclear factor of activated T-lymphocytes and Fas ligand transcription: role of mitochondrial reactive oxygen species and calcium. *Biochem J* 389**(Pt 2)**:527-539.

Kelishomi RB, Ejtemaeemehr S, Tavangar SM, Rahimian R, Mobarakeh JI and Dehpour AR.(2008). Morphine is protective against doxorubicin-induced cardiotoxicity in rat. *Toxicology* 243**(1-2)**:96-104.

Kerr JF, Wyllie AH and Currie AR.(1972). Apoptosis: a basic biological phenomenon with wide-ranging implications in tissue kinetics. *Br J Cancer* 26**(4)**:239-257.

Kimes BW and Brandt BL.(1976). Properties of a clonal muscle cell line from rat heart. *Exp Cell Res* 98**(2)**:367-381.

Kumar D, Kirshenbaum LA, Li T, Danelisen I and Singal PK.(2001). Apoptosis in adriamycin cardiomyopathy and its modulation by probucol. *Antioxid Redox Signal* 3**(1)**:135-145.

Kisielow M, Kleiner S, Nagasawa M, Faisal A and Nagamine Y.(2002). Isoform-specific knockdown and expression of adaptor protein ShcA using small interfering RNA.*Biochem J* 363:1-5.

Koch OR, Fusco S, Ranieri SC, Maulucci G, Palozza P, Larocca LM.(2008). Role of the life span determinant P66(shcA) in ethanol-induced liver damage. *Lab Invest*; 88:750–60.

Kumar S, Rajendran M, Alam SM, Lin FF, Cheng PW and Lin MF.(2011). Steroids up-regulate p66Shc longevity protein in growth regulation by inhibiting its ubiquitination. *PLoS One* 6**(1)**:e15942.

Kweon SH, Song JH and Kim TS.(2010). Resveratrol-mediated reversal of doxorubicin resistance in acute myeloid leukemia cells via downregulation of MRP1 expression. *Biochem Biophys Res Commun* 395**(1)**:104-110.

L'Ecuyer T, Sanjeev S, Thomas R, Novak R, Das L, Campbell W and Heide RV.(2006). DNA damage is an early event in doxorubicin-induced cardiac myocyte death. *Am J Physiol Heart Circ Physiol* 291**(3)**:H1273-1280.

Landshamer S, Hoehn M, Barth N, Duvezin-Caubet S, Schwake G, Tobaben S, Kazhdan I, Becattini B, Zahler S, Vollmar A, Pellecchia M, Reichert A, Plesnila N, Wagner E and Culmsee C.(2008). Bid-induced release of AIF from mitochondria causes immediate neuronal cell death. *Cell Death Differ* 15**(10)**:1553-1563.

Lebiedzinska M, Duszynski J, Rizzuto R, Pinton P and Wieckowski MR.(2009). Age-related changes in levels of p66Shc and serine 36-phosphorylated p66Shc in organs and mouse tissues. *Arch Biochem Biophys* 486**(1)**:73-80.

Lebiedzinska M, Karkucinska-Wieckowska A, Giorgi C, Karczmarewicz E, Pronicka E, Pinton P, Duszynski J, Pronicki M and Wieckowski MR.(2010). Oxidative stress-dependent p66Shc phosphorylation in skin fibroblasts of children with mitochondrial disorders. *Biochim Biophys Acta* 1797**(6-7)**:952-960.

Lebrecht D, Kokkori A, Ketelsen UP, Setzer B and Walker UA.(2005). Tissue-specific mtDNA lesions and radical-associated mitochondrial dysfunction in human hearts exposed to doxorubicin. *J Pathol* 207**(4)**:436-444.

Lebrecht D, Geist A, Ketelsen UP, Haberstroh J, Setzer B and Walker UA.(2007). Dexrazoxane prevents doxorubicin-induced long-term cardiotoxicity and protects myocardial mitochondria from genetic and functional lesions in rats. *Br J Pharmacol* 151**(6)**:771-778.

Lee BI, Lee DJ, Cho KJ and Kim GW.(2005). Early nuclear translocation of endonuclease G and subsequent DNA fragmentation after transient focal cerebral ischemia in mice. *Neurosci Lett* 386:23–27.

Lee HS and Wei YH.(2007). Oxidative Stress, Mitochondrial DNA Mutation, and Apoptosis in Aging. *Exp Biol Med.* vol. 232 no. 5 592-606.

Lee MS, Igawa T, Chen SJ, Van Bemmel D, Lin JS, Lin FF, Johansson SL, Christman JK and Lin MF.(2004). p66Shc protein is upregulated by steroid hormones in hormone-sensitive cancer cells and in primary prostate carcinomas. *Int J Cancer* 108**(5)**:672-678.

Lee V, Randhawa AK and Singal PK.(1991). Adriamycin-induced myocardial dysfunction in vitro is mediated by free radicals. *Am J Physiol* 261**(4 Pt 2)**:H989-995.

Lehtinen MK, Yuan Z, Boag PR, Yang Y, Villen J, Becker EB, DiBacco S, de la Iglesia N, Gygi S, Blackwell TK, *et al*. (2006). A conserved MST-FOXO signaling pathway mediates oxidative-stress responses and extends life span. *Cell* 125:987–1001.

Leonhard GA, Brown T and Hunter WT.(1992). Anthracycline binding to DNA. *Eur J Biochem* 204:69–74.

Li X, Klaus JA, Zhang J, Xu Z, Kibler KK, Andrabi SA, Rao K, Yang ZJ, Dawson TM, Dawson VL and Koehler RC.(2010). Contributions of poly(ADP-ribose) polymerase-1 and -2 to nuclear translocation of apoptosis-inducing factor and injury from focal cerebral ischemia. *J Neurochem* 113**(4)**:1012-1022

Li Y, Huang TT, Carlson EJ, Melov S, Ursell PC, Olson JL, *et al* (1995). Dilated cardiomyopathy and neonatal lethality in mutant mice lackingmanganese superoxide dismutase.*Nat Genet* 11:376–81.

Liu B, Chen Y and St Clair DK.(2008a). ROS and p53: a versatile partnership. *Free Radic Biol Med* 44**(8)**:1529-1535.

Liu J, Mao W, Ding B and Liang CS.(2008b). ERKs/p53 signal transduction pathway is involved in doxorubicin-induced apoptosis in H9c2 cells and cardiomyocytes. *Am J Physiol Heart Circ Physiol* 295**(5)**:H1956-1965.

Liu L, Zhang Z and Xing D.(2011). Cell death via mitochondrial apoptotic pathway due to activation of Bax by lysosomal photodamage. *Free Radic Biol Med* 51**(1)**:53-68.

Liu X, Chua CC, Gao J, Chen Z, Landy CL, Hamdy R and Chua BH.(2004). Pifithrin-alpha protects against doxorubicin-induced apoptosis and acute cardiotoxicity in mice. *Am J Physiol Heart Circ Physiol* 286**(3)**:H933-939.

Migliaccio E, Mele S, Salcini AE, Pelicci G, Lai KM, Superti-Furga G, Pawson T, Di Fiore PP, Lanfrancone L and Pelicci PG.(1997). Opposite effects of the p52shc/p46shc and p66Shc splicing isoforms on the EGF receptor-MAP kinase-fos signaling pathway. *EMBO J* 16**(4)**:706-716.

Minotti G, Menna P, Salvatorelli E, Cairo G and Gianni L.(2004). Anthracyclines: molecular advances and pharmacologic developments in antitumor activity and cardiotoxicity. *Pharmacol Rev* 56**(2)**:185-229.

Mizutani H, Tada-Oikawa S, Hiraku Y, Kojima M and Kawanishi S.(2005). Mechanism of apoptosis induced by doxorubicin through the generation of hydrogen peroxide. *Life Sci* 76**(13)**:1439-1453.

Modur, V., Nagarajan, R., Evers, B. M. and Milbrandt, J. (2002). FOXO proteins regulate tumor necrosis factor-related apoptosis inducing ligand expression. Implications for PTEN mutation in prostate cancer. *J. Biol. Chem.* 277, 47928-47937.

Monti E, Prosperi E, Supino R and Bottiroli G.(1995). Free radical-dependent DNA lesions are involved in the delayed cardiotoxicity induced by adriamycin in the rat. *Anticancer Res* 15**(1)**:193-197.

Mross K, Massing U and Kratz F.(2006). DNA-intercalators – the anthracyclines. *Drugs Affecting Growth Tumours* 19-81.

Nemoto S and Finkel T.(2002). Redox regulation of forkhead proteins through a p66shc-dependent signaling pathway.Science 295:2450–2452.

Oettl K, Greilberger J, Zangger K, Haslinger E, Reibnegger G and Jurgens G.(2001). Radical-scavenging and iron-chelating properties of carvedilol, an antihypertensive drug with antioxidative activity. *Biochem Pharmacol* 62**(2)**:241-248.

Oktem G, Uysal A, Oral O, Sezer ED, Olukman M, Erol A, Akgur SA and Bilir A.(2010). Resveratrol attenuates doxorubicin-induced cellular damage by modulating nitric oxide and apoptosis. *Exp Toxicol Pathol*.

Oliveira PJ, Bjork JA, Santos MS, Leino RL, Froberg MK, Moreno AJ and Wallace KB.(2004). Carvedilol-mediated antioxidant protection against doxorubicin-induced cardiac mitochondrial toxicity. *Toxicol Appl Pharmacol* 200**(2)**:159-168.

Oliveira PJ, Santos MS and Wallace KB.(2006). Doxorubicin-induced thiol-dependent alteration of cardiac mitochondrial permeability transition and respiration. *Biochemistry (Mosc)* 71**(12)**: 194-9.

Oliveira PJ and Wallace KB.(2006). Depletion of adenine nucleotide translocator protein in heart mitochondria from doxorubicin-treated rats-relevance for mitochondrial dysfunction. *Toxicology* 220**(2-3)**:160-168.

Orsini F, Migliaccio E, Moroni M, Contursi C, Raker VA, Piccini D, Martin-Padura I, Pelliccia G, Trinei M, Bono M, Puri C, Tacchetti C, Ferrini M, Mannucci R, Nicoletti I, Lanfrancone L, Giorgio M and Pelicci PG.(2004). The life span determinant p66Shc localizes to mitochondria where it associates with mitochondrial heat shock protein 70 and regulates trans-membrane potential. *J Biol Chem* 279**(24)**:25689-25695.

Papkovsky DB.(2004). Methods in optical oxygen sensing: protocols and critical analyses. *Methods Enzymol* 381**(**715-735.

Parsons MJ and Green DR.(2010). Mitochondria in cell death. *Essays Biochem* 47**(**99-114.

Pereira CV, Moreira AC, Pereira SP, Machado NG, Carvalho FS, Sardao VA and Oliveira PJ.(2009). Investigating drug-induced mitochondrial toxicity: a biosensor to increase drug safety? *Curr Drug Saf* 4**(1)**:34-54.

Pinton P and Rizzuto R.(2008). p66Shc, oxidative stress and aging: importing a lifespan determinant into mitochondria. *Cell Cycle* 7**(3)**:304-308.

Pradelli LA, Beneteau M and Ricci JE.(2010). Mitochondrial control of caspase-dependent and -independent cell death. *Cell Mol Life Sci* 67**(10)**:1589-1597.

Quigley GJ, Wang AH, Ughetto G, Van der Marel G, Van Boom JH and Rich A.(1980). Molecular structure of an anticancer drug-DNA complex: daunomycin plus d(CpGpTpApCpG). *Proc Natl Acad Sci U S A* 77**(12)**:7204-7208.

Racz B, Reglodi D, Horvath G, Szigeti A, Balatonyi B, Roth E, Weber G, Alotti N, Toth G and Gasz B.(2010). Protective effect of PACAP against doxorubicin-induced cell death in cardiomyocyte culture. *J Mol Neurosci* 42**(3)**:419-427.

Raffaello A and Rizzuto R.(2011). Mitochondrial longevity pathways. *Biochim Biophys Acta* 1813**(1)**:260-268.

Ravichandran KS.(2001). Signaling via Shc family adapter proteins. *Oncogene* 20**(44)**:6322-6330.

Ren D, Kratz F and Wang SW.(2011). Protein nanocapsules containing doxorubicin as a pH-responsive delivery system. *Small* 7**(8)**:1051-1060.

Rena G, WoodsYL, Prescott AR, Peggie M, Unterman TG, WilliamsMR and Cohen P. (2002). Two novel phosphorylation sites on FKHR that are critical for its nuclear exclusion. *EMBO J* 21:2263–2271.

Richard C, Ghibu S, Delemasure-Chalumeau S, Guilland JC, Des Rosiers C, Zeller M, Cottin Y, Rochette L and Vergely C.(2011). Oxidative stress and myocardial gene alterations associated with Doxorubicin-induced cardiotoxicity in rats persist for 2 months after treatment cessation. *The Journal of pharmacology and experimental therapeutics* 339 **(3)**:807-814.

Salih DAM and Brunet A (2008). FoxO transcription factors in the maintenance of cellular homeostasis during aging. *Curr Opin Cell Biol*. 2008 April ; 20**(2)**: 126–136

Santos DL, Moreno AJ, Leino RL, Froberg MK and Wallace KB.(2002). Carvedilol protects against doxorubicin-induced mitochondrial cardiomyopathy. *Toxicol Appl Pharmacol* 185**(3)**:218-227.

Sardao VA, Oliveira PJ, Holy J, Oliveira CR and Wallace KB.(2007). Vital imaging of H9c2 myoblasts exposed to *tert*-butylhydroperoxide-characterization of morphological features of cell death. *BMC Cell Biology* 8:11.

Sardao VA, Oliveira PJ, Holy J, Oliveira CR and Wallace KB.(2009a). Doxorubicin-induced mitochondrial dysfunction is secondary to nuclear p53 activation in H9c2 cardiomyoblasts. *Cancer Chemother Pharmacol* 64**(4)**:811-827.

Sardao VA, Oliveira PJ, Holy J, Oliveira CR and Wallace KB.(2009b). Morphological alterations induced by doxorubicin on H9c2 myoblasts: nuclear, mitochondrial, and cytoskeletal targets. *Cell Biol Toxicol* 25**(3)**:227-243.

Savill J and Fadok V.(2000). Corpse clearance defines the meaning of cell death. *Nature* 407**(6805)**:784-788.

Sayed-Ahmed MM, Shaarawy S, Shouman SA and Osman AM.(1999). Reversal of doxorubicin-induced cardiac metabolic damage by L-carnitine. *Pharmacol Res* 39**(4)**:289-295.

Sevrioukova IF.(2011). Apoptosis-inducing factor: structure, function, and redox regulation. *Antioxid Redox Signal* 14**(12)**:2545-2579.

Sharma H, Pathan RA, Kumar V, Javed S and Bhandari U.(2010). Anti-apoptotic potential of rosuvastatin pretreatment in murine model of cardiomyopathy. *Int J Cardiol*. 150**(2)**:193-200.

Shieh MJ, Hsu CY, Huang LY, Chen HY, Huang FH and Lai PS.(2011). Reversal of doxorubicin-resistance by multifunctional nanoparticles in MCF-7/ADR cells. *J Control Release* 152**(3)**:418-425.

Shizukuda Y, Matoba S, Mian OY, Nguyen T and Hwang PM.(2005). Targeted disruption of p53 attenuates doxorubicin-induced cardiac toxicity in mice. *Mol Cell Biochem* 273**(1-2)**:25-32.

Sokolove PM and Shinaberry RG.(1988). Na+-independent release of Ca2+ from rat heart mitochondria. Induction by adriamycin aglycone. *Biochem Pharmacol* 37**(5)**:803-812.

Spallarossa P, Fabbi P, Manca V, Garibaldi S, Ghigliotti G, Barisione C, Altieri P, Patrone F, Brunelli C and Barsotti A.(2005). Doxorubicin-induced expression of LOX-1 in H9c2 cardiac muscle cells and its role in apoptosis. *Biochem Biophys Res Commun* 335**(1)**:188-196.

Stahl M., Dijkers PF, Kops, GJ, Lens SM, Coffer PJ, Burgering BM and Medema RH.(2002). The forkhead transcription factor FoxO regulates transcription of p27Kip1 and Bim in response to IL-2. *J. Immunol* 168:5024-5031.

Steinherz L; Steinherz PG; Tan CT; Heller G; Murphy ML.(1991). Cardiac toxicity 4 to 20 years after completing anthracycline therapy. *Jama* 266 **(12):** 1672-1677.

Stennicke HR and Salvesen GS.(2000). Caspases-controlling intracellular signals by protease zymogen activation. *Biochim Biophys Acta* 1477**(1-2)**:299-306.

Stevenson LE and Frackelton AR Jr.(1998). Constitutively tyrosine phosphorylated p52 Shc in breast cancer cells: correlation with ErbB2 and p66 Shc expression. *Breast Cancer Res Treat* 49**(2)**:119-128.

Susin SA, Lorenzo HK, Zamzami N, Marzo I, Snow BE, Brothers GM, Mangion J, Jacotot E, Costantini P, Loeffler M, Larochette N, Goodlett DR, Aebersold R, Siderovski DP, Penninger JM and Kroemer G.(1999). Molecular characterization of mitochondrial apoptosis-inducing factor. *Nature* 397**(6718)**:441-446.

Susin SA, Daugas E, Ravagnan L, Samejima K, Zamzami N, Loeffler M, Costantini P, Ferri KF, Irinopoulou T, Prevost MC, Brothers G, Mak TW, Penninger J, Earnshaw WC and Kroemer G.(2000). Two distinct pathways leading to nuclear apoptosis. *J Exp Med* 192**(4)**:571-580.

Tewey KM, Chen GL, Nelson EM and Liu LF.(1984). Intercalative antitumor drugs interfere with the breakage-reunion reaction of mammalian DNA topoisomerase II. *J Biol Chem* 259**(14)**:9182-9187.

Thompson CB.(1995). Apoptosis in the pathogenesis and treatment of disease. *Science* 267**(5203)**:1456-1462.

Trinei M, Giorgio M, Cicalese A, Barozzi S, Ventura A, Migliaccio E, Milia E ,Padura IM, Raker VA, Maccarana M, Petronilli V, Minucci S, Bernardi P, Lanfrancone L and Pelicci PG.(2002). A p53-p66Shc signalling pathway controls intracellular redox status, levels of oxidation-damaged DNA and oxidative stress-induced apoptosis. *Oncogene* 21**(24)**:3872-3878.

Van der Horst A, Tertoolen LG, de Vries-Smits LM, Frye RA,Medema RH and Burgering BM.(2004). FOXO4 is acetylated upon peroxide stress and deacetylated by the longevity protein hSir2 (SIRT1). *J. Biol. Chem* 279:28873–28879.

Van Herreweghe F, Festjens N, Declercq W and Vandenabeele P.(2010). Tumor necrosis factor-mediated cell death: to break or to burst, that's the question. *Cell Mol Life Sci* 67**(10)**:1567-1579.

Veeramani S, Yuan TC, Lin FF and Lin MF.(2008). Mitochondrial redox signaling by p66Shc is involved in regulating androgenic growth stimulation of human prostate cancer cells. *Oncogene* 27**(37)**:5057-5068.

Vieira HLA, Haouzi D, El Hamel C, Jacotot E, Belzacq A.-S, Brenner C and Kroemer G. (2000). Permeabilization of the mitochondrial inner membrane during apoptosis: impact of the adenine nucleotide translocator. *Cell Death Differ*. 7: 1146–1154.

Vigneron A.and Vousden KH (2012). An indirect role for ASPP1 in limiting p53-dependent p21 expression and cellular senescence. *The EMBO Journal* 31: 471 - 480

Vogelstein B, Lane D and Levine AJ. (2000). p53:The Most Frequently Altered Gene in Human Cancer. *Nature* 408:307-310.

Vosler PS, Sun D, Wang S, Gao Y, Kintner DB, Signore AP, Cao G and Chen J.(2009). Calcium dysregulation induces apoptosis-inducing factor release: cross-talk between PARP-1- and calpain-signaling pathways. *Exp Neurol* 218**(2)**:213-220.

Wallace KB.(2007). Adriamycin-induced interference with cardiac mitochondrial calcium homeostasis. *Cardiovasc Toxicol* 7**(2)**:101-107.

Wang SQ, Han XZ, Li X, Ren DM, Wang XN and Lou HX.(2010). Flavonoids from Dracocephalum tanguticum and their cardioprotective effects against doxorubicin-induced toxicity in H9c2 cells. *Bioorg Med Chem Lett* 20**(22)**:6411-6415.

Weiss RB.(1992). The anthracyclines: will we ever find a better doxorubicin? *Semin Oncol* 19**(6)**:670-686.

Wieckowski MR, Giorgi C, Lebiedzinska M, Duszynski J and Pinton P.(2009). Isolation of mitochondria-associated membranes and mitochondria from animal tissues and cells. *Nat Protoc* 4**(11)**:1582-1590.

Wijchers PJ, Burbach JP and Smidt MP (2006). In control of biology: of mice, men and Foxes. *The Biochemical Journa*l 397**(2)**:233–246.

Yoshida S, Masaki T, Feng H, Yuji J, Miyauchi Y, Funaki T, Yoshiji H, Matsumoto K, Uchida N, Watanabe S, Kurokohchi K and Kuriyama S.(2004). Enhanced expression of adaptor

molecule p46 Shc in nuclei of hepatocellular carcinoma cells: study of LEC rats. *Int J Oncol* 25**(4)**:1089-1096.

Zhang C, Feng Y, Qu S, Wei X, Zhu H, Luo Q, Liu M, Chen G and Xiao X.(2011). Resveratrol attenuates doxorubicin-induced cardiomyocyte apoptosis in mice through SIRT1-mediated deacetylation of p53. *Cardiovasc Res* 90**(3)**:538-545.

Zhang W, Ji W, Yang L, Xu Y, Yang J and Zhuang Z.(2010). Epigenetic enhancement of p66Shc during cellular replicative or premature senescence. *Toxicology* 278**(2)**:189-194.

Zhang YW, Shi J, Li YJ and Wei L.(2009). Cardiomyocyte death in doxorubicin-induced cardiotoxicity. *Arch Immunol Ther Exp (Warsz)* 57**(6)**:435-445.

Zhou S, Starkov A, Froberg MK, Leino RL and Wallace KB (2001). Cumulative and irreversible cardiac mitochondrial dysfunction induced by doxorubicin. *Cancer Res* 61 **(2)**: 771-777.

Zunino F and Capranico G.(1990). DNA topoisomerase II as the primary target of anti-tumor anthracyclines. *Anticancer Drug Des* 5**(4)**:307-317.